Chapter 4
Processing and Properties of Starch-Based Thermoplastic Matrix for Green Composites

Laura Ribba, Maria Cecilia Lorenzo, Maribel Tupa, Mariana Melaj, Patricia Eisenberg, and Silvia Goyanes

L. Ribba
Dirección de Materiales Avanzados, Áreas del Conocimiento, INTI, CONICET, San Martín, Buenos Aires, Argentina
e-mail: ribba@df.uba.ar

L. Ribba · S. Goyanes (✉)
Departamento de Física, Facultad de Ciencias Exactas y Naturales, Universidad de Buenos Aires, Buenos Aires, Argentina
e-mail: goyanes@df.uba.ar

M. C. Lorenzo
Dirección de Materiales Avanzados, INTI-Áreas del Conocimiento, San Martín, Buenos Aires, Argentina
e-mail: clorenzo@inti.gob.ar

M. C. Lorenzo · P. Eisenberg
Instituto de Investigación e Ingeniería Ambiental, Universidad Nacional de San Martín, San Martín, Buenos Aires, Argentina
e-mail: peisenberg@unsam.edu.ar

M. Tupa · M. Melaj
Facultad de Ingeniería, ITPN. Instituto de Tecnología en Polímeros y Nanotecnología, CONICET—UBA, Buenos Aires, Argentina
e-mail: mtupa@fi.uba.ar

M. Melaj
e-mail: mmelaj@fi.uba.ar

S. Goyanes
Instituto de Física de Buenos Aires (IFIBA), CONICET—Universidad de Buenos Aires, Buenos Aires, Argentina

M. Tupa
Departamento de Ingeniería Química, Facultad de Ingeniería, Universidad de Buenos Aires, Buenos Aires, Argentina

Abbreviations

ACR	Acrylonitrile-chlorinated polyethylene styrene
a_w	Water activity
bio-PE	Bio-polyethylene
bio-PEF	Bio-polyethylene furanoate
bio-PET	Bio-polyethylene terephthalate
BP	Benzoyl peroxide
BT	Bentonite
C/OS	Corn/octenylsuccinated starch
C30B	Organically modified montmorillonite
CA	Contact angle
CAc	Citric acid
CF	Cellulose fiber
ChCl	Choline chloride
CNF	Cellulose nanofiber
CNFs	Cellulose nanofibrils
CS	Corn starch
1D	One-dimensional
2D	Two-dimensional
DES	Deep eutectic solvent
DMSO	Dimethyl sulfoxide
DMTA	Dynamic mechanical thermal analysis
DSC	Differential scanning calorimetry
EB	Elongation at break
EMA	Ethylene–methyl acrylate
EVA	Ethylene-vinyl acetate
EVOH	Poly(ethylene-co-vinyl alcohol)
Gl	Glycerol
GMA	Glycidyl methacrylate
HPDSP	Hydroxypropyl distarch phosphate
HSM	High-speed mixer
HV	3-Hydroxyvalerate
Im	Imidazole
M0	Monolayer moisture content
MA	Maleic anhydride
MCC	Microcrystalline cellulose
MFI	Melt flow index
MMT	Montmorillonite
MMTDA	Modified MMT
NCC	Nanocrystalline cellulose
nCOM	Nanoclay organically modified
O/W	Oil-in-water
OMMT	Derivate of montmorillonite

OP	Oxygen permeability
OS	Octenylsuccinated starch
OSA starch	Octenyl succinic anhydride-modified starch
PBAT	Polybutylene adipate-co-terephthalate
PBAT-g-MA	Maleate PBAT
PBT	Polybutylene terephthalate
PCF	Plasma-treated cellulose fiber
PCL	Polycaprolactone
PDA	Polydopamine
PE	Polyethylene
PEG	Polyethylene glycol
PET	Polyethylene terephthalate
pEVOH	Plasticized EVOH
PHA	Polyhydroxyalkanoate
PHB	Polyhydroxybutyrate
PHB-g-AA	Acrylic-acid-grafted PHB
PHBV	Poly-(3-hydroxybutyrate-co-3-hydroxyvalerate)
PLA	Polylactic acid
POE-g-GMA	Glycidyl methacrylate-functionalized polyolefin elastomer
POE-g-MAH	Maleic anhydride-grafted ethylene–octene copolymer
PPG	Poly propylene glycol
PS	Polystyrene
PVA	Polyvinyl alcohol
PVC	Polyvinyl alcohol
SEM	Scanning electron microcopy
SF6	Sulfur hexafluoride
SME	Specific mechanical energy
SNC	Starch nanocrystal
SO	Soybean oil
SSE	Single-screw extruder
TA	Tartaric acid
TBC	Tributyl citrate
TBoAC	Tributyl o-acetylcitrate
T_d	Decomposition temperature
TEC	Triethyl citrate
T_g	Glass transition temperature
T_m	Melting temperature
TOMC	Oxidized MCC
TPS	Thermoplastic starch
TS	Tensile strength
TSE	Twin-screw extruder
U	Urea
UM	Urea-intercalated montmorillonite
VAc	Vinyl acetate
WC	Water content

WF	Wood fiber
WS	Water sorption
WSNC	Waxy starch nanocrystal
WVP	Water vapor permeability

1   Introduction

The market for plastic materials and products faces the challenge of increasing demand for materials with higher performance and new functionalities with focus on both, biobased and biodegradable polymers as alternatives to the non-biodegradable plastics produced from fossil resources. Bioplastics can be classified into three main groups: (1) biobased, non-biodegradable materials (bio-PE, bio-PET and bio-PEF), (2) biobased and biodegradable materials (TPS, PHA, PHB, PLA), and (3) fossil-based and biodegradable materials (PBAT, PCL, PVA, mostly blended with group 2). Their input to sustainability contributes to lower carbon footprint, high recycling value and complete biodegradability/compostability [1]. The development of sustainable bioplastics made of either biobased or biodegradable polymers and the principles of the circular economy opens new opportunities to alleviate the intensive use of non-renewable sources, innovation, competitiveness, new more qualified jobs and plastic pollution [1]. In this context, global bioplastics production capacity is set to increase from around 2.11 million tonnes in 2019 to approximately 2.43 million tonnes in 2024, according to the latest market data compiled by European Bioplastics and the research institute nova-Institute [2].

Among bioplastics, starch has been widely studied for a longtime since it is an inexpensive, renewable, versatile, fully biodegradable and widely available raw material. Starch and its blends account for over 38% of the global biodegradable plastic production capacities (Fig. 1). Today, bioplastics can be used in almost all market segments and applications, but each polymer has main application fields. The fields of starch-based materials' greatest application are flexible packaging and agri- and horticulture [2]. Since starch sources, availability and structure have been discussed in many reviews as well as chapters, particularly during the last two decades, they are not going to be detailed in this chapter [3, 4].

Before being thermally processable as thermoplastic polymers, starch must be transformed into thermoplastic *starch* (TPS) by the addition of plasticizers combined with the application of elevated temperatures and shear forces. Although the clear advantages of using starch-based plastics for a sustainable development, their application is still restricted by many factors. TPS great sensitivity to water, low moisture barrier capacity and poor mechanical properties are considered as major drawbacks when compared to conventional plastics.

The addition of organic and inorganic fillers of a different nature is an efficient way to improve the performance of TPS, and some may even grant unique properties to be used in new and demanding applications. Moreover, blending TPS with other
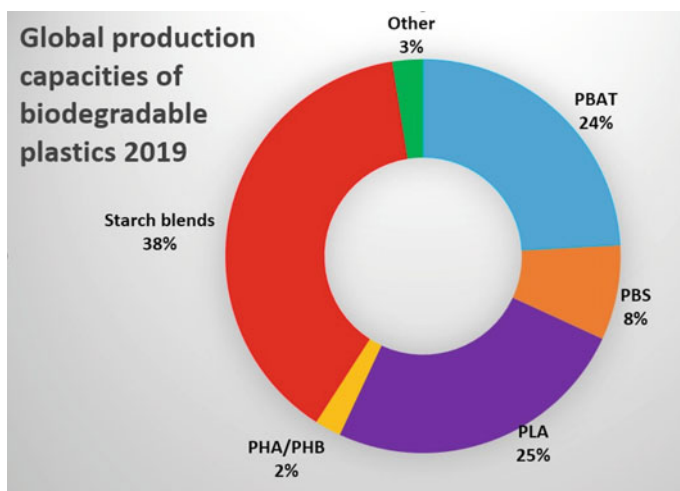
Fig. 1 Global production capacities of biodegradable plastics in 2019. *Source* European Bioplastics, nova-Institute (2019). Figure drawn by the authors

biopolymers to develop starch blend composites could bring their properties closer to those of conventional non-biodegradable plastics. A careful choice of blending polymer should be made according to the pretended application. Among biodegradable polymers, polybutylene adipate-co-terephthalate (PBAT) and polyhydroxybutyrate (PHB) have the important advantage of being biodegradable in soil. Both polymers are very stable in water due to their hydrophobic character. PHB has higher modulus and stress at break than starch but a very low elongation at break, while PBAT has higher stress at break values than that of starch and deformations at break as large as 700%, which makes it an ideal material for different applications, particularly in agriculture as mulching. One of the main drawbacks of both polyesters is their high production cost, being higher in the case of PHB. On the other hand, PBAT has the extra disadvantage of coming from fossil resources. Blending them with starch is an effective way to lower the final cost of the PHB or PBAT blends and increase the biobased character of PBAT. Moreover, the inclusion of fillers to develop starch/PHB and starch/PBAT composites could lead to superior properties. However, this poses a series of challenges to be solved mainly due to the incompatibility between polymers as a consequence of the strong difference in their polarity. While several researches that focus on the study of starch/PBAT blends can be found in the literature, there are far fewer that deal with TPS/PHB blends, possibly due to the higher cost and lower world production of the latter.

Expectations of achieving a green starch-based composite using blends with other polymers and the addition of nano-microfillers grow day by day and have already materialized in the form of commercial products, such as bags, disposable tableware and mulching. However, the costs of these products are still high compared to those of traditional plastics.

In the next sections, processing strategies for filler incorporation into starch-based composites will be described. Starch and starch blend matrices will be studied separately since different challenges are faced in each case. Then, these composites will be described from a point of view of their thermal, barrier and mechanical properties, again distinguishing between TPS and starch blend matrices. Finally, the main conclusions obtained are listed, as well as future perspectives of these materials.

2 Processing of Starch-Based Green Composites

2.1 Processing of Starch Matrix Composites

2.1.1   Usual Strategies for Processing Starch

Like most materials, polymers must be melted or solubilized, with the objective to transform them into different kinds of products with specific properties and shape. The most common ways to process polymers include extrusion, blowing, meltblown, spunbond, thermoforming and injection. The method chosen for the processing of a material will be decisive in its final properties.

Processing starch by the techniques usually used in the plastic industry is extremely complicated. Conventional equipment was designed to work with thermoplastic materials such as PE, PET, PVC or PS. Starch is not a thermoplastic, but with favorable processing conditions and proper formulation development, it can become this type of material [5, 6]. However, thermoplastic starch (TPS) processing has several additional problems, as a consequence, for example, of its high molecular weight or poor melt tenacity [7].

The melting temperature (T_m) of dry starch is generally higher than its decomposition temperature (T_d), which makes the incorporation of plasticizing agents necessary to convert it into a thermoplastic material and thus allow its processing. Although the incorporation of water is a usual strategy, for many industrial processing techniques high water content (WC) is a problem. The solution casting technique involves large amounts of water, and for that reason, it is called wet method. It is one of the most widely used techniques at laboratory scale since it is extremely simple, but as it involves drying times that are too long to permit large-scale manufacturing, it cannot be carried out at industrial scale. In this chapter, we will focus on the so-called dry methods that involve shear conditions and therefore require a lower WC in comparison with the wet process techniques, making them applicable on an industrial scale. In particular, to produce TPS from starch and plasticizers, the most widely used industrial technique is extrusion. Other usual techniques for polymer processing, such as injection, blowing or compression molding, can only be performed on thermoplastic materials. Therefore, in order to process starch in these ways, it must be first extruded together with plasticizers to become TPS.
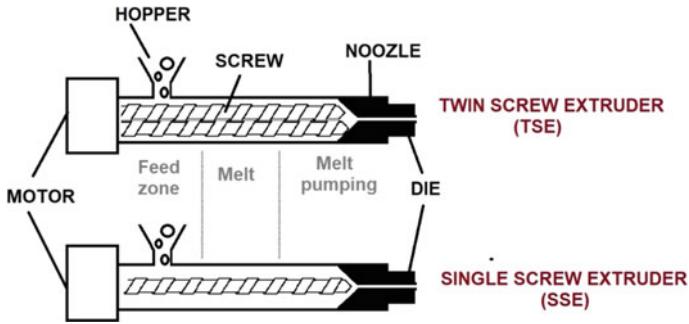
Fig. 2 Cross-sectional diagrams of a single- and a twin-screw extruder. Figure drawn by the authors

Extrusion combines high shear, temperature and pressure to break down starch granule structure, facilitating the diffusion of the plasticizers and the subsequent melting of the new blend, generating TPS. During this process, multiphase transitions occur such as gelatinization, granule expansion, melting and decomposition [8, 9].

In general form, an extruder consists of a hopper, barrel, feed screw, thermocouples and dies. There are two different extrusion equipment designs: the single-screw extruder (SSE) and the twin-screw extruder (TSE). Cross-sectional diagrams of a single- and a twin-screw extruder are shown in Fig. 2. While single-screw extrusion is ideal to produce basic and simple compounds, corotating twin-screw extrusion is better for composites which require a relatively high level of mixing in the extruder and flexibility during the process [10, 11]. Moreover, TSEs have a large operational flexibility (individual barrel zone temperature control, multiple feeding/injection ports and diverse screw configurations for different degrees of mixing/kneading). In both SSE and TSE, residence times and specific mechanical energy (SME) inputs can be controlled, achieving highly efficient production. It is worth noting that, as TSE's screws have a self-wiping ability, they are more suitable to process raw starch powder than SSEs, which may encounter the problem of conveying the starch powder at the feeding port [6].

Both the equipment configuration and its operating conditions, such as temperature profile and screw speed, will be decisive in achieving mechanical disruption and starch transformation [8, 12]. SME is the amount of mechanical energy (work) dissipated as heat inside the material, expressed per unit mass of the material. It can be calculated as

$$\mathrm{SME} = \frac{P \times \tau \times \mathrm{RPM_{act}}/\mathrm{RPM_{rated}}}{m}$$

where P is the motor power, expressed in kW, τ is the difference between the running torque and the torque when the extruder is running empty divided by the maximum allowable torque, $\mathrm{RPM_{act}}$ is the actual screw rpm, $\mathrm{RPM_{rated}}$ is the maximum allowable screw rpm and m is the mass flow rate of the system (kg/s) [13]. During TPS extrusion,

mechanical energy must be enough to break starch grains and efficiently complete its extrusion process. Different authors studied how operating parameters influence on SME [8, 14].

Ahead of the extruder's screw barrel, a die system produces shaped products to facilitate further product processing and/or to determine the properties of end products.

Sheet products can be obtained through continuous extrusion of the TPS melt through a horizontal or plate die. The uniformity of the final sample thickness and of the exit velocity distributions across the width of the die exit must be guaranteed by the design of the die [10]. Different authors used this type of die to obtain band-shaped sheets of starch and starch-based composites after extrusion [14, 15]. However, the obtained materials are usually too thick for many applications (more than 0.5 mm).

Other possibility is that the die extrudes single or multiple strands which can be cut into pellets once dried. A schematic drawing of a strand pelletizer is shown in Fig. 3. Strand extruding and pelletizing is a simple and straightforward process, but an extra step to obtain sheets or films is necessary. Generally, strands obtained from the extruder are pelletized and these pellets are converted into films through other processes such as thermocompression or single-screw extrusion followed by blowing. Many authors choose to manufacture TPS pellets using a twin-screw extruder, pelletize TPS strands and subsequently obtain films by thermocompression. For example, González-Seligra et al. [8] obtained different threads of TPS by TSE varying the screw speed used. Then, pellets from each system were obtained by the pelletization of the threads using an automatic pelletizer. TPS films were finally prepared by thermocompression using a thermostatized hydraulic press in two stages: First, pellets were heated to 140 °C for 15 min, then, pressure was
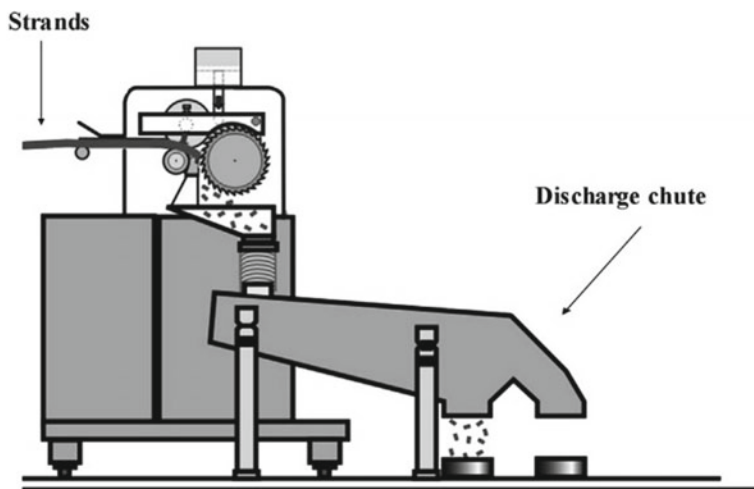
Fig. 3 Schematic drawing of a strand pelletizer. Reprinted from Drobny [18], "Processing Methods Applicable to Thermoplastic Elastomers", 33–173, Copyright (2014), with permission from Elsevier

increased to 56 kPa and temperature decreased up to 40 °C. The resultant film thickness was approximately 0.3 mm. Similarly, Estevez-Areco et al. [16] used extrusion followed by thermocompression, but in their case, they developed bioactive starch composites with antioxidant activity. They used a thermo-stated hydraulic press to convert the thermoplastic threads into films. Basically, they placed a piece of thread between Teflon sheets and heated to 130 °C for 15 min. Pressure was then increased to 45 kPa and maintained for 15 min. Finally, temperature was decreased to room temperature while keeping the pressure constant. Gutiérrez et al. [17] also prepared bio-nanocomposite films by twin-screw extrusion followed by thermo-molding, in this case from corn starch and pH-sensitive nanoclays packaged with Jamaica flower extract. After extrusion, the strands were pelletized using an automatic pelletizer and pellets were hot-pressed using a hydraulic press at 120 °C and 1×10^4 kPa for 20 min, after which a cooling cycle was applied until they reached a temperature of 30 °C.

The most common method for making plastic films, particularly for the packaging industry, is blown-film extrusion. In this process, a SSE coupled to a blower is used (Fig. 4). At the exit of the extruder, the blower has a first stage in charge of transforming the melted TPS into a hollow tube. As the tube is extruded, it expands due to a pressure increase produced by the blower. The ability to process a system by this technique will depend on the tensile properties of the melt. The melt tenacity of TPS, understanding this as the ability of the melt to deform without rupture, is not usually enough to be processed by this methodology. Thunwall et al. [19] studied possible routes for film-blowing TPS on a laboratory scale by a suitable choice of processing conditions, amount of glycerol and moisture content, finding that the
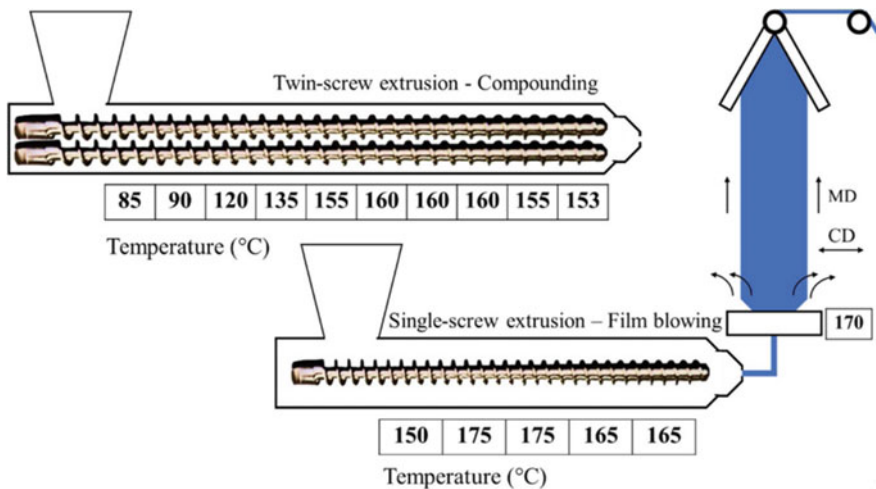
Fig. 4 Diagram of the process to obtain acetylated cassava starch composite films with pea protein isolate incorporation through blow molding, including temperature profiles. Reprinted from Huntrakul et al. [25], Copyright (2020)

possibility of obtaining films was given in a too narrow processing window. The difficulties encountered were mainly related to a sticky surface of the film, insufficient tenacity and foaming. Even in the cases in which they managed to obtain films, their final properties were poor. Several studies have explored the film blowing of starch-containing materials, introducing moderate quantities of starch (between 8 and 30 wt%) in a regular synthetic polymeric system [20, 21, 22] or developing blends with biodegradable polymers, such as poly(vinyl alcohol), poly(caprolactone) or other polyester [23, 24]. In the case of regular synthetic polymers, starch gives them the enormous benefit of its biodegradability, although it worsens its mechanical and water barrier properties. In the case of blends with other biodegradable polymers, the main benefit is economical, thanks to the low cost of starch. Other strategies to improve the melt tenacity of thermoplastic starch and allow its processing through blow molding are the development of composites. Huntrakul et al. [25] obtained acetylated cassava starch composites with pea protein isolate incorporation using a twin-screw extruder. Pellets obtained from the extruder were dried in a hot air oven at 60 °C overnight, and films were produced using a single-screw blown-film extruder connected to an annular ring-shaped film-blowing die. Temperature profiles used are shown in Fig. 4. The incorporation of pea protein isolate helped to avoid stickiness and improve processability during the blown extrusion. Moreover, the high structural deformation shown by acetylated starch films during storage was effectively prevented by pea protein isolate incorporation. Dang and Yoksan [26] improved blown-film extrusion processability of TPS films by incorporating low contents of plasticized chitosan (0.37–1.45%). The composite was extruded and pelletized, obtaining pellets which were blown into films using a single-screw extruder with an L/D 30:1, a screw diameter of 25 mm and four controlled temperature zones, connected to a film-blowing attachment with a ring-shaped die. Screw speed and nip roll speed were adjusted to 35–45 rpm and 3 rpm, respectively, while the barrel temperature profile was maintained at 130–140–140–140 °C (from feed inlet to die) and the die temperature was set at 150 °C.

Injection molding is another typical technique for thermoplastics processing, where the polymer is fed into a heated barrel, mixed (using a helical-shaped screw) and injected into a mold cavity, where it cools and hardens to the shape of the cavity. The behavior of starch during injection molding and the processing parameters have been studied by different authors during the last decades [27, 28, 29]. TPS high viscosity and poor flow properties make the application of this methodology complex [6]. Besides, TPS injection molded parts have problems related to its serious distortion and shrinkage. The only way to avoid shrinkage in hydrophilic polymers is to process them so that the products are formed at approximately the equilibrium in-use water content. For potato starch, for example, this would be water contents of around 14% used under ambient conditions. If higher contents are involved as plasticizer, the material will deform, as the equilibrium is naturally achieved after processing [29]. There are commercial products based on starch that can be injected without problems. The first commercial products made of injected molded TPS were starch capsules designed for drug delivery (Capill®). Other developments include blends of starch with eco-friendly polymers that allow to improve not only the processability

but also the final properties of the materials, such as the case of the Mater-Bi®, which is offered in molding pellet presentations.

Besides processing starch to produce TPS, extrusion can also be used for its chemical modification, addition of cross-link agents or copolymer creation in a continuous process with a more consistent product quality. Inside the extruder, very efficient mixing processes of highly viscous liquids are produced, which allows starch modification to be performed in a homogeneous medium. This methodology, called reactive extrusion, is one of the typical methods in the industrial modification of starches due to the aforementioned advantages, added to its low cost. It should be mentioned that for some particular processes special equipment designs are needed.

Ye et al. [30] synthesized citric acid-esterified rice starch using a one-step reactive extrusion method. They dissolved citric acid in distilled water and slowly added the solution to the rice starch. After equilibration in sealed bags, reactive extrusion was performed using a twin-screw extruder. The four sections of the extruder were set to 80–100–90 and 75 °C, the feed rate was 18 kg/h, and the screw (30 mm in diameter, L/D 16:1) speed was 250 rpm. The starch citrate extrudates were collected as powder, dried in an oven until constant weight at 45 °C and sieved through an 80 mesh sieve. Finally, it was washed with absolute ethanol to remove unreacted citric acid. This method to modify starch chemical structure has advantages over conventional methods because it can be carried out rapidly using a continuous process. On the other hand, Siyamak et al. [31] developed a method of synthesis based on reactive extrusion combining the benefits of continuous manufacturing with the use of green chemistry principles. They grafted four different types of starches with acrylamide monomers via free radical copolymerization using a 16-mm corotating twin-screw extruder, with a horizontally split barrel of 40:1 L/D comprising 10 barrel sections with independent temperature control zones. They designed an experimental set consisting of three different phases. The initial phase was finding optimum conditions for the gelatinization of starch using extrusion processing. The second phase involved the transfer of these optimized formulations and conditions to the development of the copolymers. Nitrogen gas was used in all experiments to eliminate oxygen from the extruder, while deionized water and acrylamide (50 wt%) solutions were sequentially injected into the barrel sections 1 and 2, followed by ammonium persulfate (5 wt%) solution, which was injected into the barrel sections 5 and 7 using peristaltic pumps. Figure 5 shows the screw profile used. Finally, the third phase consisted in
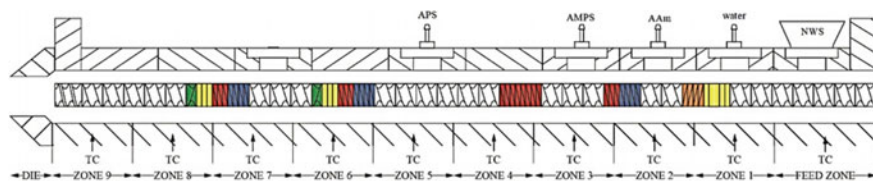
Fig. 5 Screw profile for reactive extrusion of starch copolymers. Reprinted from Siyamak et al. [31], Copyright (2020)

preparing the graft copolymers of other types of starches using the optimized conditions identified in the previous phases. The botanical origin of the starch determines the relationship between the amount of amylose and amylopectin, and the type of crystal structure. This establishes the temperature profile necessary for extrusion, as well as the efficiency and type of grafting that can be performed. Since extrusion is currently applied for large-scale manufacturing of starch-based commodities, the modification method they propose could lead to the successful production of complex smart systems based on starch-grafted copolymers.

2.1.2   Filler Incorporation During Starch Matrix Composite Processing

There are different strategies to incorporate fillers throughout the processing of composites. The final objective is to obtain a proper dispersion of the filler in the matrix, what will depend not only on the processing but also on their chemical similarity, filler's morphology and surface area [32].

One of the main factors to consider when deciding how to introduce a filler during composite processing is the chemical affinity between it and the matrix, and what interactions are expected to occur. Depending on the filler–matrix compatibility, different effects will be produced in the matrices. When the filler and the matrix are compatible and interactions between them enhance adhesion, several improvements can be achieved. For example, a good stress transfer between the matrix and the filler will occur, so that, if the filler is more rigid than the matrix, the composite will have greater Young's modulus and stress at break than the matrix material. Thermal stability, water resistance and degradation behavior can also be improved due to high compatibility and strong bonds between filler and matrix. Ilyas et al. [33] demonstrated these effects by incorporating nanocrystalline cellulose (NCC) as a reinforcing filler into sugar palm starch matrices and attributed them to the excellent compatibility achieved thanks to the presence of abundant hydroxyl groups on the NCC surface which can interact through hydrogen bonding with the hydrophilic polymer matrix.

However, on occasions fillers that are not naturally compatible with the starch matrix are used as reinforcements. In these cases, different processes can be carried out to improve filler dispersion. One possibility to incorporate a hydrophobic filler into a starch matrix is to encapsulate it. Moreover, this methodology can also provide the filler protection from temperature and stress generated during processing, as well as modulate its release kinetics in the case of active compounds [34]. Different techniques have been proposed for micro- and nano-capsule preparation and incorporation into starch matrices.

The most commonly used technique at industrial level for microencapsulation is spray-drying. In this technology, a dry powder is produced from a liquid or slurry by rapidly drying with a hot gas. The choice of the shell materials used for the encapsulation of actives is determinant in the active load of spray-dried microparticles. Talón et al. [35] employed whey protein and soy lecithin as wall materials together with maltodextrin as drying coadjuvant and oleic acid as a carrying agent,

for the production of microencapsulated eugenol through spray-drying. Different encapsulated eugenol powders were obtained by using a spray dryer with a rotary atomizer at an inlet air temperature of 180 °C. These microcapsules exhibited a mean particle diameter of around 15 µm, regardless of the wall material, and a very small percentage of finest particles (0.5 µm). To develop composite films, a pre-mixture of the starch, microcapsules and glycerol using a starch:microencapsulate powder:glycerol mass ratio of 1:0.35:0.3 was obtained in a two-roll mill at 160 °C and 12 rpm for 10 min. The obtained pellets were process through compression molding using a hot-plate press in order to obtain films. The functional properties and the release kinetics of the final materials were evaluated. They found that the incorporation of the carrying agent (oleic acid) was essential for the protective effect of microcapsules during film processing. Other possibility is to use modified starches as the shell material. Octenyl succinic anhydride-modified starch (OSA starch) is widely used in the microencapsulation of oil-soluble nutrients, flavors, agrichemicals, fragrances and pharmaceutical actives, thanks to its hydrophobic character [36]. In spray-drying microencapsulation, modified starches offer high oil retention, long shelf life and high manufacturing efficiency [37]. Figure 6 illustrates the morphological evolution of an emulsion droplet in a highly dynamic spray-drying process, together with the SEM images of spray-dried microcapsules and the cross section of a microcapsule [37].

Extrusion process can also be used for encapsulation of different agents. As it was mentioned before, during TPS extrusion starch and plasticizers are converted into a homogenous molten state, involving various structural changes, such as granule disruption, crystal melting and molecule entanglement. This molecule entanglement can be exploited for the incorporation and sustained release of the filler to be encapsulated. Several authors have used starch in extrusion encapsulation due to its ability to form stable inclusion complexes with the encapsulated agents [37–40]. Chen et al. [39], for example, presented a simple preparation of microparticles with extruded starch as the shell material, resveratrol as the core material and the thermostable α-amylase as the release-improvement reagent of resveratrol. They extruded a mixture including 10 kg of corn starch (water content was adjusted to 24%), 10 g of resveratrol and 5 g of α-amylase with 65 °C barrel temperature (50–55–60–65 °C for the four parts starting from the feed part) and 110 rpm screw speed. The extrudate was smashed by using ultra-micro-pulverizer, and microparticles with 0.15–1-mm diameter were selected. Modified starches have also been proposed for extrusion encapsulation, being CAPSUL® (product of Ingredion) a preferred choice due to its low viscosity [37].

Other possibility to encapsulate agents is through the formation of complexes with amphiphilic molecules, such as cyclodextrin. This molecule is an enzymatically modified starch which has a truncated cone shape with a hydrophobic interior, allowing the formation of an inclusion complex with oils that protects them against harsh temperature and shear conditions during extrusion [41].

The way in which the filler is incorporated into the starch matrix during processing will be highly influential in the filler's degree of dispersion, filler–matrix interaction and specific filler arrangement in the starch matrix for both, hydrophilic
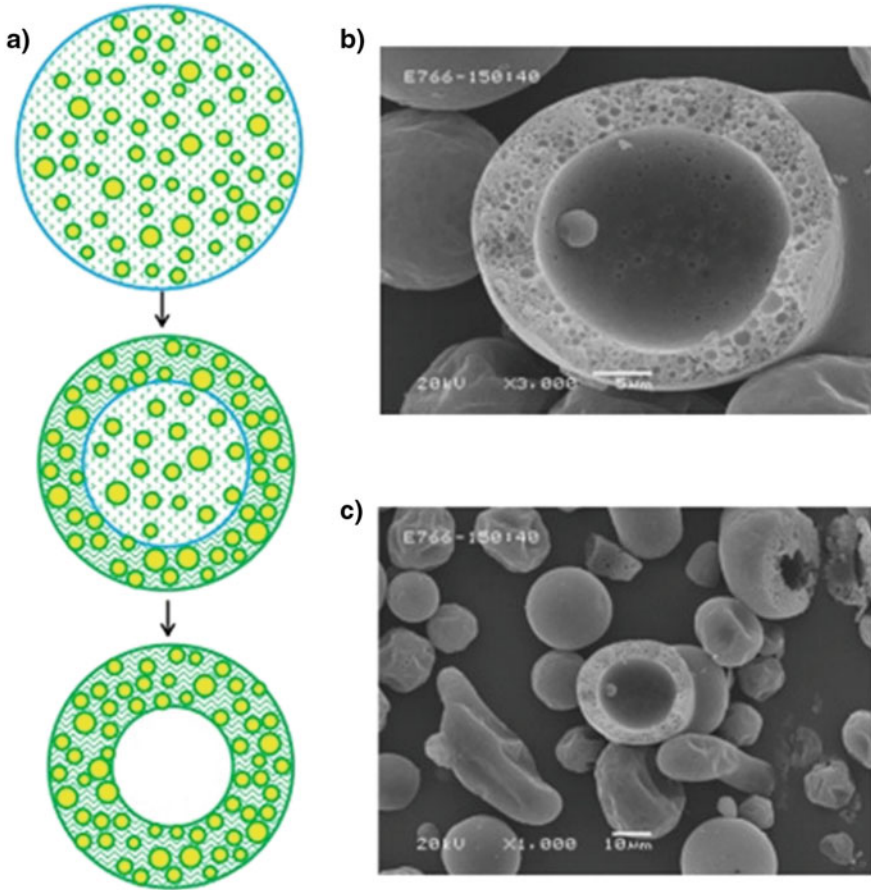
Fig. 6 a Schematic illustration of spray-drying dynamics. The big circles represent atomized water droplets, small circles represent oil droplets, and dots represent soluble carbohydrate molecules. **b** Scanning electron microcopy (SEM) images of spray-dried microcapsules and **c** the cross section of a microcapsule. Reprinted from Jin et al. [37], Copyright (2018)

and hydrophobic fillers. One possibility when producing starch-based composites through extrusion is to introduce the filler in the extruder barrel together with starch, plasticizers and/or other components. As the active compound is added at the beginning of the extrusion process, in this option, temperature and wear sensitive molecules, such as flavors, are more likely to be degraded being necessary to previously encapsulate them [38]. In the case that fillers support the temperature profile and shear stresses inside the extruder, a usual procedure is to carry out a premixed step to guarantee a proper dispersion. This is the case of Ochoa-Yepes et al. [42] who mixed cassava starch, glycerol, water and a desired amount of lentil proteins at 20 rpm for 15 min in a horizontal mixer. Mixtures sieved with a number 10 mesh were stored for 24 h in sealed containers and then extruded in a corotating twin-screw extruder at

a screw speed of 80 rpm (with feeding rate of 12 g/min) and temperature profile (from the feeder to the die) of 90–100–110–120–130–130–140–140–130–120 °C. Ghanbari et al. [43] also performed a premix, but in their case it was made manually. They mixed corn starch and glycerol in polyethylene bags for 5 min, and subsequently, the resulting blend was further mixed with the corresponding amount of cellulose nanofibers for more than 10 min. Dean et al. [44] explored three different dispersion methods to develop clay–starch mixtures before the extrusion process. Nanoclays were either dry blended with starch in a high-speed mixer (HSM); dispersed in water using conventional mixers prior to blending with starch in a HSM; or dispersed in water using ultrasonics prior to blending with starch in a HSM. All mixtures were later processed through a corotating twin-screw extruder, with diameter 30 mm and L/D 40:1, using a profile producing a melt temperature of 110 °C. They demonstrated that when the level of clay, water and starch was optimized an exfoliated structure was produced via standard mixing which exhibited comparable improvements in mechanical properties to ultrasonically treated samples.

Some authors propose to perform a double extrusion in order to enhance the filler dispersion, although this is not the most common methodology. For example, Chaves da Silva et al. [45] obtained starch films with different percentages of gelatin using a single-screw extruder in two stages. In the first stage, the starch, gelatin and a plasticizer were mixed manually and extruded to produce pellets; in the second step, the pellets were extruded to produce the films. The screw (diameter of 25 mm) speed was 30 rpm, and the zone temperature was set between 90 and 120 °C in the four heating zones for the two stages. Huang et al. [46] proceeded similarly by first extruding glycerol and corn starch to obtain small particles of TPS, which were later mixed with montmorillonite (MMT) and fed into the single-screw plastic extruder again. The temperature profile along the extruder barrel was 110–115–120–120 °C (from feed zone to die).

In some cases, for TPS extruded films a preliminary gelatinization is produced by heating a mixture of starch, distilled water and the desired plasticizer. One option for filler incorporation is to add them to the obtained gel and homogenize it. This is the case of González et al. [47], who added polysaccharide nanocrystals dispersed in distilled water by ultrasonication to a gel composed of corn starch, glycerol and water. The material was freeze-dried, then extruded using a MiniLab extruder at 120 °C and 50 rpm and pelletized. The obtained pellets were compressed at 120 °C for 5 min without pressure and 120 °C under a pressure of 2.5 t for 5 min. This work is an example of the importance of a previous mix step with high shear stresses, necessary to process this type of composites with a single-screw extruder.

Other possibility, which is recommended by some extruder's manufacturers, is the direct injection of fillers into some middle barrel section of the extruder. This approach is usually used for the addition of volatiles that can be lost due to high temperatures [38]. Basically, in the feeding section on the extruder, starch and plasticizers are metered and conveyed into the first mixing zone, where thanks to the heat and shearing, the mixture is transformed into TPS melt. In a secondary feed zone, the filler is added by means of a liquid feeding pump, reaching a further mixing zone where it is dispersed and evenly distributed into the matrix.

In most cases, the fillers are introduced at some stage of the extrusion process with the sole objective of being mixed under processing conditions that allow them to maintain their structure and properties throughout the entire process. In other cases, the extrusion process also serves as a treatment for tailoring the final properties of the filler. Such is the case of Fourati et al. [48] who produced nanocomposites based on TPS filled with cellulose nanofibrils (CNFs) in a single step by twin-screw extrusion of corn starch granules, glycerol and oxidized cellulose fibers. CNFs were produced in situ during the processing of the nanocomposite. For the extrusion process, starch granules, glycerol and fibers containing 50 wt% water were premixed manually. The mix was continuously extruded using a corotating conical twin-screw extruder at 100 rpm during 15 min at a temperature of 25 °C. Temperature was progressively increased during 10 min up to 110 °C, and the extrusion was completed at 200 rpm during 15 min to complete the gelatinization of starch and the breakdown of fibers. These nanocomposites displayed a higher strength and similar transparency degree than those produced by incorporating readily prepared CNFs.

Other processing techniques such as compression molding also offer the possibility to simultaneously process the TPS composite and modify the filler. Grylewicz et al. [49] manufactured TPS composites from potato starch, wood fiber (WF) and deep eutectic solvent (DES) based on choline chloride with urea or glycerol (Gl) as well as imidazole (Im) with Gl. The processing method included a first stage of component mechanical mixing followed by thermocompression with simultaneous WF modification. They found that DES played a triple role as starch plasticizer, as WF surface modifier and as composite component interfacial adhesion improver.

Beyond good compatibility and good dispersion, the way in which fillers are oriented within the polymeric structure will also be decisive on its final properties [50]. In the case of layered silicates, the clay platelets can be either intercalated by macromolecules and/or exfoliated, depending on the processing conditions and on the matrix–filler affinity. The best performances are commonly observed with exfoliated structures in which the clay platelets are individually delaminated and fully dispersed into the polymer matrix [51]. Different strategies have been performed to achieve these structures. For example, Adamus et al. [52] explored the possibility to modify montmorillonite through intercalation with urea. They mixed urea and montmorillonite (1:1 weight ratio) with different amounts of distilled water (0.15, 0.20 or 0.30 g H_2O/1 g M) using a laboratory mixer to obtain a homogenous material, which was subsequently extruded with an Eurolab digital laboratory extruder (L/D 40:1, screw diameter 16 mm). After extrusion, the material was dried for 2 h at 105 °C and then turned into a fine powder with mortar and pestle. The obtained powder was mixed together with starch, water and deep eutectic solvents that acted as plasticizers using laboratory mixer (25 °C, 350 rpm). After mixing, the compositions were extruded using a twin-screw extruder. The obtained extrudate was turned into 3-mm diameter pellets which were finally pressed between Teflon sheets using a hydraulic press for 5 min, at 140 °C, under pressure of 6 tonnes to obtain films. Results from the film characterization showed that an intercalated structure of MMT sheets was obtained. It must be mentioned that the inclusion of these fillers had an important effect in the processing of the material. The authors found that MMT presence helps

polymer flow through the extruder die as it decreases melt viscosities of TPS. These could be explained in terms of a limitation of polymer chain entanglement caused by intercalated clay particles. This leads to lower energy dissipation in composite materials compared with neat polymer melt and, therefore, easier movement of polymer chains. This approach results promising in the development of new starch composites, which could be easier processed by melt processing (extrusion, extrusion with film blowing, injection molding or thermocompression).

2.2 Processing of Starch Blend Matrix Composites

2.2.1 Usual Strategies for Processing Starch Blend Matrix Composites

Blending different polymers constitutes a simple and effective approach and gives the possibility to improve material or product performance, with the desired properties at a lower cost, compared to the synthesis of a new polymer. For example, through mixing technology, it is possible to improve polymer modulus and dimensional stability by blending with a more rigid and more heat-resistant polymer. In addition, it is possible to design a compounding strategy to rebuild molecular weights of partially degraded polymers, thus to produce articles from scrap or post consumer plastics. Another important advantage of polymer blending is the improvement in the processability of plastics. For example, it is possible to process a high glass transition temperature (T_g) polymer at a temperature below the thermal degradation limit by blending with a miscible polymer of lower T_g. A reduction of the pressure drop can be achieved through the incorporation of an immiscible polymer of low viscosity, thus increasing productivity. Blending allows scrap reduction and rapid change in formulations giving rise to greater adaptability and flexibility in production and market demands [53].

The performance of polymer blends depends strongly on the final morphology achieved. The morphology of immiscible polymer blends is defined by the concentration of the blended components, phase identity, viscosity ratio, compatibility and interfacial tension between components, and finally, by the processing conditions [54]. That is, in the case of polymer blends, studying the behaviour at the interface as well as the rheological response results of great importance to understand the final material'The thermal properties of starch/PHB performance [55].

As it was previously mentioned, TPS is a biobased, biodegradable and cost-effective polymer, although it cannot meet all the application requirements in terms of processability, mechanical properties and durability [56]. Its strong inherent sensitivity to moisture, high water absorption capacity and low water resistance lead to a decrease in the barrier and mechanical properties that limits its applications [57]. Many studies have been conducted to evaluate the feasibility of combining TPS with hydrophobic biodegradable polyesters, with the aim of improving its physical properties and processability [58–60]. According to Muthuraj et al. [54], the main challenges with polymer melt blending are the improvement of adhesion between

components, the reduction of interfacial tension between them and the generation of limited inclusion phase size. In this context, the addition of a reactive coupling agent or a compatibilizer is a prerequisite to improve interfacial adhesion and therefore the final properties of the blend.

The key to optimizing polymer blend performance is to control the morphology achieved after processing, as the development of a specific morphology will give rise to the desired properties [53]. For example, to optimize the material impact strength, a matrix/dispersed phase morphology is desirable, while co-continuity is expected to yield a better stiffness/ductility balance. Optimized properties, therefore, result from the proper equipment design selection, the strict control over processing conditions and the methods of generating and stabilizing the morphology, such as reactive compatibilization and the addition of coupling agents [53]. The material characteristics, such as bulk, rheological and thermal properties, have a significant impact on processing [53]. Biobased and biodegradable polymers can be processed using conventional techniques such as injection molding, extrusion and compression molding. Special attention must be paid due to their hygroscopic characteristics. Unlike starch, PHB and PBAT need to be dried before processing to avoid a drop in molecular weight and melt viscosity due to hydrolytic degradation. Furthermore, processing should be performed under controlled humidity to reduce the potential for flashing and brittle products [61]. Drying temperature and time conditions must be optimized for each material, especially when blending different polymers. The processing window of biobased and biodegradable polymers is usually narrower than most of the commodity plastics. Hence, the processing temperature profile must be designed and optimized for each system. High temperatures, the development of high shear stresses and high residence time during the process, are not desirable and can lead to polymer degradation [53, 61]. The forming stage often has a dramatic influence on the final morphology. Thus, the type of processing technology used, the equipment design and the processing conditions will determine the final morphology. During processing, the material undergoes complex deformation (e.g., elongational flow, uniaxial orientation, contraction) that affects the morphology and, thus, the material's final properties. Therefore, tailoring polymer blends for specific applications requires control of the morphology through tighter control over processing parameters [53].

Other useful strategy to improve polymer compatibility is the addition of a suitable filler which can improve interfacial adhesion between polymer phases due to preferable localization at the interface. Moreover, the addition of natural fillers can enhance the final performance of polymer blends, reducing the overall material cost and ensuring the total biodegradability of the material [62]. As in the case of neat TPS matrices, improvements in mechanical, thermal and barrier properties can be obtained when uniform filler distribution in the blend-polymer matrix is achieved. The challenge is to create a favorable interaction between the polymers and the filler, and thus avoid phase separation and agglomeration of the filler particles [63]. Polymer composites can be obtained by three different methods, in situ polymerization, melt mixing and solvent casting. Melt mixing, using conventional extrusion or injection molding technologies, is the most common method for preparing

thermoplastic-based composites at large scale [62]. When adding a filler to polymer blends with a different molar mass and viscosity, selective localization of the filler can be achieved. The preferred localization is mainly driven by thermodynamic (viz., enthalpic interaction between each polymer and particles) and kinetic factors (i.e., viscosity ratios of the two polymers). Hence, micro- and nanofillers may result in localization of the filler within different polymeric phases, specific polymeric phases and/or at the interphase [64–66]. Thus, the final properties of biocomposites can be adjusted by controlling the filler location, its distribution and the adhesion between both polymers and with the filler [66].

Melt mixing provides a high shear force method to promote dispersion and distribution of the micro- and nanofillers, providing large-scale mass production. Adjusting processing conditions such as order of mixing, mixing time and shearing forces may result in an adequate strategy to promote the desired filler location and distribution in the polymer blend. Enough shearing force and residence time must be chosen to facilitate the migration of the particle from the preferent polymeric component to the less compatible phase. If processing conditions are not enough to allow the particle to move from one polymeric phase to the other, particles will be located as a function of the shear stress and time in any of the polymers in the mixture or the interface [66]. Different mixing strategies have been described. They depend on the polymers and filler characteristics, as well as on the versatility that the processing method can offer. Simultaneous mixing of all the components and its subsequent incorporation to the processing equipment, and the addition of particles to the molten blend where polymer pairs have already been mixing for some time are the most common strategies used. In more complex systems, premixing fillers with a component that is thermodynamically preferred (or not) is the recommended choice to promote further interaction between them [66].

In addition, chemical structure and viscosity of blends may negatively affect the dispersion of fillers (usually hydrophilic and with a great tendency to agglomerate), decreasing the ultimate mechanical properties of the composite. Different methods have been proposed to overcome these issues, such as the chemical modification of fillers to decrease their inherent hydrophilicity, chemical modification of polymers and the incorporation of a suitable compatibilizer [62, 63].

There are many studies focusing on the development of green composites based on starch combined with other biobased/biodegradable polymers reported in the literature. The most common are polycaprolactone (PCL), which is incorporated in some commercial Mater-Bi® (Italy) product, and polybutylene adipate terephthalate (PBAT), which is incorporated, together with polylactic acid (PLA). In the commercial product Ecowill FS0330® (China), PLA that is easy to process is biobased and is incorporated in the commercial product INZEA® (Spain), and polyhydroxybutyrate (PHB) like starch is biobased and does not require a synthesis process in addition to being biodegradable in soil and is incorporated in the commercial product Arboblend® (Germany). In the next sections, we will focus on processing strategies of two specific blends with potential applications in agriculture: starch/PHB and starch/PBAT.

2.2.2 Processing of Starch/PHB Composites

PHB is the most common type of polyhydroxyalkanoate (PHA). PHAs are linear polyesters with good mechanical strength and similar modulus to polypropylene. They are semicrystalline, hydrophobic and biocompatible. PHAs are degraded in the environment by soil microorganisms which are able to secrete PHA depolymerases, enzymes responsible for the hydrolysis of polymer ester bonds.

PHB is a linear polyester of D(-)-3-hydroxybutyric acid (Fig. 7) that was first discovered in bacteria by Lemoigne in 1925 [67]. It is synthesized biochemically by microorganisms in response to conditions of physiological stress and then accumulated in granular form in their body as energy storage material. PHB can be fermented from a variety of sources, such as sugars, molasses or hydrogen and carbon dioxide depending on the bacteria used. Commercial PHB is synthesized by several bacterial strains such as *Alcaligenes* sp. (PHB Industrial SA, Brazil); *Cupriavidus necator* (Bio-Oil SRL, Italy); and *Ralstonia eutropha* (Tianan Biologic, China; Telles, USA; and Kaneka Corporation, Japan) [68]. Due to the high cost of production, several studies have been carried out to develop better bacterial strains, more efficient fermentation/recovery processes and the use of inexpensive carbon resources as substrates, such as cyanobacteria [69]. Bhatia et al. [70] obtained an *Escherichia coli* strain which can accumulate intracellular PHB up to 57.4% of cell dry mass. The molecular weight of PHB can vary from about 50,000 to over a million, depending on the organism, growing conditions and the extraction methodology used.

PHB is water insoluble and relatively resistant to hydrolytic degradation; it has good ultraviolet resistance and poor resistance to acids and bases. It is soluble in chlorinated solvents such as chloroform and dichloromethane, and is insoluble in non-chlorinated solvents such as hexane [68]. Besides, PHB is less "sticky" than traditional polymers when it is melted [71].

In addition, PHB can be used in food packaging applications [72], controlled drug delivery carriers [73], and wound dressing and tissue engineering [74, 75]. However, moderate mechanical, thermal and barrier properties of PHB limit its applicability in these fields. Hence, blends of PHB with other polymers are prepared in order to balance these drawbacks [76].

As previously discussed, plasticized starch films or composite starch films have low mechanical resistance and a poor barrier property toward water vapor compared

Fig. 7 Chemical structure of PHB. Figure drawn by the authors
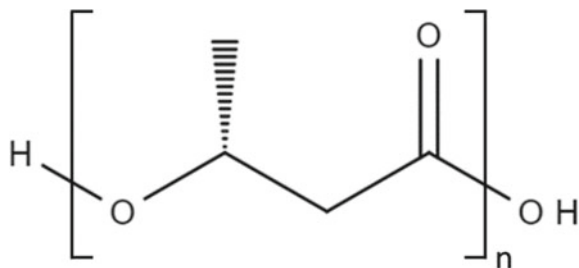
to conventional plastics. Given the background, blending starch with other biopolymers like poly-3-hydroxybutyrate, which has low deformation at break, is one approach to produce starch-based materials keeping its biodegradability and renewability while improving its Young's modulus, tensile strength and even its barrier properties and water sensitivity.

Starch/PHB blends can be produced via compression molding, extrusion and injection molding. As PHB contains bound water, it is necessary to dry pellets before processing the material. Bugnicourt et al. [71] suggest drying PHB for over 2 h at 80 °C in dry air dryers. It is important to take into account that pellets recover the original humidity within 30 min after they are removed from the dryer. On the other hand, some producers of commercial PHB recommend a maximum of 0.005 wt% of humidity before processing the material, drying the PHB at temperatures not exceeding 100 °C. Garrido-Miranda et al. [77] dried PHB at 80 °C for 12 h before processing it with a previously dried TPS.

The major inconvenience during processing starch/PHB blends is the narrow temperature range of working without degrading the polymers, owing to the poor thermal properties of PHB. This polymer has low resistance to thermal degradation that involves chain scission and a rapid drop in viscosity and molecular weight [78, 79]. It decomposes at temperatures just above its melting point (T_m = 170–175 °C). If PHB is exposed to temperatures near 180 °C, it could suffer severe degradation generating products like olefinic and carboxylic acid compounds, e.g., crotonic acid and various oligomers [71]. When PHB is processed for industrial applications, melt-processing techniques such as extrusion and/or injection expose the polymeric chains to high temperatures (above 170 °C for PHB) and shearing tension. Therefore, as degradation may occur rapidly, the acceptable residence time in the processing equipment is only a few minutes. Pachekoski et al. [80] studied the PHB degradation after being extruded and/or injected. Melt flow index (MFI) value before processing was (17 ± 2) g/10 min, and it increased up to (21 ± 2) and (26 ± 2) g/10 min after the materials were extruded, and extruded and injected, respectively. The greater fluidity was related to the increase of the polymeric chain mobility due to the reduction in molecular mass, not only as a consequence of thermal degradation but also by the shearing of the polymeric chains caused by the mechanical forces involved at extrusion and injection processes. One strategy to decrease MFI is the addition of secondary antioxidants, which increases molecular weight since they act like chain extender agents. Correa [81] found that the addition of antioxidants stabilizes the PHB during the melt mixing, increases the processing window and generates chain extension reactions that increase the melt viscosity of the matrix, allowing for better processing conditions.

After processing, the viscosity of PHB decreases due to polymer degradation. In extrusion, the molecular weight of obtained PHB is related to the residence time, and it decreases when temperature and screw speed are higher [82]. Higher temperatures also increase the biodegradation rate of PHB due to a decrease in crystallinity, aiding extracellular enzymes to attack PHB chains [83].

Some strategies have been applied to overcome the thermal drawbacks during processing of starch/PHB blends. For example, the addition of plasticizers decreases
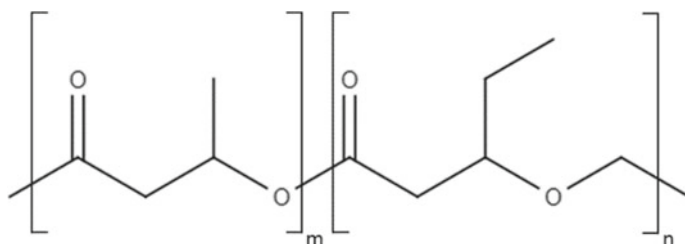
Fig. 8 Chemical structure of PHBV. Figure drawn by the authors

the glass transition and melting temperature of the mixture. However, this route is accompanied with a decrease in tensile properties; the extent depends on the amount and type of the plasticizer added [84]. Likewise, poly-(3-hydroxybutyrate-co-3-hydroxyvalerate) (PHBV) (Fig. 8) is a copolymer of PHB that is widely used to be blended to starch because it has a lesser melting temperature ($T_m = 150$–$155\,°C$) than its homopolymer [85–87]. PHBV is obtained by the incorporation of 3-hydroxyvalerate (HV) during the fermentation process (the content can reach up to 95 mol%). It is produced by a fermentative process similar to that of PHB, only differing in the use of propionic acid (responsible for the concentration of HV) with glucose, as a carbon source [88]. Higher HV contents contribute to decrease the melting point of the copolymer, expanding the processing window. Furthermore, PHBV is less crystalline, easy to mold and more resistant than its homopolymer [89–91].

Another possibility is to improve the interfacial adhesion of starch and PHB in order to increase thermal stability. For example, Don et al. [92] observed that pure PHB decreased its molecular weight in 70% when it was processed at 175 °C for 5 min, while for blends prepared with potato starch grafted with vinyl acetate the reduction was lower, reaching 46% when the composition was 20:80 of PHB:modified starch.

In general, compression molding is the most used method for obtaining starch/PHB-based blends/composites. Before this, a compounding step is carried out to obtain a homogeneous mixture of all the components. The first step is often done in a conventional mixer or in a twin-screw extruder at temperatures around to that of PHB melting. Then, the melted mixtures (frequently grounded) are processed to obtain films with desirable thickness. By compression molding, the assemblies are often processed between 160 and 180 °C, at 8–69 MPa, and for 5–30 min when PHB is used [73, 93, 94].

The resulting starch/PHB blends are often heterogeneous due to a lack of affinity between both components. Discontinuities at the interface generally lead to cracks and thus low deformation at break and poor barrier properties. Over the years, several strategies have been addressed to get better interaction between both polymers and thus obtain completely biodegradable materials with desirable properties. Among them, the adjustment of processing conditions, the extent of disruption/plasticization of starch, the botanical source and type of starch (different amylose contents), the

employment of starch/PHB derivates (physical or chemical modified starches and/or copolymers of PHB) and the use of compatibilizers have been taken into account.

The addition of fillers has also been proposed to increase the polymer compatibility. Depending on the type of filler or the simultaneous use with other additives, differences are obtained in the compatibility of the composite's components. For example, Garrido-Miranda et al. [95] investigated the influence of clay's incorporation on the properties of the resultant starch/PHB-based composite. The researchers obtained a bio-nanocomposite of PHB, TPS and clay by melt mixing with different concentrations of clay (1 and 5%). They worked with a derivate of montmorillonite (OMMT) modified by surfactants which has the same affinity for hydrophilic and hydrophobic polymers. TEM and DRX analysis indicated that OMMT structures were exfoliated and intercalated. The results showed that when concentrations of OMMT were higher (5%), only layers of clay and no starch granules were observed in the matrix. That could be attributed to the behavior of the clay as compatibilizing and reinforcing agent in PHB/TPS blend, improving the interfacial adhesion between immiscible polymers. This better compatibility of the polymers resulted in higher hardness and elastic modulus of TPS/PHB/OMMT composites with respect to that of TPS/PHB.

2.2.3　Processing of Starch/PBAT Composites

PBAT is a 100% biodegradable aliphatic–aromatic copolyester based on fossil resources. It is obtained by a polycondensation reaction between butanediol, adipic acid and terephthalic acid, using conventional polyester manufacturing technologies. Its chemical structure, shown in Fig. 9, combines the biodegradability and processability characteristic of aliphatic polyesters with the thermal and mechanical properties provided from aromatic polymers [96]. PBAT offers higher physical properties, including flexibility (elongation at break close to 700%), Young's modulus (20–35 MPa), tear resistance and tensile strength (32–36 MPa) than most biodegradable polyesters, such as poly(lactic acid) and polybutylene succinate [62]. Furthermore, its mechanical properties and processing conditions are comparable to those of low-density polyethylene. Therefore, it has become a promising biodegradable material for a wide range of potential applications [62, 97]. PBAT is a semicrystalline
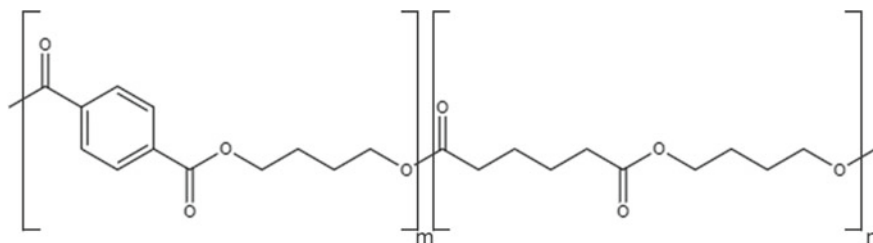
Fig. 9 Chemical structure of PBAT. Figure drawn by the authors

polymer with a thermal behavior well characterized. A crystallization exotherm is usually observed around 55–60 °C, and the melting temperature ranges from 110 to 140 °C. PBAT glass transition temperature is reported to be between −30 and − 15 °C, depending on the testing conditions [64, 96]. The moderate crystallinity and good thermal stability allow PBAT to be melt-processed by conventional techniques such as injection molding, extrusion and compression molding [61]. As reported by Dammak et al. [56], PBAT presents short molding cycles and good processability at high extrusion speeds. Typical processing temperature profile ranges from 110 to 160 °C according to the formulation, the processing technique and the characteristic of the neat PBAT. Special attention must be given to moisture removal before processing to prevent the hydrolytic degradation of PBAT. When processing biopolymers at high temperature and shear stress, the presence of moisture can accelerate polymer chain scission and promote downstream processing issues [61, 98]. The degradation routes of biodegradable polymers are generally related to a depolymerization step due to the action of external driving forces (temperature, mechanical stress, radiations, etc.) and the subsequent reactions of the radicals generated with the environment. As reported by Ferreira et al. [62], two main degradation routes have been proposed for PBAT. One considers the enzymatic action of microorganisms such as bacteria, fungi and algae in the disposal environment. The other one is based on a depolymerization process promoted by a no-enzymatic reaction (e.g., chemical hydrolysis and thermal degradation) and the subsequent assimilation and metabolization of the generated intermediates by the present microorganisms. The downsides of PBAT are its poor tensile strength, low modulus, low barrier properties and especially its relatively high production cost when compared with most conventional plastics. Hence, its biodegradability alone is not enough for consumer acceptance and makes it difficult for its large-scale application [54, 62, 65, 99]. These limitations might be addressed by blending with other biodegradable, more cost-effective polymers, and/or adding biobased fillers to design biocomposites, without compromising its biodegradability [54].

PBAT is presented as a proper candidate to combine with TPS, improving TPS toughness and water resistance while maintaining its biodegradability performance [96]. According to Manepalli and Alavi [50], blending starch (0.20–0.40 \$/lb) with high-cost polymers like PLA and PBAT (1.50–3.00 \$/lb) can be competitive in cost with respect to commodity plastics. Biodegradability degrees greater than 90% for PBAT and TPS systems were obtained by various authors. However, the rate of CO_2 production varies depending on the composition of the mixture. This variation is related to the components added to the TPS/PBAT mixture, the developed morphology and the strength of the interphase between the polymers [56].

Simple physical blending leads to the deterioration of mechanical properties caused by the incompatibility between phases, limiting the maximum TPS content in the blend to approximately 25–30 wt% [100, 101]. Hence, the major problem of the TPS/PBAT blends is the poor interfacial adhesion between the hydrophobic PBAT and the hydrophilic TPS [102, 103]. Extensive efforts have been made to lower the interfacial adhesion between TPS and PBAT, and a variety of compatibilizers, including low molecular and macromolecular compatibilizers, have been studied

[64, 102] The reactive extrusion of TPS with polyester in the presence of maleic anhydride, citric acid and tartaric acid, as well as low molecular coupling agents, has been investigated. They have been used to improve the plasticization process and to increase the compatibility between TPS and other polymers [100, 102, 104, 105]. Maleated PBAT, maleated TPS and epoxy additives have also been used to improve PBAT/TPS blend performance [106]. In all of these compatibilizers, the anhydride group of maleic anhydride, the epoxy group of glycidyl methacrylate (GMA) and the carboxyl group of acrylic acid, tartaric acid and citric acid are efficient to improve the mechanical properties of PBAT/TPS blends by enhancing the interfacial adhesion between the two phases [56].

Citric acid (CAc) is an organic tricarboxylic acid present in most fruits, especially citrus fruits such as lemon, orange and tangerine. Its molecular formula is $C_6H_8O_7$. The multi-carboxylic structure and low molecular weight make possible its use as plasticizer, cross-linking agent, hydrolytic agent and compatibilizer in polymer formulations. Several authors reported the effect of different contents of citric acid on TPS/PBAT blend properties [56, 100, 97].

Maleic anhydride (MA) is an organic compound, the acid anhydride of the bifunctional maleic acid. The anhydride group has been extensively used as an in situ or ex situ coupling agent for immiscible polymer blends due to its high reactivity with water, alcohols and amines. Maleic anhydride can react with amine and hydroxyl end groups (e.g., of polyesters) to yield the desired graft copolymer necessary for compatibilization. The MA-modified polymers can then be employed to compatibilize polyesters (e.g., PET and PBT) with other polymers due to the potential of anhydride reaction with terminal hydroxyl groups. Methods for grafting MA into polymer backbone have been studied as a technique to promote hydrophilicity, adhesion, dyeability, functionality for cross-linking and other chemical reactions in polymer development. In addition, the MA grafting has been utilized to promote compatibility between polymers and polymer/fillers [107]. Fourati et al. [100] studied the incorporation of citric acid, maleic anhydride and maleated PBAT, in PBAT/starch formulations and their effect on the mechanical properties, rheological behavior at a solid and molten state, the co-continuity and the morphology of the phases. In the work of Dammak et al. [56], the authors continued their investigation concerning the effect of MA and maleate PBAT (PBAT-g-MA) on the mechanical, rheological and biodegradability of PBAT/TPS blend with a TPS content ranging from 40 to 60%.

Tartaric acid (TA) is a dicarboxylic acid extracted from plants and fruitages, widely used as an edible acid derivative in pharmaceutical, food and general industrial chemical fields [108]. As for citric acid, it is reported that TA acts as a coupling agent by promoting esterification (grafting) and transesterification reactions (cross-linking) with polymers, improving the compatibility between them. Its effect on promoting the acid hydrolysis of starch chains has also been studied. For example, Zhang et al. [108] proposed a new facile strategy to reduce the TPS shear viscosity and improve compatibility with PBAT by adding increasing contents of tartaric acid. In their work, Olivato et al. [109] explored the use of TA as a compatibilizer of starch/PBAT blends obtained by a one-step reactive extrusion process based on a constrained mixture design.

A study of the torque recovery and polymer degradation for a TPS/PBAT blend with up to 30% of TPS, processed in a laboratory mixer with and without a commercial chain extender additive as a compatibilizer, was conducted by Marinho et al. [110]. They proposed that the compatibilizer action of the oligomer used as a chain extender is due to the presence of epoxy and methacrylate residues that can interact with the polymeric system. As an alternative for conventional macromolecular compatibilizers, Garcia et al. [111] studied the effect of using sericin (at low concentrations) in the performance of starch–PBAT blown films. Sericin protein is obtained as a by-product during silk production from the *Bombyx mori* silkworm. Its molecular weight ranges from 24 to 400 kDa, and the predominant amino acids are serine (40%), glycine (16%), glutamic acid, aspartic acid, threonine and tyrosine. Due to its chemical characteristics, sericin is reported to be used as an additive or adjuvant in polymer blends [111].

Different strategies have been proposed to process TPS/PBAT blends with the inclusion of different compatibilizers and coupling agents. The preparations of TPS/PBAT/compatibilizer (CA, MA and PBAT-g-MA) blends studied by Fourati et al. [100] first involved obtaining TPS from potato starch mixed with 20 wt% glycerol using a dough mixer (40 rpm, 10 min). The starch–glycerol blend was then extruded twice on a single-screw extruder (L/D 28:1; 200 rpm, temperature profile 110–110–120–120–130–130–120 °C from hopper to die). Before mixing with PBAT, TPS pellets were dried overnight at 70 °C. TPS and PBAT granules (Ecoflex F Blend C1200; TPS60/PBAT40) and citric acid (2 and 4%) were manually fed and extruded twice to improve the dispersion of the blend components at a screw speed of 120 rpm, with a temperature profile 120–130–145–150–150–140–130–120 °C. A flat die was used to obtain films with a thickness between 0.3 and 0.2 mm. Blends with MA (2, 4 and 6 wt%; based on the whole TPS/PBAT blend) were processed as described above for CAc. PBAT-g-MA was prepared by radical grafting in the melt of PBAT with 2% MA and benzoyl peroxide (BP) (1%) as a radical initiator, using a batch mixer (140 °C, screw speed of 45 rpm, 20 min). The PBAT-g-MA was pelletized and used without further purification. The extent of maleation was around 0.55%. Using rheological measurements, they found that the rheological behavior of the TPS60/PBAT60 blend showed a typical viscous-like behavior (G'' higher than G') and followed that of PBAT, where PBAT was the continuous phase and the TPS the dispersed one. When TPS/PBAT was processed in the presence of CA, the authors found a rheological behavior typical of a gel-like material with G' higher than G'' and nearly frequency-independent. The authors investigated the rheological properties of TPS-CA 2% blend and found that both the viscosity and G' decreased by one order of magnitude in comparison with the neat TPS. They explained the drop in viscosity, as other authors did, due to the capacity of CAc to disrupt starch inter- and intramolecular interaction and also a certain degree of starch acidolysis. The rheological behavior of TPS/PBAT/MA, at 150 °C, was also typical of a gel-like material. As the content of MA increases, a decrease of both G' (G'TPS-PBAT-2MA > G'TPS-PBAT-4MA > G'TPS-PBAT-6MA) and complex viscosity ($\eta*$) was observed. The SEM and co-continuity analysis showed a direct correlation with the rheology results. TPS/PBAT/MA 2% presented a co-continuous structure, while at 4% MA, a

phase inversion occurred (as was evidenced by SEM) with TPS being the matrix, and PBAT as droplets, the dispersed phase. In accordance with SEM results, the authors observed that the rheological behavior of TPS/PBAT-g-MA/PBAT was similar to that of the TPS/PBAT blend, dominated by a liquid-like character, where PBAT was the continuous phase and TPS the dispersed one, although PBAT represented the 40 wt% of the total weight of the blend.

Dammak et al. [56] prepared PBAT-g-MA using the same procedure and processing conditions as Fourati et al. [100]. However, the MA content grafted was 1.5%. The materials used in the work of Dammak et al. [56] were similar to the ones employed in the previously published paper [100]. However, the method of preparing the blends differs from that presented in the previous study. In their work, TPS was prepared by mixing starch with glycerol at a ratio of 80/20 wt% and 10% of water was added. Water acts as a plasticizer for starch, so the plasticizer content in this blend is higher than in the previous work [100]. Then, the starch–glycerol–water mixture was extruded in a twin-screw extruder (L/D 38:1, screw speed 100 rpm, temperature profile 130–130–130–130–135 °C) instead of the dough mixer and the two-extrusion process on a single-screw extruder previously used. Films from TPS (content 40, 50 and 60%), PBAT granules and the compatibilizer (MA and PBAT-g-MA, 2%) were extruded using the same twin-screw extruder. Films were obtained with a flat die set at the end of the extruder (thickness range 0.2 and 0.3 mm).

Zhang et al. [108] obtained TPS modified with TA by premixing dried corn starch (Langfang Starch Company) and glycerol (70:30 w/w) for 5 min with the incorporation of 0.5, 1, 2 and 4% TA (weight based on corn starch). All components were mixed for 10 more minutes. Mixtures were kept for 30 min at 80 °C, and afterward melt compounded using a twin-screw extruder (L/D 40:1) at a screw speed of 80 rpm. The temperatures of the extruder, from the feed zone to die end, were 90–120–130–140–145–145–140–135 °C. The effect of TA contents on the properties of PBAT/TPS-TA blends was studied by melt compounding TPS-TA mixtures with PBAT (TH-801, Xinjiang Blue Ridge Tunhe Chemical Industry Joint Stock Co.). TPS-TA mixtures were dried at 80 °C for 24 h and extruded with PBAT to obtain PBAT30/TPS-TA70 blends using the same equipment. The temperatures of the extruder from the feed zone to die were 140–140–150–150–155–155–160 and 150 °C, and screw speed was kept at 70 rpm. TPS and PBAT/TPS were performed at the same procedure and were considered as control materials. All PBAT/TPS-TA blends displayed a shear thinning behavior at high frequency, with complex viscosity (η^*) and storage modulus (G') of PBAT/TPS-TA higher than those of PBAT in the whole frequency region. However, η^* and G' of PBAT/TPS-TA decreased as the TA content increases from 1 to 4%, confirming that the compatibility of PBAT/TPS-TA at levels up to 1% is better than at higher contents and thus might act as a coupling agent at low content. When TA's content was higher, η^* and G' of PBAT/TPS-TA decreased, suggesting its lubricant action.

The effect of TA on the properties of a starch/PBAT blend was studied by Olivato et al. [109] using a constrained mixture design. TA proportions used ranged from 0 to 1.1%. The maximum proportion of glycerol was set to 12.0%, and the third component was a mixture of starch and PBAT with a 55:45 proportion between

the phases. Native cassava starch and PBAT (BASF) were used. The formulations were processed using a laboratory single-screw extruder (L/D 28:1), with a barrel temperature profile of 100–120–120–120 °C and the screw speed set to 40 rpm. Pellets were obtained afterward. In a second step, blown films were obtained using the same equipment with a barrel temperature profile of 100–120–120–130 °C and 130 °C for the 50-mm film-blowing die, with a screw speed of 40 rpm. The film thickness was maintained between 80 and 100 µm.

The incorporation of an oligomer with epoxy and methacrylate residues (commercial name Joncryl PR010) as chain extender and compatibilizer, in blends of PBAT with 10%, 20% and 30 wt% of TPS, was studied by Marinho et al. [110]. PBAT (Ecoflex® F Blend C1200) and thermoplastic starch (TPS Beneform 4180, Ingredion) were compounded in a laboratory internal mixer at rotor speed of 60 rpm, and chamber wall temperature kept constant at 140, 170 and 200 °C (total processing time of 15 min). PBAT and TPS were also subjected to the same process, and 1% Joncryl additive was added after 10 min without interrupting the process. The chain extender is recommended to compensate for degradation during processing in polyesters and polyamides.

Films of starch/PBAT/glycerol with increasing contents of sericin (0.5, 1.0 and 1.5 wt%) were obtained by Garcia et al. [111] using a single mixing step followed by blown-film extrusion. Cassava starch (Indemil, Brazil), PBAT (Ecoflex® S BX 7025, BASF), glycerol and sericin (extracted from silkworm cocoons, *Bombyx mori*) were manually mixed and extruded in a twin-screw extruder (L/D 35:1) to obtain pellets. The screw speed was 100 rpm, and the temperature profile used was 90–120–120–120-120 °C. In a second step, pellets were extruded using a mono-screw extruder (L/D 26:1) with a 50-mm film-blowing die. The temperature profile was 90–120–120–130 °C and 130 °C at the die, and the screw speed was 40 rpm. The control formulation contained 61, 26 and 13 wt% starch, PBAT and glycerol, respectively. As the authors' preliminary results showed that sericin could perform as a plasticizer, its addition replaced glycerol content in every formulation.

As it was mentioned before, in some cases adding fillers to polymer blends results in an improvement of the interfacial adhesion between the polymer phases caused by preferable filler localization at the interface [65]. As it was previously mentioned, the addition of low-cost materials (organic and inorganic fillers) as natural reinforcing agents is an effective way to improve the starch/PBAT properties and decrease their final cost, while maintaining (but preferably accelerating) the inherent biodegradability of the matrix. However, some concerns related to common problems of filler dispersion, the interaction between filler/matrix and reduction filler content must be overcome [62, 112]. Several factors, such as processing conditions, the miscibility and viscosity of the polymer phases, and the composition of the final mixture, will define the composite's performance.

The enhanced mechanical, thermal and barrier properties of a composite are related to the formation of strong interactions between the filler and matrix. Thus, when some external stress is applied, part of the energy can be absorbed by the filler, and part of it can be dissipated by frictions between particle–particle and particle–polymer interaction through the interphase. The uniform filler dispersion within the

starch/PBAT and the improved interactions between the filler and polymer matrix better dissipates the energy throughout the matrix.

The final properties of starch/PBAT and TPS/PBAT blends depend on several factors. The most important ones are associated with the structure of the starch in blends, influenced by the origin of the native starch, the presence of plasticizers, processing aids, use of compatibilizer agents, among others. The parameters used to obtain the thermoplastic starch and the way in which it is mixed with PBAT will influence the morphology and properties of the compound obtained [97, 101]. Different microstructures and component distributions in the starch/PBAT or TPS/PBAT blend can be achieved according to the process and processing conditions.

In order to improve the interaction between fillers and PBAT/starch (or PBAT/TPS) matrices and the filler dispersion, different strategies were proposed [62, 63]. For example, Liu et al. [103] proposed the incorporation of MA and poly(ethylene-co-vinyl alcohol) (EVOH) to improve the properties of starch-based nanocomposites/PBAT blends using nano-SiO_2 as a reinforcing agent. In their work, Zhai et al. [97] proposed a single-step process to obtain starch–glycerol/PBAT nanocomposite containing an organically modified montmorillonite as a filler and citric acid as a compatibilizer. The effect of the starch content on the morphology, mechanical properties and hydrophobicity of blown films were investigated.

The impact of different compatibilizers, including fillers, on the morphology of the TPS/PBAT blends was evaluated by several authors. Fourati et al. [100] studied by SEM the morphology of cryo-fractured cross section of TPS/PBAT (60/40 wt%) films, processed with 2 and 4% of citric acid as coupling agent, on samples with and without extraction with HCl solution (TPS extracted) and CHCl3 (PBAT soluble). Also, the continuity index was calculated as

$$\%\text{continuity} = \frac{W_{\text{init}} - W_{\text{end}}}{W_{\text{init}}} \times 100,$$

where W_{init} corresponds to the weight of PBAT or TPS before the solvent extraction step and W_{end} was the weight remaining after extraction. For TPS-PBAT (60/40), in the absence of a compatibilizer, the continuity index was about 100 and 20% for PBAT and TPS, respectively. This means that the PBAT formed the continuous matrix phase with TPS being the dispersed phase, despite its volume fraction exceeding that of PBAT. SEM images confirmed a dispersed morphology in which TPS appears as dispersed elongated droplets in the PBAT matrix (TPS droplet size between 1 and 5 µm). The presence of holes and gaps in the interfacial area between the matrix and the dispersed phase, observed in the image after the cryofracture breaking of the film, indicated a weak interfacial adhesion between TPS particles and PBAT matrix. For TPS/PBAT/2% CAc, the SEM images showed a co-continuous morphology, consisting of interconnected TPS structures with fiber-like morphology (observed in SEM image after film treatment with HCl solution). SEM micrograph for blend processed in the presence of 4% CAc showed a continuous phase of TPS and PBAT dispersed (spherical particles with a size between 2 and 4 µm). In the presence of CAc as a compatibilizer, TPS/PBAT 60/40 films totally disintegrated

in water within several minutes, especially for 4% CAc. For TPS/PBAT/2% MA, SEM images showed a co-continuous morphology, where TPS structures were interconnecting with a fiber-like morphology. This effect is highlighted in these mixture morphologies more than in those prepared with CAc. The continuity test and SEM images of TPS/PBAT/4 and 6% MA showed a dispersed morphology in which the PBAT is dispersed (droplets) in a TPS matrix. This was confirmed by the appearance of voids in the SEM micrograph of the cross section of the film after the extraction with chloroform. In addition, after immersion in the HCl solution, the film fully disintegrated, and PBAT particles (size between 1 and 4 µm) were observed. As for CA, TPS/PBAT 60/40 MA 6% totally disintegrate in water within several minutes. For the blend TPS/PBAT-g-MA/PBAT (TPS/PBAT 60/40) obtained by Fourati et al. [100], in the presence of 2% PBAT-g-MA, the morphology resembles that of TPS/PBAT (PBAT formed the continuous matrix phase with TPS being the dispersed phase). However, they observed that during cryogenic breaking for SEM evaluation a lesser number of TPS particles were pulled out and were less visible in the micrograph, compared to TPS/PBAT. They explained these results as an indication of improved interactions between TPS and PBAT when PBAT-g-MA was used as a compatibilizer.

Low interfacial adhesion and poor compatibility between TPS and PBAT were reported by several authors [108]. TPS-TA/PBAT blends presented small particles of TPS-TA phases dispersed in the PBAT matrix without agglomeration and good wettability between phases, for TA content range from 0.5 to 2%. However, the increase in the TA content from 2 to 4% leads to the phase morphology of TPS-TA/PBAT 4% with TPS-TA particles agglomerated and showing low interfacial adhesion and poor compatibility. As reported by Zhang et al. [108], increasing contents of TA in TPS mixtures improve its processability. An important reduction of the melt viscosity was reported as the melt flow index increased from 0.68 to 15.7 g/10 min when the TA contents increased from 0.5 to 4%. Melt viscosity decrease was associated with the acid hydrolysis of starch macromolecular chains observed from the viscosity-average molecular weight measurements. TA can promote the hydrolysis of starch during processing in the presence of glycerol and water vapor. FTIR and titration measurement analysis of TPS-TA presented by Zhang et al. [108] evidenced that TA does not esterify TPS or esterifying reaction degrees were very low during the extrusion process (without an external catalytic agent) and proposed that TA could be acting as a lubricant agent.

Contrary to Zhang et al. [108] results, Olivato et al. [109] demonstrated that TA was able to promote esterification reactions with the OH groups of starch (characterized by FTIR and solid-state 13C cross-polarization/magic angle spinning nuclear magnetic resonance). These esterification and transesterification reactions were responsible for the compatibilizer effect observed in starch/PBAT-TA blends. The addition of TA changes the morphology of starch–PBAT blends showing a reduction in the interfacial tension between starch and PBAT and promoting more homogeneous structures.

Olivato et al. [109] and Olivato et al. [113] published SEM images that showed a good dispersion of sepiolite in TPS80/PBAT20-sepiolite 5%, and they found no effect of nanofiller content on the morphology of the blends. TPS50/PBAT50 with and without sepiolite showed a round TPS dispersed phase. A phase inversion was

observed for TPS80/PBAT20 samples with and without nanofiller, where PBAT was the dispersion phase.

Morphology of starch/PBAT/glycerol films obtained by Garcia et al. [111] presented a fibrillar structure with effects that indicate chain orientation promoted by the blown-film process. They also reported the absence of starch granules, demonstrating that the process was adequate to enable the disruption of the starch granular structure. Sericin addition at 1.0 and 1.5 wt% resulted in more homogenous and compact structures, suggesting a cohesive effect when incorporated into polymer matrices.

Lendvai et al. [114] obtained nano-biocomposites using native maize starch, PBAT (Ecoflex® F Blend C1200, BASF), natural bentonite (BT) and an organically modified montmorillonite (OMMT, Cloisite 30B). They reported the presence of a quasi-continuous phase when 40 wt% of TPS was added to PBAT, with some less plasticized starch domains as a second phase (size range of 5–15 µm). EDS mapping for Si in 40 wt% TPS nanocomposites/PBAT blend revealed a continuous phase for TPS, with a uniform distribution of bentonite (BT). As expected from the compounding method described by the authors, BT nanoparticles were predominantly located in the TPS phase and showed an intercalated morphology when 40 wt% of TPS nanocomposite was incorporated into PBAT. The intercalated morphology progressed further with the increasing content of PBAT. These results indicated that a decrease of the melt viscosity during compounding of blends with higher PBAT content could promote the disintegration of the BT agglomerates and facilitate their dispersion on the polymer matrix. SEM micrograph for TPS-OMMT/PBAT was not presented by the authors in the discussion.

In the work of Nunes et al. [55], the effect of processing temperature and TPS contents on the rheological and mechanical performance of TPS/PBAT blends and TPS/PBAT biocomposite reinforced with babassu mesocarp was reported. Regardless of TPS content in the blends, they described that immiscible morphologies were obtained, with starch granules of heterogeneous sizes dispersed in the PBAT matrix. TPS/PBAT SEM micrograph showed poor adhesion between phases. When TPS content was increased from 10 to 30%, an increase in the agglomeration of TPS particles was observed. Biocomposite SEM micrographs also showed partial adhesion between matrix and fibers. These results are consistent with the mechanical properties reported. Blend morphology did not present significant differences as a function of the processing temperature.

In the work of Liu et al. [103], SEM micrographs showed low compatibility for the system TPS/PBAT (TPS particle-like could be found). In their work, only the influence of the compatibilizer in the TPS/PBAT blend was evaluated. When MA or plasticized EVOH (pEVOH) was used as compatibilizer, a co-continuous phase was formed. The continuous phase showed a more homogeneous structure when a combination of MA + pEVOH was added to TPS-nSiO$_2$/PBAT composites. The XRD results for the samples confirmed the absence of significant changes in the crystalline structures of starch and PBAT with the addition of nano-SiO$_2$ and the compatibilizers. The structure and morphology of TPS-nSiO$_2$ nanocomposite were not presented in their results.

X-ray diffraction analysis was used by Zhai et al. [97] to evaluate the intercalated or exfoliated structures of hydroxypropyl distarch phosphate HPDSP/PBAT/nCOM nanocomposite. The nanocomposite XRD pattern showed diffraction peaks that indicated an intercalated clay nanostructure. As the PBAT content increases, polymer chains were intercalated into nanoclay organically modified (nCOM), and the d-spacing values increase from 3.46, 3.61, 3.95, 4.16 and 4.27 nm, for PBAT contents 10, 20, 30, 40 and 50%, respectively (nanoclay d-spacing 2.76 nm). The authors proposed that the PBAT has better affinity with the hydrophobic nCOM, promoting an improvement in the fluidity of the blends and facilitating the polymer chains to enter the nanoclay interlayer during extrusion processing. He et al. [115] found that nCOM has better dispersion in PLA/PBAT two-phase blends than pure PLA or PBAT as d-spacing and relative intercalation was higher than in PLA or PBAT nanocomposites. In addition, they found that d-spacing was greater when PBAT was the continuous phase in the composite blend. They explained this result due to better compatibility of the clay organic modifier with PBAT. SEM micrographs showed smoother surfaces in HPDSP/PBAT/nCOM nanocomposite as PBAT content increased. For blends with 10% and 30% PBAT, the film's surfaces became less rough and exhibited better structural integrity than the film from 100% modified starch HPDSP. When the PBAT content was equal to 50 wt%, the surface structure of the film exhibited a smooth, dense and uniform appearance. No cracks, wrinkles or irregularities were observed on the surface of the HPDSP/PBAT 50/50, and also, the films exhibited a coarser and ductile fracture surface, probably due to a better interaction between the two polymers. The role of citric acid as a compatibilizer for HPDSP and PBAT was reflected and referenced in the work of Zhai et al. [97] through the FTIR spectra analysis, although as the peak at approximately 1713–1716 cm^{-1} (carbonyl stretch of the ester group) originally present in PBAT did not allow to find evidence of grafting and/or cross-linking reaction of the HPDSP chains, either the esterification or interesterification reaction promoted by the compatibilizer. They mentioned that these reactions are feasible to take place due to the temperatures used in the extrusion process, as was referenced by the authors.

3 Properties of Starch-Based Green Composites

3.1 Properties of Starch Matrix Composites

3.1.1 Thermal Properties of Starch Matrix Composites

Three characteristic thermal transitions may exist for such semicrystalline polymers as starch: a glass transition for the amorphous fraction (T_g); a thermal transition for the melting of crystallites (T_m); and a transition due to crystallization (T_c). Starch is partially miscible with its most used plasticizer: glycerol. For that reason, TPS films plasticized with glycerol generally have two glass transition temperatures, one

associated with the plasticizer-rich phase ($T_{\alpha 1}$) and the other with the starch-rich one ($T_{\alpha 2}$). The presence of nano-/microfillers can change this behavior through interactions with the matrix and/or the plasticizer. It has been demonstrated, for example, that waxy starch nanocrystals affect preferably the mobility of the starch-rich phase, due to strong hydrogen bonding interactions between them and the amylose/amylopectin chains of the matrix, and therefore a more remarkable shift in $T_{\alpha 2}$ is obtained [47]. It should be noted that other plasticizers could lead to different behaviors. In the case of sorbitol, for example, as it is miscible with starch, only one T_g is presented. Other possible plasticizers are currently being studied, like the use of D-isosorbide, 1,3-propanediol and deep eutectic solvents [47, 52]. In both cases, two glass transition temperatures are observed.

The effective attachment of TPS to fillers can therefore constrain the segmental motion of TPS chains by strong hydrogen bonding interactions, increasing the material's T_g. Ghanbari et al. [43], for example, found that the T_g of neat TPS film (37 °C) increased 11.5 °C with the addition of 1.5 wt% of cellulose nanofibers and ascribed this difference to the strong matrix–filler adhesion. A similar effect was found by Nessi et al. [15] for cellulose nanocrystals (CNCs)–starch nanocomposites, who proposed that CNCs may act like a junction and promote the intermolecular interaction of starch chains reducing their relaxation. In this case, the T_g of the starch-rich phase shifted from 68 °C for the TPS matrix to 75 °C for the composites with the inclusion of 2.5, 5 and 10 wt% of CNCs, regardless of the filler content.

On the other hand, the thermal degradation of TPS occurs as a three-step process. In the first stage, the initial mass decrease is in the range 60–120 °C and is related to the evaporation of water. In the second one, between 180 and 270 °C the plasticizer thermal degradation of thermoplastic starch usually occurs. Finally, the third step in thermal curves, from 280 to 350 °C, corresponds to starch degradation. All these stages may be modified due to filler addition. The first stage will depend on the possibility of fillers to modify films' moisture content. Some fillers could interact with the plasticizer, retaining it or allowing easy evaporation [16, 116, 117]. In those cases, changes in the second step are expected. Ochoa-Yepes et al. [42] showed that protein addition into TPS led to a slightly lower mass loss of the composites in the second step with respect to the matrix. When fillers with higher thermal stability than starch are incorporated into TPS matrices and many interactions occur between the polymer and the filler, a slight increase in the composite thermal stability is usually observed, due to the increasing dissociation energy. This means a delay in the decomposition of the material and has been demonstrated for gelatin [45], cellulose nanofibers [43], cassava and ahipa peels and bagasse [118], SiO_2 [103] composites, among others.

The importance of the matrix–filler interaction was demonstrated by Fazeli et al. [119], who studied TPS and TPS composite films reinforced with cellulose fibers (CFs) and plasma-treated cellulose fibers (PCFs). They found that the main decomposition temperature of the neat TPS and TPS/CF 6 wt% composite was about 260 °C, whereas the one obtained for the TPS/PCF 6 wt% composite raised to approximately 284 °C. The achieved improvements are attributed to the fact that the PCF

compounded into the TPS matrix strongly, making decomposition of the composite arduous. Hence, better thermal stability was obtained with PCF as the reinforcement.

3.1.2 Gas Barrier Properties and Water Sensitivity of Starch Matrix Green Composites

Many potential applications of starch-based materials need specific gas barrier properties, especially in the packaging field, where a product needs to be protected from the outside. Moreover, food packaging materials need the presence of specific atmospheric conditions to maintain the freshness and quality of food during storage [120]. In particular, water vapor permeability (WVP) and oxygen permeability (OP) are the two most studied gas barrier properties in the literature. In general, starch-based films show high WVP values, whereas they present better behavior against nonpolar molecules such as O_2 and CO_2, because the transport of gas molecules depends on both diffusion and solubility coefficients. The WVP of starch-based films is mainly governed by the high ability of water molecules to interact and penetrate through them because of the strong starch/water affinity and is little influenced by the type of plasticizer used. González et al. [47] showed that WVP values of starch films plasticized with glycerol and D-isosorbide had no significant differences. However, the OP was found to be strongly influenced by the type of plasticizer used. An OP value near twenty times lower for the D-isosorbide plasticized film comparing to that obtained for glycerol-plasticized one was observed. They attribute this significant decrease to the reduction of oxygen solubility due to the hydrogen bonding interactions between starch and D-isosorbide, saturating the sorption sites. On the other hand, Battegazzore et al. [121] studied the influence of ambient humidity in oxygen transmission of TPS films prepared with isosorbide as a plasticizer. They found no significant variations of oxygen permeability till 75% RH. However, over this RH, an exponential increase was found. From these results, it can be inferred the need to take into account both the plasticizer used for the development of TPS and the ambient humidity at which the material will be tested, especially for packaging applications.

The incorporation of micro- and nanofillers has proven to be highly effective in improving the barrier properties of starch films. In many cases, its success is associated with the introduction of a tortuous pathway for gas molecules to pass through. In this context, the filler shape plays a very important role in the improvement of barrier properties. Most effective fillers are usually those with platelet shape, which can create a sort of winding road hindering and delaying the passage of gases and water [13]. Most common nanofillers with this shape are clays and some starch nanocrystals. González et al. [47] compared the OP of TPS films developed from maize starch, glycerol, waxy starch nanocrystals (WSNCs) and CNC. A reduction in the OP value was found for the TPS nanocomposite containing 1 wt% of WSNC, from (108 ± 35) to (43 ± 10) cm^3 μm m^{-2} day^{-1} kPa^{-1} for the matrix and the nanocomposite, respectively. The incorporation of 1 wt% of CNC also decreased the permeability value, but the improvement was less notorious, being the OP value (70 ± 6) cm^3 μm m^{-2} day^{-1} kPa^{-1}. The greater effectiveness in the decrease of

permeability against O_2 molecules achieved by the WSNC was attributed to their platelet-shaped morphology, which gave them the capacity to generate a tortuous path for the O_2 molecules, decreasing the diffusivity. Significant improvements in permeability to both oxygen and water vapor thanks to the incorporation of platelet-shaped fillers were found by other authors [122, 123].

As it has been known for many years, the morphology of the fillers is not the only factor to consider. The way in which they are oriented within the matrix is also determinant for the produced effect in barrier properties. If the largest surface of each nanoparticle is oriented perpendicular to the direction of the gas diffusion or permeation, an optimal decreasing effect on permeability will be achieved. However, it is an extremely challenging task to achieve fillers' regular arrangements within TPS matrices, specially through industrially scalable methods. In general, the obtained composite materials have randomly oriented fillers, diminishing the impact on the decrease of permeability [124].

Possible interactions between filler and matrix components could also highly influence the composite's permeability due to the conformation of different interface morphologies. A defect-free TPS–filler interface is difficult to achieve, as the incorporation of filler particles usually modifies the properties of the neighboring polymer phase. Therefore, depending on the TPS–filler adhesion, various structures can be observed at the interface. If voids are formed in the filler–matrix interface, an increase in gas permeability can be observed, as the formation of these defects allows the gases to pass. This can occur due to poor adhesion, polymer packing disruption in the vicinity of the dispersed particles, repulsive force between the two phases or different thermal expansion coefficients, among other possible reasons. On the contrary, when the adhesion between the two phases is good, polymer chains located near the filler surface are rigidified, due to a reduction of the polymer-free volume in this region. This interfacial defect usually leads to a decrease in permeability [125, 126]. For example, while platelet-shaped starch nanocrystals can strongly reduce the permeability of cassava starch–glycerol matrices [127], the effect of these fillers is the opposite in waxy corn starch matrices. García et al. [128] proposed that this important difference was due to unlike nanocrystal distribution and interface composition. While in the case of mandioca starch matrices the nanocrystals were well distributed with excellent matrix–filler adhesion, for waxy maize starch matrices the nanocrystals were glue–glycerol bonded, forming threads with high concentration of OH groups and thus forming a preferential path for water vapor diffusion through the nanothreads.

The internal microstructure of the final composite is therefore a key aspect in its permeability properties. Whether generating impediments to the diffusion of molecules or generating pathways through which the material can penetrate thanks to chemical affinities, this property will be modified by the inclusion of fillers. Besides filler–matrix interactions, the used processing methodology can be highly influential, as due to the filler's inclusion voids and structural defects in the matrix can be created during processing. Florencia et al. [118] studied cassava and ahipa peels and bagasse as potential fillers of TPS films. They found that all TPS composite films presented WVP values similar to those of the TPS matrix. This behavior was attributed to two

offset factors. On the one hand, the filler presence increases tortuosity within the film matrix and therefore reduces water vapor diffusion. On the other hand, the processing method could promote the generation structural defects in the matrix facilitating the water molecule transport. The processing of the composite could also influence in the final water content of the composite and therefore its WVP. Ochoa-Yepes et al. [42] compared WVP of starch/lentil protein composite films obtained by extrusion/thermocompression and casting techniques. Extruded samples had lower WVP values tan that obtained by casting. This is consequence of a difference in the materials with water content. The extrusion/thermocompression process involved less water and higher temperatures than casting methodology, leading to materials with lower water contents. As water plasticizes TPS, it reduces internal hydrogen bonding between polymer chains, increasing molecular volume. It is therefore expected for materials with higher water content to have greater diffusion coefficient of water vapor and therefore to experiment increased in WVP.

Another possible strategy to improve the water vapor permeability of starch-based materials is the inclusion of hydrophobic agents, such as lipids. In general, the addition of this type of compounds to hydrophilic film matrices decreases the WVP due to the promotion of hydrophobicity and increases the OP values due to the greater oxygen solubility in the hydrophobic regions of the matrices [129]. In these cases, the addition of emulsifying or compatibilizing agents or a previous encapsulation process is mandatory to improve compatibility. Talón et al. [35] studied the effect of incorporating free or spray-dried encapsulated eugenol on the barrier properties of compression-molded corn starch composite films. Films containing non-encapsulated eugenol showed higher WVP and OP than both pure starch films and films incorporating microencapsulated eugenol. When non-encapsulated eugenol is incorporated into the starch matrix, starch–eugenol complexes are formed, in which the hydrophobic cavity of the helical conformations of amylose and amylopectin chains are involved. These complexes could limit eugenol's active role at reducing the matrix's water affinity, reaching a higher equilibrium water content which enhanced all the diffusion-dependent processes, such as water vapor or gas permeation. When microencapsulated eugenol was added to the starch films, the WVP values and water content decreased as expected for the incorporation of more hydrophobic components. Octenylsuccinated starch (OS) can act as an emulsifier for oil-in-water (O/W) system, and therefore it can be used to prepare starch–lipid composite films. The process of molecular self-assembly of film-forming components is shown in Fig. 10. Gao et al. [130] prepared corn/octenylsuccinated starch (C/OS) composite films incorporating soybean oil (SO) at 0, 0.5, 1.0, 1.5 and 2.0 wt%. The WVP of control film without SO was 2.93×10^{-12} g cm/cm^2 s Pa, while for the composite films it gradually decreased from 2.72×10^{-12} g cm/cm^2 s Pa to 2.46×10^{-12} g cm/cm^2 s Pa, when the SO concentration increased from 0.5 to 1.5%. A similar strategy was used by Kang et al. [131], who investigated the physicochemical properties of amylose–lipid inclusion complexes and their film-forming capacities. The authors used ultrasonication to promote the complexation between amylose and liquid and solid fatty acids. The WVP values of the films formed from starch–lipid composites were significantly lower than that of the native starch film. This decrease was ascribed to the presence
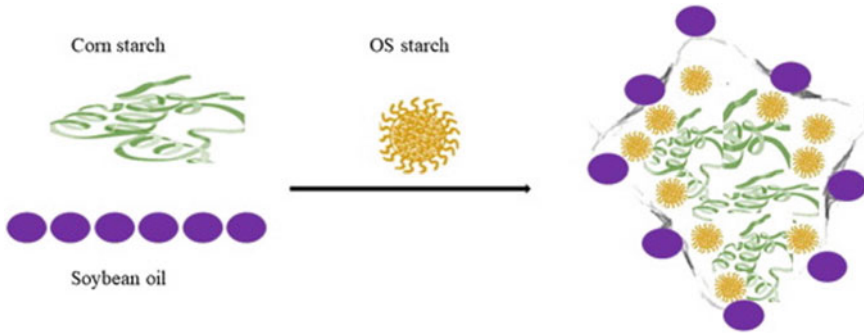
Fig. 10 Process of molecular self-assembly of corn starch, corn/octenylsuccinated starch (OS) and soybean oil. Reprinted from Gao et al. [130], Copyright (2020)

of hydrophobic carbon chains and amylose–lipid complexes in the polymer matrix. When comparing the results obtained with the incorporation of liquid or solid lipids, it was found that the former led to lower WVP values. This result is attributed to the fact that fatty acids in liquid state have shorter carbon chains than solids, so they can be more easily incorporated between the polymeric chains of the matrix, leading to a more compact structure and restricting the water permeability. Parallel, lower WVP values were found for films prepared from ultrasonicated starch–lipid complexes than those formed from untreated ones, demonstrating that the ultrasonic treatment improved the moisture resistance of films. The authors suggested that the ultrasonication process was favorable to construct a more compact and uniform structure in the polymer matrix, thus decreasing the WVP values.

The incorporated amount of filler is also of utmost importance when evaluating its effect on barrier properties of the composite. In the case of oleo-fillers, while very low contents may not be enough to hinder the passage of vapor molecules, high contents could interrupt the hydrogen bonds between the starch molecules, destroy the network structure and expand the molecular interstice of the films, thus leading to higher WVP value [130].

There are different ways to evaluate the water sensitivity of TPS composites. Due to their hydrophilic nature, it is clear that they will be highly sensitive to moisture, and this can be a problem for many applications. Depending on the aspect to be evaluated, it is possible to study the absorption isotherms, the water uptake from the environment, the wettability or directly the solubility of starch-based films. In each case, there are strategies to improve the material stability. Although the inclusion of fillers into TPS matrices cannot completely change its hydrophilic nature, if the right combination is chosen substantial improvements can be achieved.

As it was mentioned before, TPS absorbs water from the environment when the environmental RH increases or loses water while the RH decreases. This change in moisture content of TPS materials leads to modifications in their structure and, therefore in many of their properties, including mechanical, thermal and barrier ones. Moisture sorption isotherms show the relationship between water content of

TPS materials and the environmental RH, at a constant temperature. Although there are many models proposed for the behavior of these materials, no single equation can describe accurately the relationship of equilibrium moisture content and environmental RH for various TPSs over a broad range of RH and temperature, and even less in the case of composites. Therefore, for each TPS-based material, it is necessary to investigate its behavior at different RHs. Several authors used the GAB model to fit starch-based material water sorption isotherms, indicating the monolayer moisture content (M_0) as the most representative parameter [132, 133, 134]. Typically, starch and protein-rich product behavior corresponds to Type II isotherms, according to BET classification. At low RH values, film humidity content increases gradually up to a limit water activity (a_w), after which an strong increment is obtained. This significant increase of equilibrium water content is attributed to a phenomenon called "water clustering" [132].

López et al. [132] studied the influence of talc nanoparticle inclusion in corn TPS films on their sorption isotherms. Films containing talc presented a similar behavior than TPS ones, but particle incorporation reduced water sorption for $a_w > 0.4$. Strong polar interactions among starch, glycerol and mineral edge surface establish a competition mechanism which could explain the reduction of water sorption capacity of composites based on TPS by talc presence. The M_0 parameter was reduced with talc incorporation, but a net tendency with particle concentration was not evidenced. The authors explain this effect as the consequence of the low filler contents used to develop starch-based composites. Similar effects were observed by other authors, indicating that generally polymer matrix governs the sorption mechanism of TPS composites [135].

Other possibility is to study the material's water uptake while it is in a constant RH over time. Samples with the same size and equally stabilized are exposed to constant temperature and relative humidity for a time period. Water sorption (W_S) is calculated as

$$W_S(t) = \frac{W_1 - W_0}{W_0} \times 100\%$$

where W_1 is the measured moisture content at time t and W_o is the initial moisture content.

These tests can be carried out in the extreme case of 100% RH or in a particular RH value where the material is supposed to be applied, comparing how different materials (matrix and composites) absorb humidity from the environment. Fillers with lower hydrophilic character than TPS could reduce composites' moisture absorption. On the other hand, hydrophilic fillers could also reduce water uptake, as functional groups on their surface could interact with starch OHs resulting in good interfacial adhesion between the two phases and fewer sites capable of interacting with absorbed water. Cellulosic fillers have shown the ability to reduce starch-based composite water uptake thanks to this phenomenon [43, 48, 136]. However, the improvements are usually moderate. Fourati et al. [48] studied the moisture absorption maximum of TPS and TPS/CNF nanocomposites at 50% RH. They found that it was slightly

reduced by the addition of CNF decreasing from about 10% for unfilled TPS to about 8.5% for TPS/CNF. Ghanbari et al. [43] also included CNF in a TPS matrix and studied the moisture absorption, but at a RH level of 98%. They found that the water uptake of nanocomposites filled with 1.0 and 1.5 wt% of CNFs compared to the neat TPS was reduced to 6.4% and a 10% after 24 h, respectively. Other authors also found moderate improvements with the addition of sugarcane bagasse [137] and clays [138] into TPS matrices.

The wettability of TPS films can be evaluated through water contact angle (CA) measurements. Usual contact angle of glycerol-plasticized TPS films is around 40°. This value is of course related to the sample's surface polarity and can be modified thanks to the addition of fillers. One of the most hydrophobic compounds that can be introduced into TPS matrices is those of the lipid type. As it was mentioned before, the use of emulsifiers is a usual strategy for the preparation of starch–lipid composite films. Gao et al. [130] developed corn/octenylsuccinated starch (C/OS) composite films with soybean oil at 0, 0.5, 1.0, 1.5 and 2.0 wt%. OS acted as an emulsifier leading to the formation of molecular structures represented in the diagram of Fig. 10. Those conformations where a lipid-rich out layer surrounds a starch-rich phase can create a lipid-rich phase at the surface increasing the contact angle due to its higher hydrophobicity. In fact, the CA values were 39.9°, 45.4°, 58.6° and 76.1° for SO additions of 0, 0.5, 1.0 and 1.5%, respectively. However, in the presence of higher concentrations of SO, the aggregation of oil droplets in the film occurs, and therefore the conformations of Fig. 10 can no longer be formed. In this case, a lower CA value is obtained (37.0° for 2%).

Other lipophilic possible fillers are modified clays. The incorporation of MMT has turned out to be an adequate strategy to increase the contact angle of TPS films in many cases [138, 139]. In the cases of glycerol-plasticized TPS composites, a fraction of the glycerol plasticizer can migrate to the clay phase, reducing the glycerol content of the polymeric matrix and therefore its hydrophilicity [140]. Other plasticizers have proven to be successful in the reduction of TPS hydrophilicity, regardless of the incorporation of fillers. It is the case, for example, of deep eutectic solvents (DESs), which led to TPS films with contact angles in a range 80–90°. The filler–plasticizer interaction can be determinant in the final composite wettability. Adamus et al. [52] showed that the introduction of urea-intercalated montmorillonite (UM) to TPS films plasticized with two different deep eutectic solvent systems, choline chloride (ChCl) with urea (U) or with imidazole (IM), caused unlike influence on wettability depending on the particular DES. Contact angle decreased from 89° to a range 62–74° for starch/ChCl/U-UM and almost constant values 82–85° for starch/ChCl/IM-UM. The authors attribute the wettability reduction caused by the incorporation of UM to the fact that intercalated UM seems to exhibit higher polarity and then easier wettability than sodium montmorillonite itself. Differences between wettability of the films plasticized with ChCl/U and ChCl/IM are probably caused by various tendencies of particular DES to withdraw U from interlayer clay space at equilibrium state of ChCl/hydrogen donor compound into starch bulk matrix, as well as a result of specific interaction between IM and U molecules. Besides urea intercalation, there are other strategies usually applied to enhance filler compatibility

with the starch matrix. These modifications usually include the incorporation of more hydrophilic groups, which could lead to an increase in the composite's polarity. It is the case of Abreu et al. [141] who found that the incorporation of MMT modified with a quaternary ammonium salt C30B into a TPS matrix caused a significant decrease in the water contact angle value of the composite with respect to the matrix. Chen et al. [142] studied the wettability of TPS composites with the incorporation of microcrystalline cellulose (MCC) and oxidized MCC (TOMC), finding that water contact angle of TPS films (38.72°) grows with the incorporation of MCC to values between 46° and 68°, but in the case of TOMC composites its contact angle value and wettability were close to native TPS films.

Water solubility is another important aspect to be evaluated. Depending on the final application of the material, different behaviors will be needed when submerged in water. A clear example is that of coating materials for laundry condensate beads, in which different sections are expected to dissolve at different times [142]. The presence of discontinuities (microparticles) in the polymer matrix usually promotes a greater water disintegration of the films usually related to a greater solubility. Talón et al. [35] showed that the incorporation of microencapsulated eugenol into a starch matrix promoted its water disintegration. Moreover, they showed that the interfacial adhesion between the filler and the matrix plays a key role. Azevedo et al. [143] also showed this for corn starch–whey protein blend films obtained by extrusion.

3.1.3 Mechanical Properties of Starch Matrix Composites

Depending on the materials' final application, different mechanical properties will be needed. Packaging films, for example, are expected to possess high tensile strength, which helps them to endure the regular stress met while handling food, but not very high elongation at break [144]. On the other hand, films for agricultural mulches must withstand high elongations so that they can be placed on the ground without deterioration [145]. Mechanical properties of starch films are usually not enough for many potential applications. Furthermore, the great variability in these properties, due to the high water sensitivity of films, introduces an additional problem. In 0% relative humidity, starch-based composites' mechanical strength can reach values as high as 20 MPa, while when the moisture contents are high, the tensile strength may be as low as 1 MPa [144].

The improvement in mechanical properties and handling of TPS materials thanks to the incorporation of micro- and nanofillers has been known for a long time [13, 47, 136, 146]. As it has been mentioned before, interactions in the filler–matrix interface will greatly influence the composite mechanical properties. Strong interaction at the interface leads to the transmission of stress from one component to the other, so if the added filler has greater Young's modulus and tensile strength than the matrix material, these two properties will grow in the composite. On the other hand, the elongation at break depends on failure propagation. In general terms, many well-distributed nanofillers with well interaction at the interface can anchor cracks, increasing the elongation at break. Simultaneous increases in elongation and stress at break lead

to an increase in tensile toughness. In the case of microfillers, generally it is not possible to increase the elongation at break because although the achieved dispersion is excellent, there will be large domains in the matrix that do not have any filler capable of anchoring cracks. Figure 11 illustrates the difference in the distribution of nano- and microfillers in a matrix.

Beigmohammadi et al. [136], for example, worked with microfillers, investigating the effect of rye flour and cellulose as reinforcement agents in starch-based composites on mechanical properties. They found that filler incorporation had positive effect on tensile strength (TS) and Young's modulus, increasing from about 7 MPa for the starch matrix to more than 65 MPa for starch composites, reflecting the chemical and structural compatibility between starch and fillers. Unlike TS, the elongation at break decreased from 31.96 to 5.02%. On the other hand, Li et al. [139] incorporated montmorillonite (MMT) into a corn starch (CS) matrix to generate CS/MMT nanocomposite. They proposed a facile biomimetic method to enhance the interfacial adhesion between layered clay and polymer matrix based on the coating of clay nanofiller with a thin layer of polydopamine (PDA). The obtained results demonstrated that PDA coating benefited not only the intercalation and dispersion of the modified MMT (MMTDA) in the starch matrix but also the strong interfacial adhesion between filler and matrix. Thanks to this strong adhesion and the nano-character of the filler, simultaneous improvements of strain and stress at break were achieved.

Among the most widely used reinforcements for starch matrices, starch nanocrystals (SNCs) allow to create self-reinforcing starch materials. It has been demonstrated that the reinforcing effect of SNC is more significant in TPS than in other matrices, probably because of the strong interactions between the filler and amylopectin chains and a possible crystallization at the filler/matrix interface [148]. The same reinforcing effect has been reported by other authors [128, 149, 150, 151].

Other polysaccharides can also be transformed into nanofillers and introduced in starch matrices. That is the case of chitosan, which can be introduced into starch matrices as nanoparticles and thanks to their similar polysaccharide structures and

a) micro composites   b) nano composites
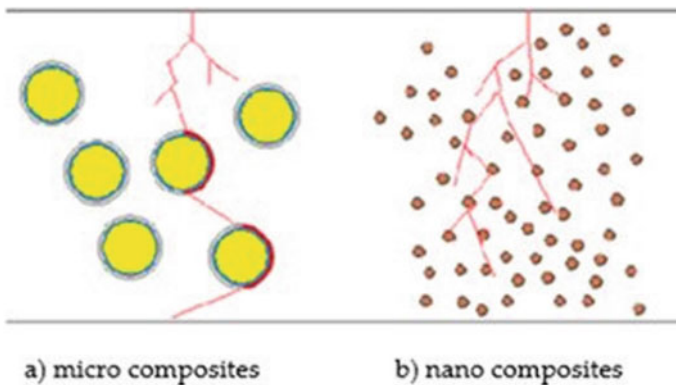
Fig. 11 Distribution of micro- and nanofillers in a matrix. Adapted from Cheng and Yu [147]

their great interaction can greatly improve the matrices' mechanical behavior [152, 153]. Moreover, chitosan has the great advantage of having antibacterial activity, which makes it very promising for applications in medicine, agriculture, drug release and edible film packaging [154].

Cellulosic reinforcements also have high affinity with starch matrices. Different authors have reported important mechanical properties' improvements thanks to this type of fillers [142], [155]. The formation of a rigid nanofiller network, the mutual entanglement between the nanofiller and the matrix, the efficient stress transfer from the matrix to the nanofiller, and the increase in the overall crystallinity of the system resulting from the nucleating effect of the fillers are the main reasons of these improvements [142], [155]. One important variable to be considered when analyzing the quality of the reinforcement is the filler morphology. It has been demonstrated that cellulose nanofibers (CNFs) have better reinforcing ability and stress transfer character than nanocrystals. This is attributed to a stronger intermolecular attraction between starch and nanofibers, consequence of a higher entanglement degree [156]. However, it is important to clarify that the degree of improvement achieved by CNF into starch matrices is considerably less than that achieved in other polymers, such as acrylics [157]. This lower reinforcing effect in TPS matrix could be due to two possible causes. On the one hand, the plasticizing agents (glycerol and water) could accumulate at the CNF/matrix interface which might reduce the possibility of interaction among neighboring fibrils through hydrogen bonding. On the other hand, the chemical similarity of CNF and starch will favor a high interfacial interaction between the two phases at the expense of CNF–CNF interaction, reducing the strength of the nanocellulose network which is known to play a key role in the mechanism of nanocellulose reinforcement [48, 158].

Besides the fillers' morphology, the way in which they accommodate in the matrix will also define the composite's mechanical properties, specially in the case of 2D fillers, such as clays and graphene sheets. Three different polymer nanocomposites can be prepared from 2D clays: (a) intercalated structure, (b) exfoliated structure and (c) flocculated structure-based nanocomposites. In general terms, exfoliated and intercalated structures will lead to greater mechanical property enhancement [159].

A useful strategy to obtain a stable dispersion of two-dimensional (2D) MMT plates in aqueous systems is through the incorporation of one-dimensional (1D) cellulose nanofibers. These systems could be used to develop starch/MMT/CNFs ternary nanocomposites. CNF can interact with MMT sheets via hydrophobic interaction between MMT sheets and specific crystalline faces (hydrophobic (200) planes) of CNF, and also with starch molecular chains from numerous hydrogen bonding through the hydroxyl groups on CNF surface. It is the case of Li et al. [138] who studied the synergistic reinforcing mechanisms of the MMT-CNFs system. They found that the tensile strength of starch/MMT/CNF ternary nanocomposites showed a remarkable improvement, which was much higher than that of the binary starch/MMT and starch/CNF nanocomposites. They ascribed this to the homogeneous dispersion of MMT, strong interfacial interaction between the fillers and matrix, and the lamellar structure with alternate stacking of 2D MMT platelet and 1D CNF fibril network layers in the ternary system. A schematic illustration for preparation
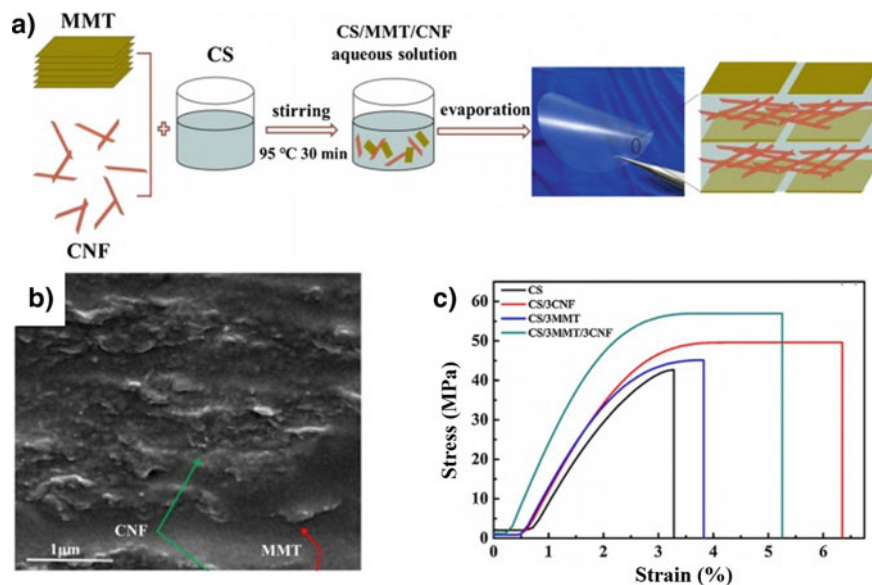
Fig. 12 **a** Schematic illustration for preparation of CS/MMT/CNF composites, **b** SEM image of CS/3MMT/5CNF × 80,000, **c** tensile stress–strain curves of CS film, binary CS/3CNF and CS/3MMT films, ternary CS/3MMT/3CNF film. Reprinted from Li et al. [138], Copyright (2019)

of starch/MMT/CNF composites, a SEM image of CS/3MMT/5CNF and tensile stress–strain curves are presented in Fig. 12.

The filler content is also determinant in the improvement effect. For each system, there will be a formulation with an optimal filler concentration that will lead to the greatest improvements in mechanical properties. Fazeli et al. [119], for example, showed that the maximum improvement in tensile strength for starch-based composite films reinforced by cellulose nanofibers was obtained for a concentration of 0.4 wt%. Tensile strength and elastic modulus increased by up to 80% and 170%, respectively. However, above 0.5 wt% CNF, tensile strength started to deteriorate. The authors proved that an excess of CNF content provokes particle agglomeration or phase separation in the starch matrix.

3.2 Properties of Starch Blend Matrix Composites

3.2.1 Introduction to Starch Blend Properties

Blend's properties can be manipulated according to their end use by correct selection of component polymers, additives and processing conditions. The properties of the

polymer blend will depend on the final morphology, making the components' misci-
bility and phase behavior a key issue. In the specific case of heterogeneous polymer
blends (obtained from immiscible polymers), the compatibility between polymer
phases decides the final achieved properties.

A very important aspect when studying the properties of a blend is knowing how
they behave with temperature, since this will influence their future processing to give
it a certain shape, by either injection, blowing or thermoforming. In PHB/starch or
PBAT/starch blends, as in the vast majority of engineering polymer blends, phase
separation occurs as a consequence of polymers' immiscibility. The glass transition
behavior associated with these systems demonstrates an elevated level of complexity,
showing multiple transitions, ascribed to pure component phases and regions of
partial mixing [160]. Properties such as crystallization and melting behavior of blends
are also strongly influenced by the miscibility of involved polymers [161]. On the
other hand, thanks to the characteristic hydrophobicity of both polymers, the water
sensitivity is expected to be improved in the blend compared to starch-based mate-
rials. This will highly depend on the compatibility achieved between phases, as
cracked morphologies will not allow the improvement of starch's moisture stability.
In the same way, poor adhesion at the interface of the polymer phases in the blend
results in diminished mechanical properties such as lower impact resistance and
elongation at break [161].

In the next sections, the properties previously described for TPS composites are
detailed for the case of composites obtained from starch blends with PHB and PBAT.
Taking into account the importance of the affinity degree achieved between the
blended polymers, the results obtained when using different compatibilizers as well
as modified polymers are detailed.

3.2.2 Properties of Starch/PHB Composites

Thermal Properties of Starch/PHB Composites

The thermal properties of starch/PHB blend strongly influence their process-
ability. As discussed earlier, melting point of PHB limits the temperature range
for processing it with starch. PHB is a thermoplastic polymer with relatively high
melting temperature which is in the range of 170 and 176 °C [73, 77, 92, 94, 162].

In the case of starch/PHB blends, the melting temperature of the binary mixtures is
slightly reduced by the increment of starch amount in the mixture as consequence of
the lower melt viscosity of starch contrary to that of PHB [162, 163]. For example,
Liao and Wu [163] prepared PHB/starch blends by compression molding method
using the acrylic-acid-grafted PHB (PHB-g-AA) as an alternative to PHB. With
both, PHB and the grafted polymer, the melting temperature of the mixtures gradually
decreased up to 4 °C from 0 to 30% of starch added.

On the other hand, the incorporation of plasticizers into the formulation has
been applied to considerably reduce the melting and glass transition temperatures
of the starch/PHB mixtures, thus enhancing the blend processability. For example,

Innocentini-Mei et al. [164] blended native and modified starches (starch adipate and grafted starch–urethane) with PHB by injection molding. Triacetin was added as plasticizer of PHB resulting in blends with lower melting temperatures ($T_m =$ 141.5–159.1 °C) and glass transition temperature ($T_g = -19.2$ °C and -38.9 °C) than that of neat PHB ($T_m = 171$ °C and $T_g = 0.7$ °C). Likewise, the utilization of glycerol as plasticizer of starch led to reduce the melting temperature range of the binary blends (TPS/PHB, 70:30 wt%) by 10 °C compared to that of pure PHB [165].

As it was mentioned before, the blend glass transitions will depend on the components' miscibility. While TPS plasticized with glycerol typically shows two T_gs, PHB exhibits just one T_g between -2.5 and 0.7 °C [92], [164]. In the case of TPS/PHB blends, the three T_gs are maintained due to the inherent immiscibility of both components. However, the Tgs of starch on the blends cannot always be observed using the differential scanning calorimetry (DSC) technique because of the chain rigidity and the strong hydrogen bonding of starch molecule [92]. In addition, the temperature at which transitions occur can vary. For example, Innocentini-Mei et al. [164] prepared three types of blends based on PHB (plasticized with triacetin) and TPS from native starch, starch adipate and grafted starch–urethane by injection molding. The amount of starch added to the plasticized PHB matrix varied from 10 to 30%. The plasticized PHB matrix had a T_g at -25.7 °C. However, this T_g value shifted to a lower (-19.2 °C) or higher (-38.9 °C) temperature in the three kinds of TPS/PHB blends depending on the amount of PHB and the type and amount of starch used. For blends of PHB with native and adipate starches, no other T_g values were observed. However, the blends prepared with grafted starch–urethane at concentrations over 20% showed an extra T_g in an interval of -42.2 °C and -58.8 °C attributed to the glass transition of these modified starches.

The thermal decomposition of PHB-TPS blend has also been studied. Generally, it occurs in three stages that are associated with the decompositions of the PHB and the TPS. As it was mentioned before, TPS has three-step degradation. The first step corresponds to the loss of water, the second to the degradation of other plasticizers, such as glycerol, and the third to starch degradation ($T_d = 323$ °C). On the other hand, degradation of PHB occurs in two steps [77, 166]. The first is associated with the rupture of the ester groups, and the second is attributed to the plasticizer in the commercial PHB [166]. In the PHB-TPS blend, three stages of decomposition have been found and associated with the decompositions of PHB and TPS [77]. PHB stability is expected to be improved by blending it with starch due to the formation of hydrogen bonding between hydroxyl groups of starch and carbonyl groups of PHB that may inhibit early PHB degradation [94]. Different authors have reported that with the addition of PHB, the beginning of thermal decomposition of starch/PHB blends remains as that of the starch and the maximum temperature at which it occurs is shifted to higher temperatures as PHB amount increases [93, 165].

The inclusion of fillers into starch/PHB blends can influence its thermal stability. The effect of clay and eugenol inclusion was studied by Garrido-Miranda et al. [77], who observed temperatures for 5 wt% weight loss (T95%) and 10 wt% weight loss (T90%). The T95%, corresponding to the first step of starch degradation (water loss), was displaced to higher temperatures. This could be attributed to a reorganization

caused by the clay's inclusion that restricted starch chains, and therefore, higher energy for the degradation process is needed.

Gas Barrier Properties and Water Sensitivity of Starch/PHB Composites

One of the main causes that motivates the formulation of starch/PHB blends is the necessity of reducing the water uptake of starch and therefore enhances and extends the range of application of starch-based materials. An inherent characteristic of PHB is its hydrophobic character as a result of the large number of carbonyl groups in its structure, which makes it a suitable material for packaging applications. In this context, blending starch with PHB may improve the starch WVP and water sensitivity if both polymers are compatibilized, obtaining a co-continuous phase without the presence of cracks at the interface. It should be noted that PHB barrier properties against other gases, such as oxygen, are poorer than starch ones, being the OP 13.4 mL * 700 μm/(m^2 * 24 h * 0.21 atm O$_2$) and 9.1 mL * 700 μm/(m^2 * 24 h * 0.21 atm O$_2$) for PHB and starch, respectively [167]. Taking into account that the property to improve in starch matrices is their moisture barrier capacity, in this section we will focus on WVP along with other aspects of materials' water sensitivity.

Thiré et al. [93] explored the water absorption of PHB/starch blends by contact angle assay studying the kinetics of spreading a drop of water on the materials' surface every 15 s. To prepare the blends, previously melted PHB and different amounts of starch (0–50%) were processed by injection molding. PHB film showed the highest value of contact angle owing to its hydrophobic character and intrinsic rigidity, contrary to that in TPS films in which the drop of water rapidly spread on their surface due to its high water adsorption tendency. These values were intermediate for all blends with starch content from 20 to 40%. Over time, an increase in the water absorption rate was observed with the increment in starch content. The contact angle for PHB80/starch20 was 76° and diminished to 69° for PHB60/starch40. Likewise, Liao and Wu [163] showed similar findings on the study of water absorption of PHB/starch blends produced by compression molding for six weeks. The study included different contents of starch (10–50 wt%), and the possibility to include acrylic-acid-grafted PHB was also studied. Better water resistance was obtained with PHB-g-AA/starch than with PHB/starch at the same amount of starch. These results were attributed to the formation of ester carbonyl function groups by the reaction between starch's hydroxyl groups and anhydride carbonyl groups of PHB-g-AA. In addition, the increment of starch content in the blends led to higher water uptake again which was assigned to lower miscibility of both polymers. The positive effect of PHA on the increasing water resistance was showed also in TPS matrix combined with other polymer. Tingwei [168] prepared TPS/PBAT/modified-PHA biodegradable films with enhanced water repellency to be applied in a variety of industries such as sanitary products.

The addition of less hygroscopic fillers into TPS/PHB blends could improve the water sensitivity and barrier properties even more. Magalhães and Andrade [169]

showed that the incorporation of PHBV and an organically modified montmorillonite (C30B) into a starch matrix was able to reduce the moisture absorption of the extruded materials in more than a 50%. While the maximum water absorption of TPS was about 14% of its dry weight, this value was reduced to 6.3% for the PHBV50/TPS50 neat blend, decreasing up to 3% when C30B was added. This result is in agreement with the property of organoclays as a barrier against humidity.

Mechanical Properties of Starch/PHB Composites

At room temperature, TPS films are soft and ductile while PHB films are rigid and brittle with high Young's modulus and tensile strength at break due to its high crystallinity (about 80%). PHB brittleness is attributed to the formation of large volume-filling spherulites from few nuclei which are accompanied by interspherulitic cracks, and to the secondary crystallization of the amorphous phase which takes place during storage at room temperature [170].

The crystallinity level of PHB is usually tuned by crystallization rate that affects the nucleation rate and spherulite size [171]. Generally, PHB presents slow crystallization rates which will depend on the production method. At temperatures between 80 and 100 °C, the crystallization rate is fast, but it is slow below 60 °C and above 130 °C resulting in a higher crystallinity. In addition, PHB suffers recrystallization with aging at room temperature, and a progressive reduction of the amorphous content in the partially crystalline polymer, changing its mechanical properties with time, for example, an increase in yield stress and modulus, and decrease in elongation at break and fracture toughness. The incorporation of some additives such as plasticizers and nucleating agents contributes to the reduction of crystallization process and to impart flexibility and toughness to the material. Râpă et al. [172] investigated the incorporation of three plasticizers, triethyl citrate (TEC), tributyl o-acetylcitrate (TBoAC) and tributyl citrate (TBC) in PHB via melt-mixing procedure and studied the effect of these additives on thermal and mechanical properties. Then, the incorporation of plasticizers into PHB decreased tensile strength and Young's modulus, but increased elongation at break; PHB/plasticizer blends exhibited a wider melt-processing window with a lower melting temperature.

Mechanical properties of starch/PHB blends are mainly affected by their degree of compatibility and miscibility to a greater or lesser extent, as well as processing conditions. As morphological characteristics of blends are strictly related to the mechanical properties, they will be also described along this section. Poor interfacial interaction between starch and PHB often leads to heterogeneous blends. Zhang and Thomas [94] investigated the effect of blending two types of starch (high amylose corn starch and regular corn starch) with PHB in a ratio of 30:70. No plasticizer or other additives were added in the formulation. Starch and PHB were melted at 175 °C for 10 min at 50 rpm, and then the assembly was hot-pressed at 180 °C. According to dynamic mechanical thermal analysis (DMTA), high amylose starch had better interfacial bonding with PHB due to its linear structure compared to regular starch. On the other hand, SEM micrographs of cryogenic fracture blends' surfaces showed

that starch granules still kept their structure which negatively affected the blends' mechanical properties according to the researchers. As the major component of the blend was PHB and starch granules were not disintegrated through processing, the researchers inferred that starch acted as a filler of PHB matrix. Similar results were obtained by Thiré and collaborators [93]. The authors prepared PHB/starch blends with different contents of maize starch (0–50%) by compression molding. Herein, PHB was melted in a mixer at 165 °C for 15 min, then a mixture of starch, glycerol and water was added into the melted PHB, and this resulting mixture was continuously mixed for 30 min at 60 rpm. Then, the mixes were hot-pressed at 160 °C and 69 MPa for 30 min to form sheets. TPS for comparative purposes was prepared at 60 °C and 20 rpm for 20 min, and then films were obtained by hot-pressing at 90 °C. SEM micrographs of fractured surface samples obtained after tensile tests revealed that starch granules were not disintegrated during processing. These granules kept their original size and were dispersed throughout the matrix, forming agglomerates when starch content was higher. Starch incorporation of up to 30 wt% into PHB matrix resulted in materials as hard as pure PHB ones. Young's modulus of blends with those starch contents remained practically constant in a value around 1300 MPa. If the amount of starch was increased, the module's value decreased until reaching 850 MPa for a starch content of 50%. These values are much higher than that reported by the authors for TPS (300 MPa). However, all the binary blends were much less flexible than TPS films and PHB since they presented lower values for elongation at break. The authors explained these results by the lack of interfacial adhesion between starch and PHB and by the heterogeneous dispersion of starch granules over PHB-rich matrix, and they concluded that both polymers were processed at very light processing conditions which did not allow starch degradation.

In addition to the polarity differences of starch and PHB, the difficulty of an adequate process of starch is added when it is blended with PHB. A suitable gelatinization/destructurization and/or plasticization of starch is required to promote the compatibilization between starch and PHB to produce blends with higher performance of their mechanical properties. Lai et al. [173] prepared TPS/PHB blends from potato, corn and soluble potato starches. The starches were gelatinized at different degrees, adding glycerol (25 and 33%) and water (25 and 17%) at 90 °C for corn starch and 70 °C for both potato starch and soluble potato starch, during 30 min at 50 rpm. TPSs and PHB (1–7%) were mixed for 10 min at 180 °C. Then, the prepared batch was compression-molded to obtain 1-mm-thin sheet. In all cases, the dimension of starch granules in the sheets was in the order of 1 μm according to SEM micrographs. Besides, as PHB content increased, tensile strength of blends generally grew from 0.6 to 5.8 MPa, which was attributed to the high strength of PHB and a reasonable compatibility between TPS and PHB. In addition, the higher molecular weight and the more compact structure of potato starch with respect to soluble potato starch and corn starch conferred it better tensile properties. The authors ascribed the better performance of the blends to the suitable gelatinization of starch.

A processing method that could lead to the development of materials with better properties is reactive extrusion, in which interfacial adhesion between components can be enhanced. Avella et al. [174] developed PHBV/starch blends using between 20

and 30% of a high amylose content starch by both traditional and reactive extrusions. They found that in the case of traditional extrusion, as the starch content increases, impact resistance decreases, and attribute this behavior to the poor interfacial addition between polymers and failure propagation. In the case of reactive extrusion in the presence of peroxides, a better interaction between the two components is achieved, which is responsible for good stress transfer. In particular, with a 20% of starch the blend's impact resistance improves, while with a 30% of starch it is in the same order, in both cases comparing with PHBV.

Researchers have been exploring other alternatives for enhancing mechanical and physical properties of starch/PHB blends through upgrading their compatibility. Recently, Florez et al. [165] modified the surface of PHB with an atmospheric plasma treatment to compatibilize its particles with the matrix of TPS. The selected gases for the mentioned process were atmosphere air and sulfur hexafluoride (SF6) gas which caused surface ablation of the particles. Starch (35–75%), glycerol (25–35%) and PHB (10–30%) were melted at high rotation for short times (1800 RPM for 20 s followed by 3600 RPM for 5 s). Disks of ≈2 mm of thickness were obtained after hot-pressing the melted mass at 90 °C for 15 s with 8 tonne force. Pristine TPSs had homogeneous surface suggesting that processing was capable of promoting disruption of the starch granules; however, the blends exhibited bimodal morphology of the equiaxed and elongated PHB grains dispersed in the starch matrix. Besides, agglomerations of PHB particles were also found on the surface of blends. These agglomerations could be generated during plasma treatment leading to a fragile starch/PHB blends that induced the rupture of the materials, especially when PHB content was higher.

Knowing the miscibility degree between polymers is critical to choose compatibilizing strategies. Concerning this, binary blends of starch and PHB were produced using modified starches such as acetate starch, adipate starch and grafted starches [164]. These starches are characterized by their less hydrophilicity that might result in better affinity and interaction with the hydrophobic PHB. For example, Innocentini-Mei et al. [164] investigated the behavior of starch derivatives (10, 20, 30 wt%) blended with PHB by injection molding. Triacetin (30 wt%) was used as plasticizer of PHB. The assayed starches were natural starch, starch adipate and grafted starch–urethane. Grafted starches were obtained with 0.25 mol of PEG, PPG or Rucoflex polyester as grafting agents and the addition of 0.25 mol of diisocyanate. Before the injection molding process, natural starch and starch adipate were gelatinized in dimethyl sulfoxide (DMSO) (50 wt%) in a mechanical mixer. However, starches retrograded as a result of a presumable migration of DMSO to PHB, due to their affinity. Therefore, stiffer and brittle materials with poor mechanical properties were obtained as a consequence of the insufficient amount of DMSO employed and the poor affinity of these starches with PHB, even for the adipate starch as its modification level was very low according to its FTIR spectrum. On the other hand, for grafted starches/PHB, Young's modulus and tensile strength showed slightly higher performance than those obtained with the natural and adipate starch due to a greater affinity of its structure with PHB. However, elongation at break of all modified starches remained as that of natural starch.

Other proposed modifications include grafting EVA [175] or poly(vinyl acetate) [92, 162] to starch chains or acrylic acid to PHB [163]. Ma et al. [175] showed that the presence of EVA chemically bounded with starch inhibited the starch agglomeration and enhanced the toughness of starch–EVA/PHB materials as shown by an increment of elongation at break and tensile-fractured energy. Similarly, the increased compatibility between PHB and soluble potato starch grafted with vinyl acetate (VAc) resulted in blends with higher toughness than pure PHB [92]. However, all these strategies do not achieve enough improvements for many of the applications proposed for these materials. Going one step further, Yingxin et al. [176] used compatibilizers and at the same time included a new polymer in the blend. They used different combinations of compatibilizers, including glycidyl methacrylate (GMA)-functionalized polyolefin elastomer (POE) (POE-g-GMA), maleic anhydride-grafted ethylene–octene copolymer (POE-g-MAH), ethylene–methyl acrylate (EMA), acrylonitrile-chlorinated polyethylene styrene (ACR), ethylene–vinyl acetate (EVA), and different combinations of coupling agents, including silane, titanate and aluminate, to develop starch-based degradable polypropylene/PHB materials by extrusion process with good mechanical properties (high tensile strength, elongation at break and impact strength).

Filler incorporation into PHB/TPS matrices has been a successful strategy to improve the blends' mechanical properties. Garrido-Miranda et al. [77] analyzed the influence of eugenol and clay incorporation into a PHB/TPS matrix on mechanical properties. They worked with a derivate of montmorillonite (OMMT) modified by surfactants which has the same affinity for hydrophilic and hydrophobic polymers. The authors found that the OMMT presence improves the interaction between PHB and TPS by the formation of hydrogen bonds between eugenol and the available hydroxyl groups of the components. Then, the elastic modulus of the nanocomposites was higher than that of PHB-TPS. These results were explained by the reinforcing effect of the OMMT which caused partial immobilization of the polymer chains and the increment of the composites' rigidity. Another derivate of MMT was used by Magalhaes and Andrade [169] to produce bio-nanocomposite with TPS and PHBV. The researchers investigated the properties of 1:1 PHBV (with 3.4 mol% hydroxyvalerate units) and TPS nanocomposites, prepared by melt extrusion in the presence of the different contents of an organically modified montmorillonite (C30B, 2.5, 5.0, 7.5 and 10.0 wt%). Due to the reinforcement effect of the organoclay and the rigidity of PHBV, the nanocomposites were stiffer as the organoclay content increased resulting in a lower elongation at break and an increase in the Young modulus and tensile strength.

On the other hand, a recent alternative proposed to include starch in PHB materials is through the use of starch nanocrystals. Zhang et al. [177] used SNC to make matrices of immiscible PHB and PBS mixtures compatible. More degraded and nearly disappeared banded spherulite morphology was obtained with the addition of SNC to the matrix of PHB as SNC loading increased, which evidences the SNCs compatibilizer role. Consequently, improved phase adhesion and reinforcement were obtained resulting in a rigid material with a deformation at break 4 times greater than PHB.

3.2.3 Properties of Starch/PBAT Composites

Thermal Properties of Starch/PBAT Composites

Following the principles detailed in Sect. 3.2.1, the final blend's processability of starch/PBAT blend differs from that of the neat polymers. Generally, there is a new T_m of the blend, as well as a new viscosity and rheological behavior. PBAT has good crystallization and thermal stability, and it melts at about 123 °C and crystallizes at about 60 °C. As a result, it has good processing stability to be used alone or blended with other material [96].

When PBAT is blended with TPS, its melting point can slightly increase due to the stabilizing effect of TPS caused by the hydrogen bond interaction between the polymeric chains after mixing with PBAT. Lendavi et al. [114] reported an increase in the T_m of PBAT, from 123 °C to 125.7 °C for the blend PBAT50/TPS50.

Filler inclusion can increase the blends' T_m. Olivato et al. [113] showed a slight T_m increase of PBAT phase in TPS50/PBAT50 (124 °C) and TPS80/PBAT20 (124 °C) with the incorporation of 3 wt% of sepiolite nanoclay (126–127 °C). An increase in the nanoclay content from 3 to 5 wt% did not significantly affect composites' T_m. On the other hand, both blends exhibited a crystallization peak at 79 °C for TPS50/PBAT50 and 63 °C for TPS80/PBAT20. A significant increase in the T_c (84–86 °C) and decrease in the crystallinity content were obtained with the addition of sepiolite. The authors proposed that the clay was acting in the crystallization process mainly during the nucleation step, but could reduce the crystallinity degree, possibly due to confinement effect and steric hindrance, which restrain the crystal growth. Liu et al. [103] studied the T_m and T_c of TPS-SiO$_2$ composite blended with PBAT in a 60:40 ratio. They found that Tm of the PBAT phase in the composite did not differ from that of PBAT. Moreover, they found that the addition of two compatibilizers, MA and EVOH, to the blend caused no influence in the melting point. In the case of crystallization temperature of the PBAT phase, an important shift occurred for the TPS-nSiO$_2$/PBAT composite (83 °C) compared to neat PBAT (45 °C). The authors explained that this sharp increase could be due to the TPS-nSiO$_2$ particles acting as a nucleating agent. When MA and pEVOH were incorporated into the TPS-nSiO$_2$/PBAT blend, a higher T_c was observed for PBAT phase (88–89 °C).

These results suggest that, unlike the case of PHB, when blending PBAT with TPS, the melting temperature of the PBAT phase does not undergo significant changes. Moreover, the addition of the additives, such as compatibilizers or fillers, had no significant influence on the melting transitions of the composites. However, this is not the case of crystallization temperatures, which could be highly affected, modifying the properties of the final material.

As it was mentioned before, TPS plasticized with glycerol has two T_gs, one related to the plasticizer's rich phase and the other to the starch's one. In the case of PBAT, the principal T_g is found in the range −16 to −35 °C and is associated with its soft segments (aliphatic). In some cases, other T_g is observed around 60 °C, which is associated with the T_g of the hard segment (aromatics). In the case of starch/PBAT blends, as they are immiscible polymers, all the T_gs of the components are expected

to be present. Generally, three distinct transitions (from low to high temperature) are reported: the secondary relaxation of the glycerol-rich domain, the principal glass transition of the PBAT phase and the glass transition of the starch-rich phase which is overlapped with the one of PBAT's hard segments. This behavior was reported by several authors [100, 103, 108].

The addition of compatibilizing agents can have different effects. Better compatibility between phases tends to generate a shift in their T_gs toward each other. This effect has been reported as a consequence of the inclusion of different compatibilizers [97, 178]. In particular, Zhai et al. [97] found that the T_gs of the phases rich in PBAT and starch shifted toward each other when the content of the two polymers became close. They proposed that during the reactive extrusion process of a TPS/PBAT blend in the presence of CAc, some interactions may have occurred between starch and PBAT at the molecular level. CAc could graft single ester groups in the starch chains, decreasing their hydrophilicity and increasing their compatibility with PBAT. Simultaneously, if the interfacial adhesion is strong, T_g shifts to higher temperatures can occur, as more energy will be needed for molecules to gain mobility. For example, it has been demonstrated that the inclusion of PBAT-g-MA into TPS/PBAT blends leads to an upward shift of the relaxation temperatures of PBAT (+5 °C) and TPS (+20 °C) [100]. Zhai et al. [97] deduced that in HPDSP/PBAT 50/50 film, using citric acid as a compatibilizer, hydroxypropyl distarch phosphate interacts with PBAT, from changes in the alpha phase relaxation temperatures of both polymers. They found a slight shift in the T_g of the PBAT phase from −24.9 to −22.6 °C for HPDSP/PBAT 10 to 50 wt%. The glass transition for the HPDSP phase decreased from 84.4 to 81.7 °C. The authors suggested that during extrusion, some interactions between PBAT and HPDSP may have occurred and also a graft reaction between citric acid and modified starch HPDSP. Zhang et al. [108] blended PBAT with a previously extruded starch with glycerol as plasticizer and tartaric acid as modifier (TPS-TA). Using the blend PBAT30/TPS-TA70, they demonstrated that the compatibility between starch and the polyester matrix could be improved when starch had been pretreated. The incorporations of TPS-TA into PBAT shift the T_g associated with the polyester's soft segment (aliphatic) from −16.4 to −13.8 °C and one of the primary glass transitions of the starch-rich phase from 28 to 11.8 °C. These variations in glass transition temperatures demonstrate the compatibility of PBAT/TPS-TA composites. Starch modification with TA serves as a coupling reagent and reduces the phase separation.

Some compatibilizers can also act as plasticizers, and therefore its effect can be varied. DMA analysis of starch/PBAT/glycerol blends with different amounts of sericin performed by Garcia et al. [111] showed both sericin's plasticizing and compatibilizing effects depending on its concentration in the blends. For contents up to 1 wt%, T_g of the starch-rich phase was shifted to a higher temperature indicating that the molecular mobility of the starch chains was reduced and that sericin could be acting as a compatibilizer. The highest content of sericin (1.5 wt%) showed the opposite behavior, indicating a plasticizing effect. The authors proposed that the short-chain segments of sericin could act as plasticizers improving the mobility of the starch short-chain segments, while the larger sericin segments could act as compatibilizers between polymers, increasing stiffness.

The addition of fillers can, of course, also have effects on material transitions. Depending on whether the filler is located in the interface or if it tends to be interacting only in one phase, its effect will be different. For example, Olivato et al. [113] studied the effect of sepiolite inclusion in TPS50/PBAT50 blend. They found that strong interaction between starch molecules and sepiolite limited the mobility of the starch chains, producing a shift in the T_g of starch-rich phase to higher temperatures. This gives account of the high interfacial interactions between sepiolite and starch. When the filler is highly interacting with one of the polymers, then part of the plasticizer can migrate to the other phase. Lendvai et al. [114] blended PBAT with TPS nanocomposites (reinforced with BT and OMMT). They found that for blended nanocomposites both T_gs of TPS increased, probably due to the depletion of the plasticizer in the TPS phases that could have migrated into the PBAT phase. Similar results were found by Liu et al. [103], who blended PBAT with TPS-nSiO$_2$ nanocomposite. Compared with that for the pure PBAT ($T_g = -30$ °C), the glass transition of the PBAT phase in each of the composites was observed at a lower temperature by about 5–6 °C. They explained this as a consequence of the increased plasticizing effect on the PBAT phase by the migration of glycerol from TPS. The glass transition of the starch-rich phase for the TPS-nSiO$_2$ (60 °C) shifted to a higher temperature (70 °C) in TPS-nSiO$_2$/PBAT sample. The authors explained this result probably due to the poor compatibility between TPS and PBAT and the weakened plasticizing of the starch-rich phase from the migration of glycerol, which reduced the mobility of the starch chain segment. On the contrary, after the addition of the compatibilizer of MA, EVOH and MA + EVOH, the glass transition of the starch-rich phase in the nanocomposites shifted to a lower temperature (about 60 °C for MA, 62 °C for EVOH and 55 °C for MA + EVOH) than that for the sample without compatibilizer (about 70 °C). The lowered transition temperatures indicated that the introduction of both MA or/and EVOH could improve the compatibility between TPS and PBAT, resulting in the increased mobility of the starch chain segment. When the combination of MA and EVOH was used, the T_g of the starch-rich phase was the lowest (about 55 °C).

While neat PBAT decomposes in one step at 400 °C, thermal degradation of TPS/PBAT blends occurs as a three-step process, including a first stage attributed to the elimination of water and plasticizers (50–250 °C), a second much sharper transition at ≈320 °C, which represents the degradation of TPS components amylose and amylopectin, and a final third stage around 400 °C corresponding to the PBAT degradation [114].

The inclusion of fillers could cause changes in the different stages, depending on their interactions. Lendvai et al. [114] blended TPS-OMMT and TPS-BT nanocomposites with PBAT. They found a lower temperature and faster plasticizer degradation step for PBAT60/TPS-OMMT40 than for PBAT60/TPS-BT40 composite and PBAT60/TPS40 neat blend. This phenomenon was also observed in torque measurements, which revealed that OMMT-filled composites presented a higher degree of dehydration than the others. TGA results revealed that BT and OMMT incorporation on TPS affected its dehydration and degradation, suggesting that the clays remained predominantly in the TPS phase, where they were initially introduced. Liu et al. [103]

also blended a TPS nanocomposite with PBAT, but in their case it was TPS-SiO$_2$. The thermal stability of starch and PBAT in the PBAT40/TPS-SiO$_2$60 sample was not affected by the blending of PBAT with the starch nanocomposite. Moreover, when MA or/and plasticized EVOH were added as compatibilizers, the two main degradation temperatures were similar to those for the PBAT40/TPS-SiO$_2$60 nanocomposite, which indicated that the compatibilizers had no significant influence on the thermal stability of the composites.

Gas Barrier Properties and Water Sensitivity of Starch/PBAT Composites

While PBAT presents a good balance between biodegradability and thermal–mechanical performance, its barrier properties are lower comparing to traditional petrochemical non-biodegradable polymers. As it is well known, compared to starch, PBAT has lower WVP but its barrier properties against oxygen are poorer. Therefore, depending on the needed property different combinations can be performed. Generally, increasing the PBAT content in PBAT/TPS blends decreases the WVP and simultaneously increases the OP [97, 179, 180]. In this section, we will focus on water vapor permeability, as it is the property to improve in starch matrices.

When additives with compatibilizing action are added to starch/PBAT blends, stronger intramolecular bonds are expected, which could lead to the formation of a tighter structure that could restrict water vapor diffusion. It is the case of Garcia et al. [111], who incorporated sericin protein to improve the compatibility of a starch/PBAT/glycerol blend and found a reduction of almost 20% in the WVP of sericin containing films with respect to the blend without compatibilizer.

As in the cases of starch/PHB blends, blending starch with PBAT together with fillers using an appropriate processing strategy and conditions to promote an intercalated nanostructure, where better polymer–nanofiller interaction is achieved, will result in better barrier properties of the TPS/PBAT composite [181].

Manepalli and Alavi [50] used the modified Nielsen equation to model the WVP of the ternary blend of PLA/PBAT/TPS with the inclusion of nanocrystalline cellulose (NCC), as a function of filler morphology, filler content and the degree of filler–polymer interaction. As expected, more TPS contents lead to larger WVP values, since both PLA and PBAT have a more hydrophobic response than TPS. In the same way, as it was predictable due to the tortuousness generated by the addition of nanofillers, the incorporation of NCC to the PBAT6/TPS40/PLA54 matrix decreased the WVP to 15 and 32%, for a filler content of 1 and 2 wt%, respectively. Similarly, nanocomposite films obtained by Zhai et al. [97] showed a significant reduction in WVP when PBAT content increased in PBAT/HPDSP/nCOM composite (PBAT10/HPDSP90 24%; PBAT20/HPDSP80 38%; PBAT30/HPDSP70 40%; PBAT40/HPDSP60 57%; and PBAT60/HPDSP50 66%). Moreover, they showed that the PBAT content increases the *d*-spacing values (evaluated by XDR), evidencing an increase in the intercalated nanostructure in the composite, due to better polymer interaction with the nanoclay. The increase in the PBAT content (less water sensitivity) and the appropriate melt extrusion condition that promote

the formation of an intercalated nanostructure, due to better PBAT interaction with the organic modified clay, results in better water vapor barrier properties of the TPS/PBAT composite.

In agreement with the WVP results, the surface hydrophobicity of the films increased with increasing PBAT content, especially beyond 30 wt%. In contrast to the WVP of the HPDSP/PBAT/nCOM, the oxygen and carbon dioxide permeability values increased with increasing PBAT content. Although the addition of PBAT promoted the formation of a filler-intercalated nanostructure, which could prevent oxygen and carbon dioxide molecules from passing through the film matrix, the clay's dispersion was not enough to generate a tortuous path homogeneously distributed to reduce the permeability of oxygen and carbon dioxide efficiently.

As in the case of PHB, due to its hydrophobic character, it is expected that the incorporation of PBAT in starch matrices will lead to more stable blends in water, compared to TPS. The composition and morphology of PBAT/TPS blends will be decisive in the amount of water they can absorb from the environment. Depending on whether the predominant phase is TPS or PBAT, the behavior will be very different. Dammak et al. [56] showed that when TPS was the continuous phase in the blends of TPS/PBAT, this phase was accessible to water by diffusion from the surface increasing film's water absorption. This will be influenced by compatibilizer's presence. Fourati et al. [100] found that the moisture absorption for PBAT40/TPS60 was affected by the compatibilizer, reaching the highest level around 6% in the presence of MA and CAc, and the minimum was observed in the absence of the compatibilizer and in the presence of PBAT-g-MA. This evolution is connected with the continuity index for PBAT, as the lowest moisture absorption was attained when the PBAT is the continuous phase. For example, PBAT40/TPS60 formulated with CAc 2, 4 and 6% and presented a 33% increase regardless of CAc content, where the TPS formed a co-continuous (2% CAc) or continuous phase (4 and 6%) in the composite.

Changes in moisture content usually lead to differences in surface properties. Zhang et al. [108] showed that the incorporation of tartaric acid influenced the water absorption and contact angle of PBAT/TPS-TA blends. The authors reported that when 0.5% of TA was added, the water contact angle of PBAT/TPS-TA-0.5 increased from that neat PBAT and TPS/PBAT blend. These results confirmed the TA coupling effect in PBAT/TPS-TA-0.5. In these materials, TPS-TA-0.5 particles dispersed uniformly in the PBAT matrix to achieve a homogeneous phase, where the interface intensity was stronger than that of PBAT/TPS and prevented water molecules from permeating the boundary. On the contrary, the introduction of TPS and TPS-TA with higher TA content enhanced the hydrophilicity of PBAT, resulting in a decrease in the contact angle and an increase in water absorption. This is probably due to a new phase morphology reverse from the homogeneous phase of PBAT/TPS-TA-0.5.

Investigations of Spiridon et al. [182] revealed that the addition of ground and sieved particles of grape pomace, celery, treated waste of *Asclepias syriaca* floss and poplar seed hair fibers used as biomass fillers in starch/PBAT blends increased the water uptake capacity, compared to starch/PBAT. This result was awarded by the authors due to the strong hydrophilic character of the biomass fillers, related to the presence of hydroxyl groups present in the fibers. However, slight differences were

found depending on the biomass incorporated into the mixture, due to a different cellulose and lignin content in the biomass fiber composition [183]. When lignin was added to the formulation, a reduction in the water uptake capacity was observed. Vapor sorption capacity of biocomposites in the dynamic regime and isothermal conditions was also studied. The authors reported that the addition of biomass fillers to the starch/PBAT system did not change the shape of the isotherms, though the water uptake capacity was higher than that of the reference sample in the whole range of the curve. Other fillers, such as clays, have also been successful in reducing the blend water absorption. For example, sepiolite nanoclay's addition, studied by Olivato et al. [113], in PBAT80/TPS20 and PBAT20/TPS80 decreased the water adsorption rate and the water absorption capacity of nano-biocomposites, due to intermolecular links between starch and sepiolite silanol groups.

Mechanical Properties of Starch/PBAT Composites

The mechanical properties of the final blend will strongly depend on the compatibilization degree achieved. The role of various compatibilizers on TPS/PBAT mechanical properties was evaluated by several authors. The effect achieved by a compatibilizer will depend on the way in which it is added. For example, both Dammak et al. [56] and Fourati et al. [100] studied the case of maleic anhydride inclusion, placed as a compatibilizer in the blend or through a graft in PBAT (PBATg-MA). Dammak et al. [56] presented stress–strain curves for PBAT40/TPS60, PBAT50/TPS50 and PBAT60/TPS40 with and without compatibilizer. All blends exhibited three regions involving elastic, plastic deformation and strain hardening behavior. The tensile strength and the elongation at break of the samples improved as the TPS content decreased in the presence and absence of MA. For PBAT50/TPS50 blends, the tensile strength and elongation at break attained 12.8 MPa and 205% in the absence of any additive, reaching, respectively, 15.1 MPa and 614% when PBATg-MA was used as a compatibilizer, but decreasing to 6.5 MPa and 36%, respectively, when the blend was processed in the presence of 2% MA. In the blend PBAT50/TPS50 without compatibilizer, starch was in the form of dispersed droplets of about 2–10-µm diameter, with a low connection between them, while in the presence of MA, a full continuous morphology was observed, where the TPS formed an interconnected structure. This continuous morphology of the TPS phase was not observed when the blend was processed in the presence of PBATg-MA, where a dispersed morphology was obtained. These important morphological changes could be the reason for the marked differences in the materials' mechanical properties. Similarly, Fourati et al. [100] studied the mechanical properties of PBAT40/TPS60 processed in the presence of MA or PBATg-MA. They also found that the important improvements of strain at break achieved by blending TPS with PBAT (185%) reversed when MA was added (to values between 12 and 30%). The tensile strength of films also decreased in the presence of MA from 10 MPa for the blend without compatibilizer to around 8 MPa. By including PBATg-MA in the blends, the negative effect of MA was no longer observed, but on the contrary, strength and strain at break values around 12 MPa

and 380%, respectively, were obtained. The effective interfacial adhesion brought by the PBAT-g-MA coupling agent explains the improvement in the performance of the TPS/PBAT blends. The negative effect of MA on mechanical properties of PBAT50/TPS50 and PBAT40/TPS60 seems to be in disagreement with previous works highlighting the beneficial effect of MA in PBAT-TPS blends [105, 184]. Nevertheless, it is worth noting that all these results are being compared for blends with compositions close to that for which phase inversion occurs (PBAT40/TPS60 and PBAT45/TPS55). It is possible then that the difference in behavior obtained for the MA is due to morphological changes that produce different physical–chemical responses.

In summary, the effect of compatibilizer's inclusion in blend's mechanical properties is strongly dependent on the PBAT/TPS ratio and on the way in which it is included. In all cases, more important improvements are obtained when the compatibilizer is modified with one of the blend's components to maximize the interaction between them. The enhancement of tensile strength and elongation at break when PBATg-MA was included in PBAT/TPS blends confirmed the efficiency of this reactive compatibilizer to promote the interfacial adhesion between both phases. A presumably reason for this effect is the ester linkage between grafted MA onto PBAT and TPS.

Zhang et al. [108] show a case where the compatibilizer (tartaric acid) is initially mixed with starch and glycerol for the manufacture of TPS-TA, which is later blended with PBAT. Tensile test analysis of PBAT30/TPS-TA70 blends revealed that the use of TA at 0.5% increased the tensile strength value of the blend from 15 to 16 MPa and the elongation at break from 942 to 1311%. However, it was observed that increasing the TA content leads to a continuous decrease in these values, with a tensile strength of 9 MPa and elongation at break of 942% for a TA addition of 4%. A combination of different factors was proposed by the authors to explain this behavior. They observed a drastic reduction in the molecular weight of TPS-TA as the TA content increased. In addition, the interface interaction between phases decreased in the presence of excessive TA concentration. These facts lead to a reverse in the morphology and the presence of TPS-TA particle agglomerations, all of which promoted a decrease in the tensile strength for TA contents higher than 0.5%.

Other additives, such as proteins, have been used as compatibilizers. It is the case of Garcia et al. [111] who reported that in PBAT/starch/glycerol blends (61, 26 and 13 wt%) the addition of sericin increased the Young modulus and tensile strength but decreased the strain at break. These results were observed for all studied sericin contents (0.5–1.5%). As the sericin content increased from 0.5 to 1%, the tensile strength was slightly improved, from 5.7 to 6.4 MPa, Young's modulus increased from about 66–91 MPa and the deformation remained unchanged. By increasing more the sericin concentration, to 1.5%, the authors found no differences in the tensile strength values, but a strong increment in the Young modulus (to approximately 130 MPa) and an important decrease in elongation at break (of about a 50%) were obtained, compared with the blend containing 1% of sericin. These results were attributed to the fact that the presence of sericin reduced the molecular mobility of starch and PBAT chains, and due to its amphoteric character, it could act similarly to a

surfactant agent. The side chains of amino acid residues with hydrophobic character (such as glycine) and hydrophilic character (such as serine, aspartate and asparagine) could interact with PBAT and starch, respectively, leading to molecular interactions when located in the interface. The compatibilizer effect explains the mechanical performance and the more homogeneous and compact morphology observed from sericin containing PBAT/starch/glycerol films.

The influence of compatibilizers' inclusion on the material's mechanical properties was also studied in the case of composites. In these cases, the compatibilizers' effect needs to be reevaluated, as new effects can appear. Liu et al. [103] blended a TPS composite reinforced with $nSiO_2$ (TPS-$nSiO_2$) and PBAT, and studied the influence of adding compatibilizers in mechanical properties. They worked with MA, one of the typical compatibilizers of these systems, and plasticized EVOH, which meets the requirement of a starch–PBAT compatibilizer, as it has a lipophilic long chain on one end and many hydroxyl groups on the other. The authors showed that the addition of MA reduces dramatically the impact strength and elongation at break of PBAT40/TPS-$nSiO_2$60/MA compared to PBAT40/TPS-$nSiO_2$60. This decrease was explained as a consequence of a plasticization effect of MA or its participation in hydrolysis reactions of the polymer chains. The impact strength of PBAT40/TPS-$nSiO_2$60/pEVOH was higher than for PBAT40/TPS-$nSiO_2$60/MA, and close to the PBAT40/TPS-$nSiO_2$60hg, without compatibilizer. CA is other possible compatibilizer usually used in these systems. Garcia et al. [102] stated that it might promote not only cross-linking reactions, which could reduce film flexibility but also starch hydrolysis or plasticization, reducing hydrogen bonds between starch chains that weaken the blend structure. De Campos et al. [57] found that the addition of 0.75 wt% of curcumin into a PBAT30/starch49/glycerol21 blend with CAc caused a significant increase in the evaluated mechanical properties (Young's modulus increases 32%, tensile strength 7% and 39% elongation at break), compared to the film without the addition of curcumin. They explained that the presence of curcumin could hinder or inhibit the interaction between citric acid and starch, so better mechanical properties were observed. Furthermore, the change in mechanical properties was not associated with a plasticizing effect since this behavior was undetected by DSC, and they did not find evidence of improvement in compatibilization when comparing the glass transition temperature of the individual materials and the produced blends.

The degree of improvement achieved by filler inclusion usually depends on their dispersion in the polymer matrix as well as their properties. Manepalli and Alavi [50] not only studied the effect of NCC inclusion in PLA/PBAT/TPS blends, but also made a detailed description of the filler's morphology effect on mechanical properties and predicted them by applying the well-known Halpin–Tsai model. They found that the addition of NCC increased the mechanical properties of PLA/PBAT/TPS films and predicted that the increase in aspect ratio (L/d of the particle) and modulus of nanofiller lead to a nanocomposites' modulus increase.

The affinity of the filler to each component of the blend will define its reinforcement effect. Olivato et al. [113] studied the effect of sepiolite addition on PBAT/TPS blends' mechanical properties, varying PBAT/TPS ratio and nanofiller content. Their results suggested that sepiolite was more compatible with the TPS phase, probably

due to its more hydrophilic character. For blends with higher TPS content, the dispersion of sepiolite was facilitated and so its relative contribution to blend final mechanical properties. In some cases, significant improvements are achieved when the filler is incorporated into one of the polymers, but in the case of the blend this positive result is no longer observed. Lendvai et al. [114] reported a different mechanical behavior as a function of clay characteristics, when studying the effect of increasing contents of TPS nanocomposites in PBAT. The incorporation of BT and OMMT particles into the starch formulation resulted in the typical reinforcement effect, showing a significant increase in TPS composite strength and modulus without affecting elongation at break with respect to TPS. The incorporation of increasing contents of TPSnBT to PBAT, however, had no significant effect on the strength and modulus data when compared to neat TPS/PBAT blend with the same TPS content. Elongation at break for blends with contents of TPSnBT up to 60% exceeded that of the neat TPS/PBAT blends suggesting a compatibilizing effect of BT particles. When TPSnOMMT was incorporated into PBAT at contents of 40 and 50%, mechanical properties (tensile strength, modulus and elongation at break) were similar to blends without clay.

The costs of industrial processes and new environmental legislation promoted development of composites containing directly natural fibers, in particular from biomass residues. Its cellulose and lignin content strongly depend on the chosen waste, and these values greatly affect the composite's mechanical properties. Spiridon et al. [182] explored the effect of incorporating waste biomass fibers into the PBAT/starch blends in mechanical properties. Young's modulus of biocomposites registered an increase in the rage of 141–191% with respect to starch/PBAT blend as the content of cellulose in fibers increased. Tensile strength values obtained for the biocomposites were similar to those of the starch/PBAT blend, demonstrating that low interactions between fibers and the polymer matrix were achieved. At the same time, the ductility of biocomposites was significantly reduced with the addition of waste fibers. The presence of rigid fibers could restrain the matrix deformation and therefore reduce the elongation of biocomposites. Nunes et al. [55] found similar effects studying the reinforcing effect of babassu mesocarp fiber into PBAT70/TPS30 blends. Their biocomposite presented higher elastic modulus and lower elongation at break with regard to neat PBAT and PBAT70/TPS30. When lignocellulosic fibers are dispersed in a polymer matrix with low affinity (as with PBAT), and the system is stretched, they tend to hinder chain mobility and lower the elongation at break despite maintaining or improving tensile strength and Young's modulus. Although morphological analysis showed poor adhesion between the fiber and the polymer matrix, the increase reported in the elastic modulus for the biocomposite could be due to some interactions of the hydroxyl groups present in TPS and cellulose fiber. The composition of the employed fiber resulted influential in the achieved effect. Spiridon et al. [182] found that higher lignin contents of fiber could result in an improved fiber distribution promoting the interaction with the matrix. Furthermore, lignin addition to the biocomposites resulted in more homogeneous structures, with improved interfacial adhesion due to partial miscibility between cornstarch and lignin. A slight increase in plastic deformation, higher elastic modulus, impact performance and tensile strength was achieved when compared to the neat PBAT/starch blend and PBAT/starch/waste

biomass fibers without lignin. The improvement observed could be due to the partial miscibility related to the formation of interactions such as hydrogen bonding and other physical forces between lignin and the polymer matrix.

Zhai et al. [97] simultaneously used two strategies to improve the performance of the material: using a modified starch and adding a filler. They developed PBAT/TPS blends using hydroxypropyl distarch phosphate (HPDSP), citric acid as compatibilizer and a nanoclay as filler (an organic montmorillonite modified with octadecyl dimethyl benzyl ammonium chloride). The authors found that at fixed amounts of nanofiller and compatibilizer content, an increase in the amount of PBAT improved mechanical strength and flexibility, especially for nanocomposite films with PBAT content higher than 30%. The maximum tensile strength of the PBAT50/HPDSP50 nanocomposite film was approximately five times higher than that of the HPDSP, and the elongation at break (EB) was seven times higher than that of the starch nanocomposite film. The maximum tensile strength and elongation at break of the PBAT50/HPDSP50 nanocomposite films were 7.4 MPa and 614%, respectively.

4   Conclusions and Future Perspectives

Although the proposal to replace conventional plastics with starch-based materials is a very attractive idea from an ecological and economical point of view, the properties of TPS are not enough to meet the requirements of many applications. The development of starch-based composites with the incorporation of natural fillers helps improve their performance, but it is still a long way from commodity plastics.

The best strategy found so far is the use of starch blends with biodegradable polyesters that improve the properties of TPS together with the inclusion of fillers. The results obtained by different researchers show that a critical key to achieving the desired properties is the proper design of compounding–processing strategies. However, desirable properties such as good processability, thermal stability, mechanical strength and improved barrier properties still must be achieved to increase the market share among commodity materials. Hence, further studies, including the introduction of new biobased plasticizers, cross-linkers, additives and/or different types of micro-nanofillers, are required, to fulfill the needs of each particular plastic sector. Rationally designing these materials, including higher biomass contents as a valuable resource, and the use of green methodologies to obtain them, would establish a sustainable production value.

One of the most promising fields of application for these materials is agri-horticulture. In much of the recent scientific works and published patents related to agricultural materials, modified starches blended with other biopolymers are used, being today the critical points to solve the compatibility and processing problems of the mixtures [185, 186]. In relation to plastics destined for agriculture, a strong growth in mulching and covering materials is expected, being PBAT one of the most attractive candidates to be used since it gives the mixture high toughness and elongation at break while maintaining its biodegradability [99, 108]. PHB is other excellent

candidate that has the extra advantage of being biobased, but which production cost is much higher and can be used in applications where hydrophobicity improvements are required, as well as higher Young's modulus and stress at break [165].

Although PBAT is still fully fossil derived, sustainable alternatives have been proposed looking for obtaining a whole biobased PBAT. In this sense, the production of biobased 1,4 butanediol (BDO) has been achieved through industrial biological fermentation; sebacic acid (as a substitute of adipic acid) coming from castor oil has been used as a monomer to prepare poly(butylene sebacinate-co-butylene terephthalate) (PBSeT) co-polyesters; 2, 5-furandicarboxylic acid (FDCA) has been regarded as a biobased alternative to the petroleum-based terephthalic acid.

PHB, on the other hand, has the great advantage of being fully biobased and biodegradable in soil. However, the challenge of obtaining good compatibility with TPS remains unsolved. At this moment, the studies carried out were orientated to develop different strategies to improve compatibility and therefore the physical and mechanical properties of the blends. These strategies were focused on using TPS from various botanical sources, modified polymers and the addition of compatibilizing agents as well as micro-nanofillers.

The amount of filler incorporated into the composites is usually very small, most of the times much lower than 5%. When choosing the reinforcement to use, a cost–benefit analysis must be carried out in all cases. The only truly green fillers are renewable, biobased and biodegradable, such as cellulose. However, other fillers, such as clays, are much more economical, do not generate a high environmental impact and can generate strong improvements if a good dispersion is achieved. For that reasons, they were and are one of the most studied fillers as reinforcement of starch blend. In some cases, it is preferred to choose fillers that do not generate the most important improvements, but that are completely green. However, this can be tricky, since the method of obtaining/purifying them can include the use of non-environmentally friendly processes, as happens for example with some cellulosic reinforcements. To date, there is not enough experimental evidence to show that 100% green starch-based composites with suitable properties to replace commodity plastics can be produced, including the use of green chemistry to obtain the modified starches or to make the grafts in the bioplastics with which it is usually combined.

Nowadays, trend aims to generate plastics with the least environmental impact. Phrases like "a better bioplastic for a better world", "plastic more sustainable, compostable, and eco-friendly" or "zero waste to make a difference" are the head of many of today's developments and even appear on the presentation pages of many companies. In this framework, starch composites such as those presented in this chapter have great potential to be inserted into the agricultural and packaging industry. It is expected that the problems that still persist in these materials' properties will be solved in the near future, responding to the demands of society for a sustainable world.

References

1. Rameshkumar S, Shaiju P, O'Connor KE (2020) Bio-based and biodegradable polymers—state of the art, challenges and emerging trends. Curr Opin Green Sustain Chem 21:75–81
2. Skoczinski P, Chinthapalli R, Carus M, Baltus W, de Guzman D, Käb H, Raschka A, Ravenstijn J (2020) Global markets and trends of bio-based building blocks and polymers 2019–2024. Carus M (Publ) Nova-Institut GmbH, Germany
3. Villar MA, Barbosa SE, García MA, Castillo LA, López OV (eds) (2017) Starch-based materials in food packaging. Processing, characterization and applications. Academic Press, United Kingdom and United States
4. Visakh PM (2015) Starch: state-of-the-art, new challenges and opportunities. In: Visakh PM, Yu L (eds) Starch-based blends, composites and nanocomposites. RSC Green Chemistry, United Kigndom, pp 1–16
5. Ribba L, Garcia NL, D'Accorso N, Goyanes S (2017) Disadvantages of starch-based materials, feasible alternatives in order to overcome these limitations. In: Villa MA, Barbosa SE, Garcia MA, Castillo LA, Lopez OV (eds) Starch-based materials in food packaging, 1st edn. Academic Press, Cambridge, pp 37–76
6. Xie F, Zhang B, Wang DK (2017) Starch thermal processing: technologies at laboratory and semi-industrial scales. In: Villa MA, Barbosa SE, Garcia MA, Castillo LA, Lopez OV (eds) Starch-based materials in food packaging, 1st edn. Academic Press, Cambridge, pp 187–227
7. Thunwall M, Boldizar A, Rigdahl M, Kuthanová V (2006) On the stress-strain behavior of thermoplastic starch melts. Int J Polym Anal Charact 11(6):419–428
8. González-Seligra P, Guz L, Ochoa-Yepes O, Goyanes S, Famá L (2017) Influence of extrusion process conditions on starch film morphology. LWT 84:520–528
9. von Borries-Medrano E, Jaime-Fonseca MR, Aguilar-Mendez MA (2016) Starch–guar gum extrudates: microstructure, physicochemical properties and in-vitro digestion. Food Chem 194:891–899
10. Bouvier JM, Campanella OH (2014) Extrusion processing technology: food and non-food biomaterials. Wiley, Hoboken
11. Lawal A, Kalyon DM (1995) Mechanisms of mixing in single and co-rotating twin screw extruders. Polym Eng Sci 35(17):1325–1338
12. Lai LS, Kokini JL (1991) Physicochemical changes and rheological properties of starch during extrusion (a review). Biotechnol Prog 7(3):251–266
13. García NL, Famá L, D'Accorso NB, Goyanes S (2015) Biodegradable starch nanocomposites. Adv Struct Mater 75:17–77
14. Jebalia I, Maigret JE, Réguerre AL, Novales B, Guessasma S, Lourdin D, Della Valle G, Kristiawan M (2019) Morphology and mechanical behaviour of pea-based starch-protein composites obtained by extrusion. Carbohydr Polym 223:115086
15. Nessi V, Falourd X, Maigret JE, Cahier K, D'orlando A, Descamps N, Gaucher V, Chevigny C, Lourdin D (2019) Cellulose nanocrystals-starch nanocomposites produced by extrusion: structure and behavior in physiological conditions. Carbohydr Polym 225:115123
16. Estevez-Areco S, Guz L, Famá L, Candal R, Goyanes S (2019) Bioactive starch nanocomposite films with antioxidant activity and enhanced mechanical properties obtained by extrusion followed by thermo-compression. Food Hydrocolloids 96:518–528
17. Gutiérrez TJ, Toro-Márquez LA, Merino D, Mendieta JR (2019) Hydrogen-bonding interactions and compostability of bionanocomposite films prepared from corn starch and nano-fillers with and without added Jamaica flower extract. Food Hydrocolloids 89:283–293
18. Drobny JG, (2014) Handbook of thermoplastic elastomers. PDL (Plastics Design Library)/William Andrew, Pensilvania
19. Thunwall M, Kuthanova V, Boldizar A, Rigdahl M (2008) Film blowing of thermoplastic starch. Carbohydr Polym 71(4):583–590
20. Fishman ML, Coffin DR, Onwulata CI, Willett JL (2006) Two stage extrusion of plasticized pectin/poly (vinyl alcohol) blends. Carbohydr Polym 65(4):421–429

21. Jana T, Maiti S (1999) A biodegradable film, 1. Pilot plant investigation for production of the biodegradable film. Angew Makromolek Chem 267(1):16–19
22. Otey FH, Westhoff RP, Doane WM (1987) Starch-based blown films. 2. Ind Eng Chem Res 26(8):1659–1663
23. Halley P, Rutgers R, Coombs S, Kettels J, Gralton J, Christie G, Jenkins M, Beh H, Griffin K, Jayasekara R, Lonergan G (2001) Developing biodegradable mulch films from starch-based polymers. Starch-Stärke 53(8):362–367
24. Matzinos P, Tserki V, Kontoyiannis A, Panayiotou C (2002) Processing and characterization of starch/polycaprolactone products. Polym Degrad Stabil 77(1):17–24
25. Huntrakul K, Yoksan R, Sane A, Harnkarnsujarit N (2020) Effects of pea protein on properties of cassava starch edible films produced by blown-film extrusion for oil packaging. Food Packaging Shelf 24:100480
26. Dang KM, Yoksan R (2016) Morphological characteristics and barrier properties of thermoplastic starch/chitosan blown film. Carbohyd Polym 150:40–47
27. Abbégs B, Ayad R, Prudhomme JC, Onteniente JP (1998) Numerical simulation of thermoplastic wheat starch injection molding process. Polym Eng Sci 38(12):2029–2038
28. Onteniente JP, Abbès B, Safa LH (2000) Fully biodegradable lubricated thermoplastic wheat starch: mechanical and rheological properties of an injection grade. Starch-Stärke 52(4):112–117
29. Stepto RFT (2009) Thermoplastic starch. Macromol Symp 279:163–168
30. Ye J, Luo S, Huang A, Chen J, Liu C, McClements DJ (2019) Synthesis and characterization of citric acid esterified rice starch by reactive extrusion: a new method of producing resistant starch. Food Hydrocolloids 92:135–142
31. Siyamak S, Luckman P, Laycock B (2020) Rapid and solvent-free synthesis of pH-responsive graft-copolymers based on wheat starch and their properties as potential ammonium sorbents. Int J Biol Macromol 149:477–486
32. Okonkwoa EG, Aigbodiona VS, Akinlabib ET, Daniel-Mkpumea CC (2020) Starch-based composites and their applications. In: Al-Ahmed A, Inamuddin (eds) Advanced applications of polysaccharides and their composites, 1st edn. Materials Research Forum LLC, Millersville, pp 73–198
33. Ilyas RA, Sapuan SM, Ibrahim R, Abral H, Ishak MR, Zainudin ES, Atiqah A, Atikah MSN, Syafri E, Jumaidin R (2020) Thermal, biodegradability and water barrier properties of bio-nanocomposites based on plasticised sugar palm starch and nanofibrillated celluloses from sugar palm fibres. J Biobased Mater Bio 14(2):234–248
34. Valencia-Sullca C, Jiménez M, Jiménez A, Atarés L, Vargas M, Chiralt A (2016) Influence of liposome encapsulated essential oils on properties of chitosan films. Polym Int 65(8):979–987
35. Talón E, Vargas M, Chiralt A, González-Martínez C (2019) Eugenol incorporation into thermoprocessed starch films using different encapsulating materials. Food Packaging Shelf 21:100326
36. Wandrey C, Bartkowiak A, Harding SE (2010) Materials for encapsulation. In: Zuidam NJ, Nedovic V (eds) Encapsulation technologies for active food ingredients and food processing, 1st edn. Springer Science & Business Media, New York, pp 31–100
37. Jin Y, Li JZ, Nik AM (2018) Starch-based microencapsulation. In: Sjöö M, Nilsson L (eds) Starch in food: structure, function and applications, 1st edn. Woodhead Publishing, Cambridge, pp 661–690
38. Castro N, Durrieu V, Raynaud C, Rouilly A, Rigal L, Quellet C (2016) Melt extrusion encapsulation of flavors: a review. Polym Rev 56(1):137–186
39. Chen S, Zong J, Jiang L, Ma C, Li H, Zhang D (2020) Improvement of resveratrol release performance and stability in extruded microparticle by the α-amylase incorporation. J Food Eng 274:109842
40. Zhu F (2017) Encapsulation and delivery of food ingredients using starch based systems. Food Chem 229:542–552
41. Yuliani S, Torley PJ, D'Arcy B, Nicholson T, Bhandari B (2006) Extrusion of mixtures of starch and d-limonene encapsulated with β-cyclodextrin: flavour retention and physical properties. Food Res Int 39(3):318–331

42. Ochoa-Yepes O, Di Giogio L, Goyanes S, Mauri A, Famá L (2019) Influence of process (extrusion/thermo-compression, casting) and lentil protein content on physicochemical properties of starch films. Carbohydr Polym 208:221–231

43. Ghanbari A, Tabarsa T, Ashori A, Shakeri A, Mashkour M (2018) Preparation and characterization of thermoplastic starch and cellulose nanofibers as green nanocomposites: extrusion processing. Int J Biol Macromol 112:442–447

44. Dean K, Yu L, Wu DY (2007) Preparation and characterization of melt-extruded thermoplastic starch/clay nanocomposites. Compos Sci Technol 67(3–4):413–421

45. Chaves da Silva NM, Fakhouri FM, Fialho RLL, Cabral Albuquerque ECDM (2018) Starch–recycled gelatin composite films produced by extrusion: physical and mechanical properties. J Appl Polym Sci 135(19):46254

46. Huang MF, Yu JG, Ma XF (2004) Studies on the properties of montmorillonite-reinforced thermoplastic starch composites. Polymer 45(20):7017–7023

47. González K, Iturriaga L, González A, Eceiza A, Gabilondo N (2020) Improving mechanical and barrier properties of thermoplastic starch and polysaccharide nanocrystals nanocomposites. Eur Polym J 123:109415

48. Fourati Y, Magnin A, Putaux JL, Boufi S (2020) One-step processing of plasticized starch/cellulose nanofibrils nanocomposites via twin-screw extrusion of starch and cellulose fibers. Carbohydr Polym 229:115554

49. Grylewicz A, Spychaj T, Zdanowicz M (2019) Thermoplastic starch/wood biocomposites processed with deep eutectic solvents. Compos Part A Appl Sci Manuf 121:517–524

50. Manepalli PH, Alavi S (2019) Mathematical modeling of mechanical and barrier properties of poly(lactic acid)/poly(butylene adipate-co-terephthalate)/thermoplastic starch based nanocomposites. J Food Eng 261:60–65

51. Chivrac F, Pollet E, Dole P, Avérous L (2010) Starch-based nano-biocomposites: plasticizer impact on the montmorillonite exfoliation process. Carbohydr Polym 79(4):941–947

52. Adamus J, Spychaj T, Zdanowicz M, Jędrzejewski R (2018) Thermoplastic starch with deep eutectic solvents and montmorillonite as a base for composite materials. Ind Crop Prod 123:278–284

53. Utracki LA (ed) (2002) Polymer blends handbook. Kluwer Academic Publishers, Dordrecht

54. Muthuraj R, Misra M, Mohanty AK (2018) Biodegradable compatibilized polymer blends for packaging applications: a literature review. J Appl Polym Sci 135(24):45726

55. Nunes MABS, Marinho VAD, Falcão GAM, Canedo EL, Bardi MAG, Carvalho LH (2018) Rheological, mechanical and morphological properties of poly(butylene adipate-co-terephthalate)/thermoplastic starch blends and its biocomposite with babassu mesocarp. Polym Test 70:281–288

56. Dammak M, Fourati Y, Tarrés Q, Delgado-Aguilar M, Mutjé P, Boufi S (2020) Blends of PBAT with plasticized starch for packaging applications: mechanical properties, rheological behaviour and biodegradability. Ind Crop Prod 144:112061

57. de Campos SS, de Oliveira A, Moreira TFM, da Silva TBV, da Silva MV, Pinto JA, Bilck AP, Gonçalves OH, Fernandes IP, Barreiro M-F, Yamashita F, Valderrama P, Shirai MA, Leimann FV (2019) TPCS/PBAT blown extruded films added with curcumin as a technological approach for active packaging materials. Food Packaging Shelf 22:100424

58. Nesic A, Castillo C, Castaño P, Cabrera-Barjas G, Serrano J (2020) Bio-based packaging materials. In: Galanakis CM (ed) Biobased products and industries, 1st edn. Elsevier, Amsterdam, pp 279–309

59. Platt DK (2006) Biodegradable polymers—market report. Smithers Rapra Limited, United Kingdom

60. Shogren R, Wood D, Orts W, Glenn G (2019) Plant-based materials and transitioning to a circular economy. Sustain Prod Consum 19:194–215

61. Ashter SA (2016) Introduction to bioplastics engineering. William Andrew Publishing, Oxford

62. Ferreira FV, Cividanes LS, Gouveia RF, Lona LMF (2019) An overview on properties and applications of poly(butylene adipate-co-terephthalate)–PBAT based composites. Polym Eng Sci 59:E7–E15

63. Markovic G, Visakh PM (2017) Polymer blends: state of art. In: Visakh PM, Markovic G, Pasquini D (eds) Recent developments in polymer macro, micro and nano blends, 1st edn. Woodhead Publishing, UK, pp 1–15

64. Liu W, Liu S, Wang Z, Liu J, Dai B, Chen Y, Zeng G (2020) Preparation and characterization of compatibilized composites of poly(butylene adipate-co-terephthalate) and thermoplastic starch by two-stage extrusion. Eur Polym J 122:109369

65. Mochane MJ, Sefadi JS, Motsoeneng TS, Mokoena TE, Mofokeng TG, Mokhena TC (2020) The effect of filler localization on the properties of biopolymer blends, recent advances: a review. Polym Compos 1–22. https://doi.org/10.1002/pc.25590

66. Ray SS, Salehiyan R (2019) Nanostructured immiscible polymer blends: migration and interface. Elsevier, Amsterdam

67. Lemoigne M (1926) Produit de deshydratation et de polymerisation de l'acide b-oxybutyrique. Bull Soc Chim Biol 8:770–782

68. Kumar M, Rathour R, Singh R, Sun Y, Pandey A, Gnansounou E, Lin KYA, Tsang DCW, Thakur IS (2020) Bacterial polyhydroxyalkanoates: opportunities, challenges, and prospects. J Clean Prod 121500:1–20

69. Balaji S, Gopi K, Muthuvelan B (2013) A review on production of poly β hydroxybutyrates from cyanobacteria for the production of bio plastics. Algal Res 2(3):278–285

70. Bhatia SK, Shim YH, Jeon JM, Brigham CJ, Kim YH, Kim HJ, Seo HM, Lee JH, Kim JH, Yi DH, Lee YK, Yang YH (2015) Starch based polyhydroxybutyrate production in engineered *Escherichia coli*. Bioproc Biosyst Eng 38(8):1479–1484

71. Bugnicourt E, Cinelli P, Lazzeri A, Alvarez VA (2014) Polyhydroxyalkanoate (PHA): review of synthesis, characteristics, processing and potential applications in packaging. Express Polym Lett 8(11):791–808

72. Manikandan NA, Pakshirajan K, Pugazhenthi G (2020) Preparation and characterization of environmentally safe and highly biodegradable microbial polyhydroxybutyrate (PHB) based graphene nanocomposites for potential food packaging applications. Int J Biol Macromol 154:866–877

73. Souza Jd, Chiaregato CG, Faez R (2018) Green composite based on PHB and montmorillonite for KNO₃ and NPK delivery system. J Polym Environ 26:670–679

74. Coltelli MB, Danti S, Trombi L, Morganti P, Donnarumma G, Baroni A, Fusco A, Lazzeri A (2018) Preparation of innovative skin compatible films to release polysaccharides for biobased beauty masks. Cosmetics 5(4):70

75. Coltelli MB, Panariello L, Morganti P, Danti S, Baroni A, Lazzeri A, Danti S, Baroni A, Lazzeri A, Fusco A, Donnarumma G (2020) Skin-compatible biobased beauty masks prepared by extrusion. J Funct Biomater 11(2):23

76. Din MI, Ghaffar T, Najeeb J, Hussain Z, Khalid R, Zahid H (2020) Potential perspectives of biodegradable plastics for food packaging application—review of properties and recent developments. Food Addit Contam A 37(4):665–680

77. Garrido-Miranda KA, Rivas BL, Pérez-Rivera MA, Sanfuentes EA, Peña-Farfal C (2018) Antioxidant and antifungal effects of eugenol incorporated in bionanocomposites of poly (3-hydroxybutyrate)-thermoplastic starch. LWT-Food Sci Technol 98:260–267

78. Weinmann S, Bonten C (2019) Thermal and rheological properties of modified polyhydroxybutyrate (PHB). Polym Eng Sci 59(5):1057–1064

79. Corre YM, Bruzaud S, Audic JL, Grohens Y (2012) Morphology and functional properties of commercial polyhydroxyalkanoates: a comprehensive and comparative study. Polym Test 31(2):226–235

80. Pachekoski WM, Dalmolin C, Agnelli JAM (2013) The influence of the industrial processing on the degradation of poly (hidroxybutyrate)-PHB. Mater Res 16(2):237–332

81. Correa JP (2018) Nanocompuestos poliméricos: estudio de la interacción de mezclas de polímeros biodegradables con refuerzos químicamente modificados. Ph. D. thesis, Universidad de San Martín, Buenos Aires, Argentina

82. Yamaguchi M, Arakawa K (2006) Effect of thermal degradation on rheological properties for poly (3-hydroxybutyrate). Eur Polym J 42(7):1479–1486

83. Renstad R, Karlsson S, Albertsson AC (1999) The influence of processing induced differences in molecular structure on the biological and non-biological degradation of poly (3-hydroxybutyrate-co-3-hydroxyvalerate), P (3-HB-co-3-HV). Polym Degrad Stabil 63(2):201–211

84. Janigová I, Lacík I, Chodák I (2002) Thermal degradation of plasticized poly (3-hydroxybutyrate) investigated by DSC. Polym Degrad Stabil 77(1):35–41

85. Koller I, Owen AJ (1996) Starch-filled PHB and PHB/HV copolymer. Polym Int 39(3):175–181

86. Kotnis MA, O'Brien GS, Willett JL (1995) Processing and mechanical properties of biodegradable poly (hydroxybutyrate-co-valerate)-starch compositions. J Polym Environ 3(2):97–105

87. Rosa DDS, Rodrigues TC, Gracas Fassina Guedes CD, Calil MR (2003) Effect of thermal aging on the biodegradation of PCL, PHB-V, and their blends with starch in soil compost. J Appl Polym Sci 89(13):3539–3546

88. Gomes Brunel D, Pachekoski WM, Dalmolin C, Marcondes Agnelli JA (2014) Natural additives for poly (hydroxybutyrate-CO-hydroxyvalerate)-PHBV: effect on mechanical properties and biodegradation. Mater Res 17(5):1145–1156

89. Chen L, Zhu M, Song L, Yu H, Zhang Y, Chen Y, Adler H (2004) Crystallization behavior and thermal properties of blends of poly-(3-hydroxybutyrate-co-3-hydroxyvalerate) and poly(1,2-propandiolcarbonate). Macromol Symp 210:241–250

90. Modi SJ (2010) Assessing the feasibility of poly-(3-hydroxybutyrate-co-3-hydroxyvalerate) (PHBV) and poly-(lactic acid) for potential food packaging applications. M.Sc. thesis, The Ohio State University, EEUU

91. Yu L (2009) Biodegradable polymer blends and composites from renewable resources. Wiley, Hoboken

92. Don TM, Chung ChY, Lai SM, Chiu HJ (2010) Preparation and properties of blends from poly(3-hydroxybutyrate) with poly(vinyl acetate)-modified starch. Polym Eng Sci 50(4):709–718

93. Thiré RM, Ribeiro TA, Andrade CT (2006) Effect of starch addition on compression-molded poly (3-hydroxybutyrate)/starch blends. J Appl Polym Sci 100(6):4338–4347

94. Zhang M, Thomas NL (2010) Preparation and properties of polyhydroxybutyrate blended with different types of starch. J Appl Polym Sci 116(2):688–694

95. Garrido-Miranda KA, Rivas BL, Pérez MA (2017) Poly (3-hydroxybutyrate)–thermoplastic starch–organoclay bionanocomposites: surface properties. J Appl Polym Sci 134(34):45217(1–8)

96. Jian J, Xiangbin Z, Xianbo H (2020) An overview on synthesis, properties and applications of poly(butylene-adipate-co-terephthalate)–PBAT. Adv Ind Eng Polym Res 3(1):19–26

97. Zhai X, Wang W, Zhang H, Dai Y, Dong H, Hou H (2020) Effects of high starch content on the physicochemical properties of starch/PBAT nanocomposite films prepared by extrusion blowing. Carbohydr Polym 239:116231

98. Meraldo A (2016) Introduction to bio-based polymers. In: Wagner JR (ed) Multilayer flexible packaging, 2nd edn. Plastics design library. William Andrew Publishing, New York, pp 47–52

99. Nunes MABS, Castro-Aguirre E, Auras RA, Bardi MAG, Carvalho LH (2019) Effect of babassu mesocarp incorporation on the biodegradation of a PBAT/TPS blend. Macromol Symp 383:1800043

100. Fourati Y, Tarrés Q, Mutjé P, Boufi S (2018) PBAT/thermoplastic starch blends: effect of compatibilizers on the rheological, mechanical and morphological properties. Carbohydr Polym 199:51–57

101. Ivanič F, Kováčová M, Chodák I (2019) The effect of plasticizer selection on properties of blends poly(butylene adipate-co-terephthalate) with thermoplastic starch. Eur Polym J 116:99–105

102. Garcia PS, Grossmann MVE, Shirai MA, Lazaretti MM, Yamashita F, Muller CMO, Mali S (2014) Improving action of citric acid as compatibiliser in starch/polyester blown films. Ind Crop Prod 52:305–312

103. Liu W, Liu S, Wang Z, Dai B, Liu J, Chen Y, Zeng G, He Y, Liu Y, Liu R (2019) Preparation and characterization of reinforced starch-based composites with compatibilizer by simple extrusion. Carbohydr Polym 223:115122

104. Da Roz AL, Carvalho AJF, Gandini A, Curvelo AAS (2006) The effect of platicizers on thermoplastic starch compositions obtained by melt processing. Carbohydr Polym 63:417–424

105. Olivato JB, Grossmann MVE, Yamashita F, Eiras D, Pessan LA (2012) Citric acid and maleic anhydride as compatibilizers in starch/poly(butylene adipate-co-terephthalate) blends by one-step reactive extrusion. Carbohydr Polym 87(4):2614–2618

106. Wei D, Wang H, Xiao H, Zheng A, Yang Y (2015) Morphology and mechanical properties of poly(butylene adipate-co-terephthalate)/potato starch blends in the presence of synthesized reactive compatibilizer or modified poly(butylene adipate-co-terephthalate). Carbohydr Polym 123:275–282

107. Robeson LM (2007) Polymer blends: a comprehensive review. Hanser, Munich

108. Zhang S, He Y, Lin Z, Li J, Jiang G (2019) Effects of tartaric acid contents on phase homogeneity, morphology and properties of poly (butyleneadipate-co-terephthalate)/ thermoplastic starch bio-composites. Polym Test 76:385–395

109. Olivato JB, Müller CMO, Carvalho GM, Yamashita F, Grossmann MVE (2014) Physical and structural characterisation of starch/polyester blends with tartaric acid. Mater Sci Eng C 39:35–39

110. Marinho V, Pereira CAB, Vitorino MBC, Silva AS, Carvalho LH, Canedo EL (2017) Degradation and recovery in poly(butylene adipate-co-terephthalate)/thermoplastic starch blends. Polym Test 58:166–172

111. Garcia PS, Turbiani FRB, Baron AM, Yamashita F, Eiras D, Grossmann VE (2018) Sericin as compatibilizer in starch/polyester blown films. Polímeros (São Carlos, Online) 28(5):389–394

112. Xiong SJ, Pang B, Zhou SJ, Li MK, Yang S, Wang YY, Shi Q, Wang SF, Yuan TQ, Sun RC (2020) Economically competitive biodegradable PBAT/lignin composites: effect of lignin methylation and compatibilizer. ACS Sustain Chem Eng 8(13):5338–5346

113. Olivato JB, Marini J, Yamashita F, Pollet E, Grossmann MVE, Avérous L (2017) Sepiolite as a promising nanoclay for nano-biocomposites based on starch and biodegradable polyester. Mater Sci Eng C 70:296–302

114. Lendvai L, Apostolov A, Karger-Kocsis J (2017) Characterization of layered silicate-reinforced blends of thermoplastic starch (TPS) and poly(butylene adipate-co-terephthalate). Carbohydr Polym 173:566–572

115. He H, Liu B, Xue B, Zhang H (2019) Study on structure and properties of biodegradable PLA/PBAT/organic-modified MMT nanocomposites. J Thermoplast Compos Mater 1–18. https://doi.org/10.1177/0892705719890907

116. Guz L, Famá L, Candal R, Goyanes S (2017) Size effect of ZnO nanorods on physicochemical properties of plasticized starch composites. Carbohydr Polym 157:1611–1619

117. Morales NJ, Candal R, Famá L, Goyanes S, Rubiolo GH (2015) Improving the physical properties of starch using a new kind of water dispersible nano-hybrid reinforcement. Carbohydr Polym 127:291–299

118. Florencia V, López OV, García MA (2020) Exploitation of by-products from cassava and ahipa starch extraction as filler of thermoplastic corn starch. Compos Part B Eng 182:107653

119. Fazeli M, Keley M, Biazar E (2018) Preparation and characterization of starch-based composite films reinforced by cellulose nanofibers. Int J Biol Macromol 116:272–280

120. Pandit P, Nadathur GT, Maiti S, Regubalan B (2018) Functionality and properties of bio-based materials. In: Ahmed S (ed) Bio-based materials for food packaging: green and sustainable advanced packaging materials, 1st edn. Springer, Singapore, pp 81–103

121. Battegazzore D, Bocchini S, Nicola G, Martini E, Frache A (2015) Isosorbide, a green plasticizer for thermoplastic starch that does not retrograde. Carbohydr Polym 119:78–84

122. Preetha B, Sreerag G, Geethamma VG, Sabu T (2019) Mechanical and permeability properties of thermoplastic starch composites reinforced with cellulose nanofiber for packaging applications. J Siberian Federal Univ Biol 12(3):287–301

123. Sadegh-Hassani F, Nafchi AM (2014) Preparation and characterization of bionanocomposite films based on potato starch/halloysite nanoclay. Int J Biol Macromol 67:458–462

124. Wolf C, Angellier-Coussy H, Gontard N, Doghieri F, Guillard V (2018) How the shape of fillers affects the barrier properties of polymer/non-porous particles nanocomposites: a review. J Membr Sci 556:393–418

125. Rybak A, Rybak A, Sysel P (2018) Modeling of gas permeation through mixed-matrix membranes using novel computer application MOT. Appl Sci 8(7):1166

126. Vinh-Thang H, Kaliaguine S (2013) Predictive models for mixed-matrix membrane performance: a review. Chem Rev 113(7):4980–5028

127. García NL, Ribba L, Dufresne A, Aranguren MI, Goyanes S (2009) Physico-mechanical properties of biodegradable starch nanocomposites. Macromol Mater Eng 294(3):169–177

128. García NL, Ribba L, Dufresne A, Aranguren MI, Goyanes S (2011) Effect of glycerol on the morphology of nanocomposites made from thermoplastic starch and starch nanocrystals. Carbohydr Polym 84(1):203–210

129. Jiménez A, Fabra MJ, Talens P, Chiralt A (2012) Effect of re-crystallization on tensile, optical and water vapour barrier properties of corn starch films containing fatty acids. Food Hydrocolloids 26(1):302–310

130. Gao W, Wu W, Liu P, Hou H, Li X, Cui B (2020) Preparation and evaluation of hydrophobic biodegradable films made from corn/octenylsuccinated starch incorporated with different concentrations of soybean oil. Int J Biol Macromol 142:376–383

131. Kang X, Liu P, Gao W, Wu Z, Yu B, Wang R, Cui B, Qiu L, Sun C (2020) Preparation of starch-lipid complex by ultrasonication and its film forming capacity. Food Hydrocolloids 99:105340

132. López OV, Castillo LA, Barbosa SE, Villar MA, Alejandra García M (2018) Processing–properties–applications relationship of nanocomposites based on thermoplastic corn starch and talc. Polym Compos 39(4):1331–1338

133. Moghaddam MRA, Razavi SMA, Jahani Y (2018) Effects of compatibilizer and thermoplastic starch (TPS) concentration on morphological, rheological, tensile, thermal and moisture sorption properties of plasticized polylactic acid/TPS blends. J Polym Environ 26(8):3202–3215

134. Müller CM, Laurindo JB, Yamashita F (2012) Composites of thermoplastic starch and nanoclays produced by extrusion and thermopressing. Carbohydr Polym 89(2):504–510

135. Masclaux C, Gouanve F, Espuche E (2010) Experimental and modelling studies of transport in starch nanocomposite films as affected by relative humidity. J Membr Sci 363(1–2):221–231

136. Beigmohammadi F, Barzoki ZM, Shabanian M (2020) Rye flour and cellulose reinforced starch biocomposite: a green approach to improve water vapor permeability and mechanical properties. Starch-Stärke 72(5–6):1900169

137. dos Santos BH, de Souza do Prado K, Jacinto AA, da Silva S, Aparecida M (2018) Influence of sugarcane bagasse fiber size on biodegradable composites of thermoplastic starch. J Renew Mater 6(2):176–182

138. Li J, Zhou M, Cheng G, Cheng F, Lin Y, Zhu PX (2019) Fabrication and characterization of starch-based nanocomposites reinforced with montmorillonite and cellulose nanofibers. Carbohydr Polym 210:429–436

139. Li J, Zhou M, Cheng F, Lin Y, Zhu P (2019) Bioinspired approach to enhance mechanical properties of starch based nacre-mimetic nanocomposite. Carbohydr Polym 221:113–119

140. Gutiérrez TJ, Ollier R, Alvarez VA (2018) Surface properties of thermoplastic starch materials reinforced with natural fillers. In: Thakur VK, Thakur MK (eds) Functional biopolymers, 1st edn. Springer International Publishing, Cham, pp 131–158

141. Abreu AS, Oliveira M, de Sá A, Rodrigues RM, Cerqueira MA, Vicente AA, Machado AV (2015) Antimicrobial nanostructured starch-based films for packaging. Carbohydr Polym 129:127–134

142. Chen J, Chen F, Meng Y, Wang S, Long Z (2019) Oxidized microcrystalline cellulose improve thermoplastic starch-based composite films: thermal, mechanical and water-solubility properties. Polymer 168:228–235

143. Azevedo VM, Borges SV, Marconcini JM, Yoshida MI, Neto ARS, Pereira TC, Pereira CFG (2017) Effect of replacement of corn starch by whey protein isolate in biodegradable film blends obtained by extrusion. Carbohydr Polym 157:971–980

144. Niranjana Prabhu T, Prashantha K (2018) A review on present status and future challenges of starch based polymer films and their composites in food packaging applications. Polym Compos 39(7):2499–2522

145. Merino D, Gutiérrez TJ, Alvarez VA (2019) Potential agricultural mulch films based on native and phosphorylated corn starch with and without surface functionalization with chitosan. J Polym Environ 27(1):97–105

146. Famá, LM, Goyanes, S, Pettarin, V, Bernal, CR (2015) Mechanical behavior of starch–carbon nanotubes composites. In: Kar KK, Pandey JK, Rana S (eds) Handbook of polymer nanocomposites. Processing, performance and application. Springer, Berlin, pp 141–171

147. Cheng Y, Yu G (2020) The research of interface microdomain and corona-resistance characteristics of micro-nano-ZnO/LDPE. Polymers 12(3):563

148. Angellier H, Molina-Boisseau S, Dole P, Dufresne A (2006) Thermoplastic starch−waxy maize starch nanocrystals nanocomposites. Biomacromolecules 7(2):531–539

149. Dai L, Zhang J, Cheng F (2020) Cross-linked starch-based edible coating reinforced by starch nanocrystals and its preservation effect on graded Huangguan pears. Food Chem 311:125891

150. Li X, Qiu C, Ji N, Sun C, Xiong L, Sun Q (2015) Mechanical, barrier and morphological properties of starch nanocrystals-reinforced pea starch films. Carbohydr Polym 121:155–162

151. Mukurumbira AR, Mellem JJ, Amonsou EO (2017) Effects of amadumbe starch nanocrystals on the physicochemical properties of starch biocomposite films. Carbohydr Polym 165:142–148

152. Chang PR, Jian R, Yu J, Ma X (2010) Fabrication and characterisation of chitosan nanoparticles/plasticized-starch composites. Food Chem 120(3):736–740

153. Othman SH, Kechik NR, Shapi'i RA, Talib RA, Tawakkal IS (2019) Water sorption and mechanical properties of starch/chitosan nanoparticle films. J Nanomater. https://doi.org/10.1155/2019/3843949

154. Shapi'i RA, Othman SH, Nordin N, Basha RK, Naim MN (2020) Antimicrobial properties of starch films incorporated with chitosan nanoparticles: in vitro and in vivo evaluation. Carbohydr Polym 230:115602

155. Siqueira G, Bras J, Dufresne A (2010) Cellulosic bionanocomposites: a review of preparation, properties and applications. Polymers 2(4):728–765

156. Balakrishnan P, Gopi S, Geethamma VG, Kalarikkal N, Thomas S (2018) Cellulose nanofiber vs nanocrystals from pineapple leaf fiber: a comparative studies on reinforcing efficiency on starch nanocomposites. Macromol Symp 380:1800102

157. Boufi S, Gandini A (2015) Triticale crop residue: a cheap material for high performance nanofibrillated cellulose. RSC Adv 5:3141–3151

158. Anglès MN, Dufresne A (2000) Plasticized starch/tunicin whiskers nanocomposites. 1. Structural analysis. Macromolecules 33(22):8344–8353

159. Iqbal MZ (2016) Structure-property relationships in graphene/polymer nanocomposites. Ph. D. thesis, Colorado School of Mines, Arthur Lakes Library

160. Kalogeras IM (2016) Glass-transition phenomena in polymer blends. In: Isayev AI (ed) Encyclopedia of polymer blends, vol 3: structure. Wiley-VCH, Weinheim, pp 1–134

161. Jabarin SA, Majdzadeh-Ardakani K, Lofgren EA (2016) Crystallization and melting behavior in polymer blends. In: Isayev AI (ed) Encyclopedia of polymer blends, vol 3: structure. Wiley-VCH, Weinheim, pp 135–190

162. Lai SM, Sun WW, Don TM (2015) Preparation and characterization of biodegradable polymer blends from poly (3-hydroxybutyrate)/poly (vinyl acetate)-modified corn starch. Polym Eng Sci 55(6):1321–1329

163. Liao HT, Wu ChS (2007) Performance of an acrylic-acid-grafted poly(3-hydroxybutyric acid)/starch bio-blend: characterization and physical properties. Des Monomers Polym 10(1):1–18

164. Innocentini-Mei LH, Bartoli JR, Baltieri RC (2003) Mechanical and thermal properties of poly(3-hydroxybutyrate) blends with starch and starch derivatives. Macromol Symp 197:77–88

165. Florez JP, Fazeli M, Simão RA (2019) Preparation and characterization of thermoplastic starch composite reinforced by plasma-treated poly (hydroxybutyrate) PHB. Int J Biol Macromol 123:609–621

166. Panaitescu DM, Nicolae CA, Frone AN, Chiulan I, Stanescu PO, Draghici C, Iorga M, Mihailescu M (2017) Plasticized poly(3-hydroxybutyrate) with improved melt processing and balanced properties. J Appl Pol Sci 134(19):1–14

167. Petersen K, Nielsen PV, Olsen MB (2001) Physical and mechanical properties of biobased materials starch, polylactate and polyhydroxybutyrate. Starch-Stärke 53(8):356–361

168. Tingwei W (2020) PHA-modified TPS/PBAT biodegradable resin and preparation method therefor. WO2020088214 (A1), 7 May 2020

169. Magalhães NF, Andrade CT (2013) Properties of melt-processed poly (hydroxybutyrate-co-hydroxyvalerate)/starch 1: 1 blend nanocomposites. Polímeros 23(3):366–372

170. Bhattacharyya B, Behera HT, Mojumdar A, Raina V, Ray L (2019) Polyhydroxyalkanoates: resources, demands and sustainability. In: Jamil N, Kumar P, Batool R (eds) Soil microenvironment for bioremediation and polymer production, 1st edn. Wiley, Hoboken, pp 253–270

171. Kushwah BS, Kushwah AVS, Singh V (2016) Towards understanding polyhydroxyalkanoates and their use. J Polym Res 23:153

172. Râpă M, Darie-Niţă RN, Grosu E, Tănase EE, Trifoi AR, Pap T, Vasile C (2015) Effect of plasticizers on melt processability and properties of PHB. J Optoelectron Adv Mater 17:1778–1784

173. Lai SM, Don TM, Huang YC (2006) Preparation and properties of biodegradable thermoplastic starch/poly (hydroxy butyrate) blends. J Appl Polym Sci 100(3):2371–2379

174. Avella M, Errico ME, Rimedio R, Sadocco P (2002) Preparation of biodegradable polyesters/high-amylose-starch composites by reactive blending and their characterization. Appl Polym Sci 83(7):1432–1442

175. Ma P, Xu P, Chen M, Dong W, Cai X, Schmit P, Spoelstra AB, Lemstra PJ (2014) Structure–property relationships of reactively compatibilized PHB/EVA/starch blends. Carbohydr Polym 108:299–306

176. Yingxin H, Tianci H, Peng W (2019) Starch-based degradable PP/PHB composite material and preparation method thereof. CN109679305 (A), 26 Apr 2019

177. Zhang G, Xie W, Wu D (2020) Selective localization of starch nanocrystals in the biodegradable nanocomposites probed by crystallization temperatures. Carbohydr Polym 227:115341

178. Pan HW, Ju DD, Zhao Y, Wang Z, Yang HL, Zhang HL, Dong LS (2016) Mechanical properties, hydrophobic properties and thermal stability of the biodegradable poly(butylene adipate-co-terephthalate)/maleated thermoplastic starch blown films. Fiber Polym 17:1540–1549

179. Hablot E, Dewasthale S, Zhao Y, Zhiguan Y, Shi X, Graiver D, Narayan R (2013) Reactive extrusion of glycerylated starch and starch–polyester graft copolymers. Eur Polym J 49(4):873–881

180. Stagner JA, Alves VD, Narayan R (2012) Application and performance of maleated thermoplastic starch–poly (butylene adipate-co-terephthalate) blends for films. J Appl Polym Sci 126(S1):E135–E142

181. Rhim J-W, Park H-M, Ha C-S (2013) Bio-nanocomposites for food packaging applications. Prog Polym Sci 38(10):1629–1652

182. Spiridon I, Anghel NC, Darie-Nita RN, Iwańczuk A, Ursu RG, Spiridon IA (2019) New composites based on starch/Ecoflex®/biomass wastes: mechanical, thermal, morphological and antimicrobial properties. Int J Biol Macromol. https://doi.org/10.1016/j.ijbiomac.2019.11.185

183. Spiridon I, Darie-Nita RN, Hitruc GE, Ludwiczak J, Cianga Spiridon IA, Niculaua M (2016) New opportunities to valorize biomass wastes into green materials. J Clean Prod 133:235–242

184. Olivato JB, Grossmann MVE, Yamashita F, Nobrega MM, Scapin MRS, Eiras D, Pessan LA (2011) Compatibilisation of starch/poly(butylene adipate co-terephthalate) blends in blown films. Int J Food Sci Technol 46:1934–1939
185. Lekube BM, Fahrngruber B, Kozich M, Wastyn M, Burgstaller C (2019) Influence of processing on the mechanical properties and morphology of starch-based blends for film applications. J Appl Polym Sci 136(39):47990
186. Sun S, Liu P, Ji N, Hou H, Dong H (2018) Effects of various cross-linking agents on the physicochemical properties of starch/PHA composite films produced by extrusion blowing. Food Hydrocolloids 77:964–975